Ion Channels in Microbes

BORIS MARTINAC, YOSHIRO SAIMI, AND CHING KUNG

*School of Biomedical Sciences, The University of Queensland, Brisbane, Queensland, Australia;
and Laboratory of Molecular Biology and Department of Genetics, University of Wisconsin, Madison, Wisconsin*

Martinac B, Saimi Y, Kung C. Ion Channels in Microbes. *Physiol Rev* 88: 1449–1490, 2008; doi:10.1152/physrev.00005.2008.—Studies of ion channels have for long been dominated by the animalcentric, if not anthropocentric, view of physiology. The structures and activities of ion channels had, however, evolved long before the appearance of complex multicellular organisms on earth. The diversity of ion channels existing in cellular membranes of prokaryotes is a good example. Although at first it may appear as a paradox that most of what we know about the structure of eukaryotic ion channels is based on the structure of bacterial channels, this should not be surprising given the evolutionary relatedness of all living organisms and suitability of microbial cells for structural studies of biological macromolecules in a laboratory environment. Genome sequences of the human as well as various microbial, plant, and animal organisms unambiguously established the evolutionary links, whereas crystallographic studies of the structures of major types of ion channels published over the last decade clearly demonstrated the advantage of using microbes as experimental organisms. The purpose of this review is not only to provide an account of acquired knowledge on microbial ion channels but also to show that the study of microbes and their ion channels may also hold a key to solving unresolved molecular mysteries in the future.

I. INTRODUCTION

The earth is 4.6 billion years old (Fig. 1*A*). Since it became a living planet some 3.8 billion years ago, microbes represent the largest group of living organisms on it (394). Microbes are much more diverse than animals and plants (393) and outweigh all other living organisms by far in terms of their biomass. They include prokaryotes (bacteria and archaea) and eukaryotes (protozoa, algae, and fungi), occupying numerous evolutionary branches

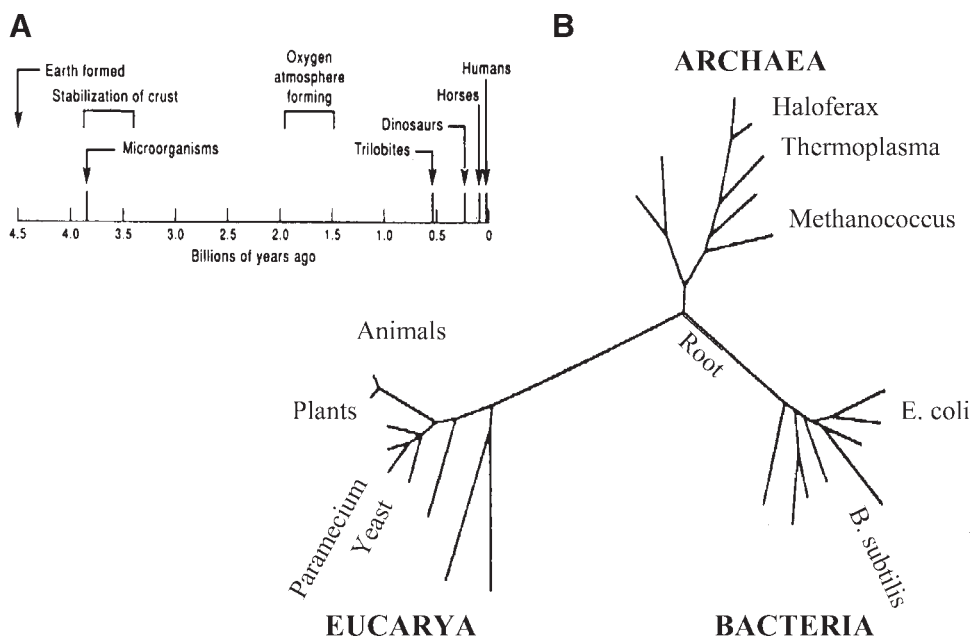0031-9333/08 $18.00 Copyright © 2008 the American Physiological Society

FIG. 1. Diversity of life forms on Earth. *A*: timeline of the planet Earth showing the early emergence of various life forms on it. [From Woese (393), with permission from American Society for Microbiology.] *B*: universal phylogenetic tree showing the organization of life on Earth in three kingdoms of living organisms: Archaea, Euakarya, and Bacteria. [Modified from Woese (393).]

on the universal phylogenetic tree (Fig. 1*B*). Their diversity, number, and adaptability to environments characterized by extreme temperatures, salinity, or acidity (270) have enabled them to inhabit all the niches of life on the planet and will in all likelihood allow them to outlive any future global cataclysm.

Why study ion channels in microbes? Microbes are not only very interesting study objects in their own right, but they also offer specific experimental advantages for studies of structure and function of ion channels. Highlighted by the 2003 Nobel Prize in Chemistry "for structural and mechanistic studies of ion channels" in which bacterial ion channels played an essential role (229), microbes have in the past often been used to advance our understanding of basic biochemical or physiological cellular processes. They are uniquely suited for genetic manipulation and are the prime subject of recombinant DNA technology. They have very short replication times and some are simple to grow, allowing for large yields in laboratory cultures, which is a prerequisite for a large-scale production of milligram amounts of ion channel proteins required for structural studies by X-ray crystallography or magnetic resonance spectroscopy. Microbes also provide a unique opportunity to study evolutionary origins and primordial design of ion channels. Channel prototypes may be deduced from the commonalities of channels of extant samples from all three domains.

A. A Brief History

Beginning with Galvani's discovery, bioelectricity is largely the concern of animal physiology, with the excitation of nerve and muscle being the centerpiece. This animalcentric view is further accentuated in recent years because of human health concerns. Ion channels, the molecular bases of excitation and beyond, are therefore continued to be studied mainly in the human, mouse, and fly. Two developments broadened our horizon, revealing the existence of ion channels in all three domains of life (Fig. 1). First, patch-clamp survey of the model bacterium *Escherichia coli* (238; see sect. II*A1*) and the model unicellular eukaryote *Saccharomyces cerevisiae* (114, 115; see sect. IV*C1*) revealed unitary ion conductances on their membranes. These findings not only showed that ion channels exist in microbes but also showed that they are not necessarily associated with motility, an impression previously reinforced by the study of *Paramecium* behavior (see sect. IV*A*). Second, the ever-increasing number of microbial genome sequences revealed gene products akin to animal channels. Because of the relative ease in microbial culture, milligrams of bacterial and archaeal channel proteins can be purified, yielding diffractable crystals (80; see sect. III). The results are microbial ion-channel structures of atomic resolutions, leading to insights that revolutionized our understanding of ion channels.

Structural and functional studies of ion channels in prokaryotic cells are some of the best examples of how microbes as model systems have contributed towards our understanding of general principles underlying the structure and function relationship in biological molecules. A multidisciplinary approach that can be employed in studies of bacterial mechanosensitive channels (13, 22, 27, 44, 202, 238, 300–302, 366, 367, 401), K^+ channels (11, 80, 298, 299, 340), Na^+ channels (294, 321), Cl^- channels (83), cNMP-gated channels (53), and glutamate receptor channels (47) as well as archaeal mechanosensitive channels

(161, 162, 164, 165) and Ca^{2+}-gated K^+ channel (206) enhanced our understanding of the function of ion channels in living cells in ways that could not have been done by studying animal channels only.

Not only for historical reasons but also for keeping an accurate record of achievements of the pioneers in electrophysiology, it is worth mentioning here that the first intracellular electrical recordings from a living organism were obtained from a microbial cell. It was a protozoon *Paramecium* that in 1934 was impaled by a glass microelectrode to register the resting membrane potential of this microbe (150). This work was later overshadowed by the great work of Alan. L. Hodgkin and Andrew. F. Huxley on neuronal excitation and conduction in squid giant axon (134, 139).

B. Scope of This Review

The focus of this review is on the structural and functional characterization of ion channels in prokaryotic (bacteria and archaea) and eukaryotic microbes (algae, ciliates, and fungi). Some of these microorganisms have been excellent experimental objects amenable to modern electrophysiological techniques. Probing their cellular membranes by glass microelectrodes connected to amplifiers, oscilloscopes, and computers has made a great contribution towards our understanding of the workings, functional role, and evolutionary origins of ion channels in living cells. Conceptually, this review consists of two major parts: the first one focusing on ion channels in prokaryotic cells and the second one describing ion channels in eukaryotic microbes. For completeness, we also included in the review two sections that are briefly touching upon the channels formed by microbial toxins and ion channels found in viruses.[1] Space concern does not allow us to cover other channels such as porins, aquaporins, organelle channels such as VDAC, nuclearpore, etc. Comprehensive reviews on these subjects are available elsewhere.

C. Voltage-Clamp and Patch-Clamp Investigation of Microbial Cells

With the exception of some large protozoa and algae, the classical electrophysiological techniques of the whole cell current clamp and voltage clamp using two glass microelectrodes were for a long time not applicable to microorganisms because of their very small size. The patch-clamp method (118) provided means to overcome this shortcoming. Prior to the advent of the patch-clamp

technique, electrophysiological measurements in microbial cells could only be carried out in large protozoan or algal cells in vivo or in vitro by reconstituting ion channels into planar lipid bilayers (87, 263, 395). The patch-clamp technique allowed, for the first time, the study of electrical properties of very small cells by examining ionic currents flowing through individual ion channels in their cellular membranes in situ. Whereas little modification of recording solutions, glass pipettes, and electrophysiological equipment is required to record ionic currents from microbial cells, appropriate preparations of microbial cell membranes amenable for giga-seal formation and patch-clamp recording present a major challenge. The following examples may illustrate the variety and architectural complexity of microbial cell envelopes.

A single *Paramecium* cell is covered by ∼5,000 cilia, and the cell membrane is covered by a thick extracellular matrix consisting mainly of the "immobilization antigen" protein (228). In yeast (single-celled fungi), the cell membrane is covered by a cell wall made of glucans, mannans, proteins, and lipids (269). The cytoplasmic membrane of Gram-positive bacteria is enclosed by a thick cell wall made of peptidoglycan that provides the rigidity necessary to maintain cell integrity, whereas Gram-negative bacteria have in addition a second chemically distinct outer membrane attached to the peptidoglycan layer on its external side (385). The situation with archaea is further complicated by the large diversity of extreme habitats to which archaea have adapted, which greatly influenced the chemical composition and architecture of their cell membranes (162). Not only the cell wall structure, which varies considerably among archaeal species, but also the composition of cell membranes of archaea is very different from bacterial membranes. Archaeal membranes are not made of phospholipids, but consist of diphytanyl-glycerol-diether or -tetraether or both (79). Consequently, there is no single method that can be applied to all microbes to expose their membranes for the purpose of patch-clamping. Each type of microbial cell has to be approached individually. For example, the examination of a bacterial cell membrane by the patch-clamp technique became possible some 20 years ago with development of a "giant spheroplast" preparation in *E. coli*, which has led to a discovery of MS channels in these microbes (238, 328) (Fig. 2). Briefly, a culture of *E. coli* cells is grown in media containing antibiotic cephalexin until strings of bacteria, called "snakes," of the appropriate length are formed as observed under the microscope. Giant spheroplasts are then obtained by addition of EDTA and lysozyme to perforate the outer membrane and break glycosidic linkages in the cell wall structure causing the "snakes" to round up into spheroplasts of 5–10 μm in diameter. This giant spheroplast preparation has recently been optimized for studies of MmaK, a putative cyclic nucleotide-gated K^+ channel cloned from *Magnetospiril-*

---

[1] Although viruses are not microbes, but encapsulated parasitic fragments of DNA or RNA, we have also included in this review a brief account of viral ion channels, because of their minimalistic structure matching the simplicity of microbial channel-forming toxins and of some of the extant channels.
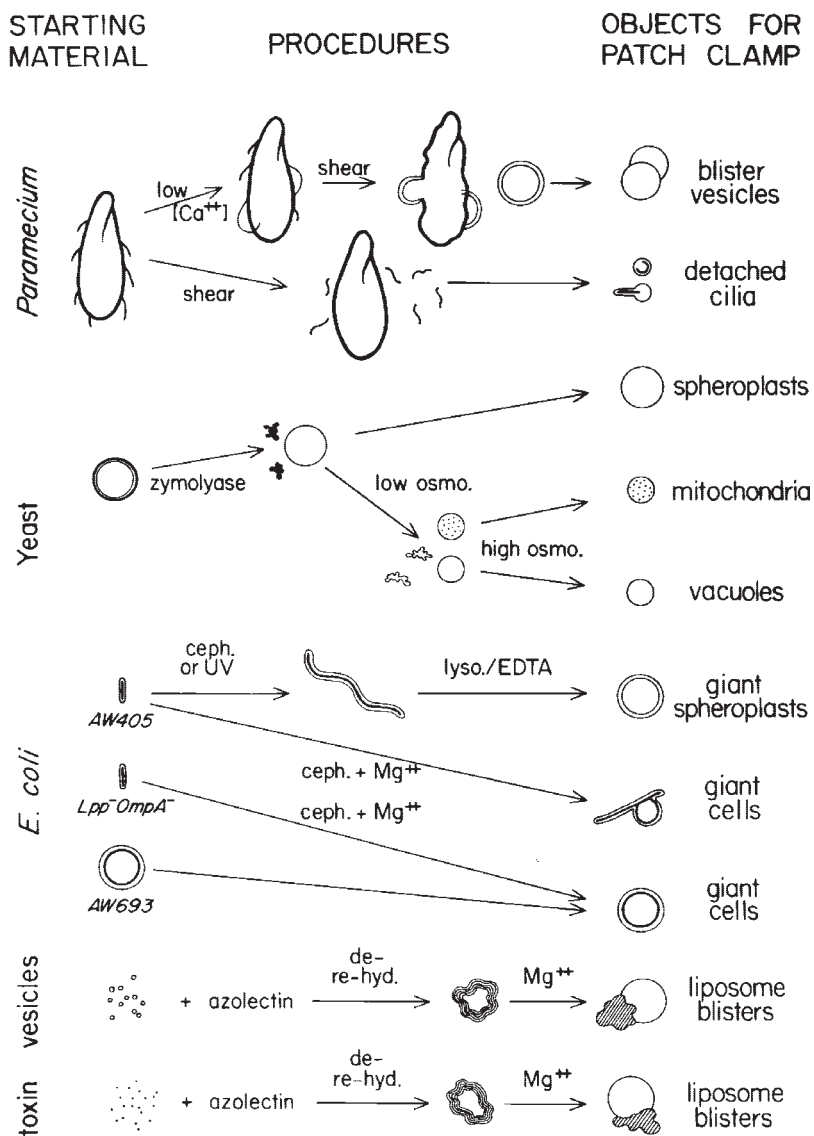
FIG. 2. Different procedures used to generate microbial objects suitable for patch-clamp studies. The starting material (*left*) (*Paramecium*, *Saccharomyces cerevisiae*, *Escherichia coli*, membrane vesicles, and yeast killer toxin) have dimensions on the order of 100, 10, 1, 0.1, and 0. 01 μm, respectively. The procedure briefly shown in the center converts the microbes to objects used successfully for the patch-clamp recording. The objects (*right*) are all 5–15 μm in diameter, except detached cilia from *Paramecium* and yeast mitochondria and vacuoles, which are $\sim$2 and $\sim$3 μm in size, respectively. For details of the procedures for preparations of the microbial objects, see Saimi et al. (334); figure used with permission from Elsevier.

lum magnetotacticum (194). A diagram summarizing several of the methods used for patch-clamp recording from microbial cells is shown in Figure 2. Details of these methods (334) are described in references cited under individual organisms detailed below.

II. LARGE-CONDUCTANCE MECHANOSENSITIVE CHANNELS OF PROKARYOTES

A. Mechanosensitive Channels of Bacteria: MscL, MscS, and MscK

Although they conduct ions and are usually characterized by their ionic conductance and selectivity, prokaryotic MS ion channels are often referred to as MS channels rather than MS ion channels. This is because in bacteria (and possibly also in Archaea) they primarily serve to transport cellular osmoprotectants other than ions by acting as osmosensors that regulate the cellular turgor (see sect. IIC). Bacterial MscL and MscS channels have large conductances of $\sim$3 and $\sim$1 nS, respectively, and lack ionic specificity by passing anything smaller than $\sim$1,000 molecular weight including proline, potassium glutamate, trehalose, and ATP (117). MscL is nonselective for both anions and cations (62, 368), whereas MscS exhibits a slight preference for anions over cations with a permeability ratio $P_{Cl}:P_K = 1.5$–3.0:1 (238, 354, 364, 368).

1. MscL (mechanosensitive channel of large conductance)

The technical advance of the "giant spheroplast" preparation in *E. coli* (238, 328) opened a window of

opportunities for structure and function studies of mechanosensitive (MS) class of membrane proteins in prokaryotes. Prokaryotic MS channel currents have most extensively been studied in *E. coli* (236, 238, 239, 297, 362, 416), which harbors several MS channels in its cell envelope: MscL (large), MscS/MscK (small/kalium, i.e., potassium), and MscM (mini), named for their single-channel conductances of ~3, ~1, and ~0.3 nS, respectively (19). Given that bacteria can be grown in large quantities delivering the milligram amounts of channel proteins required for structural studies, three-dimensional structures of MscL from *Mycobacterium tuberculosis* (44) (Fig. 3*A*) and MscS from *Escherichia coli* (13) (Fig. 3*C*) were solved by X-ray crystallography only a few years after identification and cloning of both channels in *E. coli* (202, 366). MscK was cloned simultaneously with MscS (202), whereas MscM (19) still remains to be identified at the molecular level.

The strategy used for cloning of MscL consisted of detergent solubilization and fractionation of *E. coli* membrane constituents by column chromatography combined with the patch-clamp examination of the individual protein fractions reconstituted into artificial liposomes (366, 367). Given that mechanosensitivity of MscL is fully preserved upon the reconstitution of the channel protein into liposomes (367, 368), the protein fraction containing MscL activity could be identified, which enabled the isolation of the MscL protein comprising 136 amino acid residues followed by the cloning of its corresponding *mscL* gene (366). The expression of the gene *in trans* as well as with an in vitro transcription/translation system confirmed that the *mscL* gene alone was required and sufficient for the MscL activity.

Three-dimensional structure of the MscL homolog from *M. tuberculosis* obtained at 3.5 Å resolution shows a homopentameric channel, most likely in a closed state (Fig. 3*A*) (44). The channel monomer consists of two α-helical transmembrane (TM) domains, TM1 and TM2, cytoplasmic NH_2- and COOH-terminal domains and a central periplasmic domain. The channel pore is formed by five transmembrane TM1 helices organized as a tightly packed bundle. At the cytoplasmic side, the five helices funnel into a hydrophobic constriction of 2 Å functioning as the channel gate. The diameter of the channel pore at the gate expands from 2 to 30 Å during the channel opening as determined by electrophysiological perme-
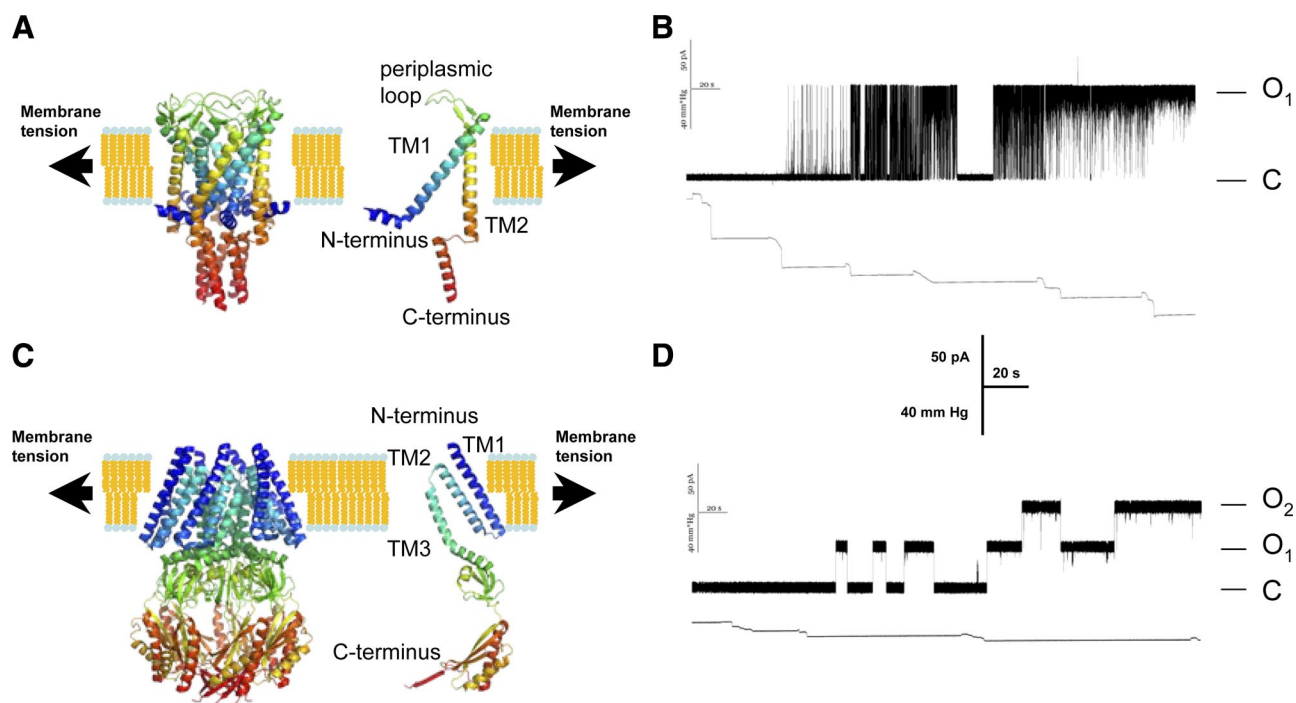
FIG. 3. Bacterial MS channels. *A*: the structure of the pentameric MscL channel (*left*) and a channel monomer (*right*) from *M. tuberculosis* according to the 3-dimensional structural model (357). *B*: a current trace of a single MscL channel reconstituted into azolectin liposomes (wt/wt protein/lipid of 1:2,000) recorded at +30 mV pipette potential. The channel gated more frequently and remained longer open with increase in negative pressure applied to the patch-clamp pipette (trace shown below the channel current trace). *C*: 3-dimensional structure of the MscS homoheptamer (*left*) and a channel monomer (*right*) from *E. coli* (358). *D*: current traces of two MscS channels reconstituted into azolectin liposomes (wt/wt protein/lipid of 1:1,000) recorded at +30 mV pipette voltage. Increase in pipette suction (trace shown below the channel current trace) caused an increase in the activity of both channels. C and O_n denote the closed and open state of the n number of channels.

ation studies using large organic cations (62) and electron paramagnetic resonance (EPR) spectroscopy combined with cysteine scanning mutagenesis and site-directed spin labeling (SDSL) (300–302). FRET spectroscopic analysis confirmed these findings by showing that the overall change in diameter of the MscL pentamer between its closed and open state is 16 Å (59). This result is consistent with the very large conformational changes that MscL undergoes during gating, which are necessary to accommodate the opening of the large pore of the channel. Mutational studies that led to isolation of either gain-of-function (GOF) or loss-of-function (LOF) mutant strains helped further in identifying functionally important residues and structural regions in MscL (208, 242, 283, 400, 401).

Since the publication of a three-dimensional structure of MscL (44), a large number of computer simulation studies aimed at understanding the gating mechanism of the channel by changes in membrane tension or composition. Simulations examining the stability of the protein structure when embedded in the lipid bilayer membrane indicated large conformational changes occurring when the MscL protein is influenced by an external force, in agreement with the results of the experimental studies. The simulations that have been carried out to investigate the nature and sequence of these conformational changes differ mostly in the way that the external force is applied to the MscL protein and conditions that affect the interactions between the lipid and the protein (25, 54, 90, 112, 113, 170) (for review on computational studies of bacterial MS channels, see also Ref. 58).

The TM1 and TM2 helices of MscL are connected by a structurally not well defined periplasmic loop, which is thought to function as a spring, resisting the channel opening (2, 290). This view has been supported by a molecular dynamics study of MscL embedded in a curved bilayer (246). According to this study, the periplasmic loop is the first domain of MscL to change its structure leading to channel opening. At the cytoplasmic end of MscL, the short NH$_2$-terminal domain comprising approximately a dozen amino acids has been proposed to function as a second channel gate working in accord with the hydrophobic gate formed by the TM1 helix bundle (22, 365). Although results from a recent study, which utilized cysteine trapping of single-cysteine mutated channels, do not support the "second-gate" concept (144), the NH$_2$ terminus is nevertheless an important structural domain of MscL, as demonstrated by amino acid deletion and substitution studies showing that structural changes in the NH$_2$ terminus severely affect MscL function (30, 122). The precise role of the NH$_2$ terminus for the MscL gating thus remains to be determined. The COOH-terminal domain, which forms an α-helical bundle at the cytoplasmic end of the channel (44) (Fig. 3A), appears to be the least important structural domain for the channel gating, since a deletion of 27 COOH-terminal residues constituting a large portion of the COOH terminus was shown not to significantly affect mechanosensitivity of the channel (22, 29, 365). Although the precise physiological role of the COOH-terminal domain is unclear at present, a current view of its role is that of a size-exclusion filter, which should prevent a loss of essential metabolites at the cytoplasmic side of the MscL channel pore (5). Recently, it has been shown that the structural stability of the COOH-terminal bundle is pH dependent (160), suggesting that in addition to its role of a size-exclusion filter, COOH terminus may also influence the channel gating in a pH-dependent manner. Furthermore, it has recently been shown that the COOH terminus may actively participate in the channel gating, since the opening of MscL is accompanied by the dissociation of the COOH-terminal helix bundle and pore formation (402).

2. MscS and MscK (mechanosensitive channel of smaller conductances)

MscS and MscK were cloned several years after MscL (202). Two genes, *yggB* and *kefA*, corresponding to MscS and MscK respectively, were identified on the *E. coli* chromosome. Deletion of these genes led to the abolishment of the MS currents corresponding to the MS channel of small conductance, leaving the activity of MscL intact in *E. coli* giant spheroplasts. Originally, MscS and MscK appeared indistinguishable in the patch-clamp experiments (238). However, MscS was later shown to differ functionally from MscK by exhibiting a rapid inactivation upon sustained application of pressure (173). A distinguishing property of MscK on the other hand is its sensitivity to the extracellular ionic environment (207). Structurally, MscS is a small membrane protein of 286 amino acids, whereas MscK is a much larger, multidomain membrane protein comprised of 1,120 amino acid residues. Both proteins share a common structural feature such that the primary amino acid sequence of MscS closely resembles the sequence of the last two domains of the MscK protein (202).

A three-dimensional crystal structure of MscS of *E. coli* obtained at 3.9 Å resolution (13) shows a channel folded as a homoheptamer (Fig. 3C). Each of the seven subunits is composed of three transmembrane domains with NH$_2$ termini facing the periplasm and COOH termini facing the cytoplasm. Initially, the three-dimensional structure of MscS was thought to depict an open channel (13). However, recent computer simulation studies have cast doubt on this assertion (58). The TM1 and TM2 transmembrane domains, which are in direct contact with the surrounding lipids, are thought to constitute the sensor for membrane tension as well as a voltage sensor because of the presence of three arginine residues in their structure (13, 23). Since the precise contribution of these charged residues to the channel voltage dependence is

not known, their role in the channel gating remains to be established experimentally. TM3 helices line the channel pore. As a distinguishing feature, the channel has a large, cytoplasmic domain (Fig. 3*C*), which is in contact with the cytoplasm through multiple openings. Its major characteristic is a large interior chamber of 40 Å in diameter. The cytoplasmic domain is a dynamic structure that undergoes significant conformational changes upon the channel gating (172). It passively follows the movement of the TM1-TM2 "hairpin" and the membrane portion of the TM3 helix by expanding during the channel gating. In addition to its role in the channel gating, this domain has been suggested to also play a role in the channel desensitization and stability (248, 342) as well as in ion transport and selectivity (86).

Most of the computational studies that have appeared since the publication of the crystal structure of the MscS channel (13) have attempted to answer the question on the conduction state of the crystallized structure. The crystal structure of the protein showing a large nonoccluded pore passing across the membrane has suggested that the protein had most likely been imaged in an open state. Closer inspection of the structure, however, indicates that the narrowest region of the pore has a diameter of only ~3.5 Å and is surrounded by two rings of nonpolar leucine residues (L105 and L109). Such narrow hydrophobic pores can, however, prevent the passage of ions without presenting a physical occlusion as indicated by a number of molecular dynamic investigations of model pores (17, 18) and the nicotinic acetylcholine receptor (16, 57), which have shown that water tends to evacuate the hydrophobic regions of such pores under certain conditions. If the radius of a pore is increased to 4.0–4.5 Å or a more polar surface is introduced, then water will fully hydrate the channel. As the radius of the constriction in the MscS pore is below the critical radius for hydration seen for other pores, it is likely that a similar hydrophobic gating mechanism could play a role in the MscS gating. Consequently, the MscS crystal structure could represent a closed or nonconductive state rather than an open conformation as originally proposed. Molecular dynamics studies of the MscS pore indicated that water does indeed evacuate the constricted region of the pore and provided some of the first evidence for a hydrophobic gating mechanism in a real channel rather than model (6, 353).

3. Force transmission from the lipid bilayer

Both channels, MscL and MscS, directly sense membrane tension developed in the lipid bilayer alone (123, 234, 237, 300, 301, 364, 383) (Fig. 3, *B* and *D*). The bilayer mechanism, as this mechanism of the MS channel gating has been named (119), has been well documented for MS channels of prokaryotes (236, 303), since the prokaryotic MS channels preserve their mechanosensitivity after re-constitution into artificial liposomes. The fact that MscL and MscS can be activated by amphipaths, known to insert preferentially in one leaflet of the lipid bilayer (237, 346), provided a basis for a recent spectroscopic and patch-clamp studies. In these studies, structural changes in MscL induced by either hydrophobic mismatch or curving the bilayer by insertion of the amphipath lysophosphatidylcholine (LPC) were examined by combining cysteine-scanning mutagenesis with SDSL, EPR spectroscopy, and patch-clamp functional analysis of MscL reconstituted into liposomes (300, 301). The studies demonstrated that hydrophobic surface matching could stabilize intermediate conformations of MscL, requiring less tension to open the channel in thin bilayers (<18 hydrocarbons/acyl chain) compared with thick bilayers (>18 hydrocarbons/acyl chain), but was insufficient to fully open the channel. However, curving the bilayer by asymmetric insertion of LPC opened MscL without applying membrane tension, indicating that the mechanism of mechanotransduction in MS channels is defined by both local and global asymmetries in the transbilayer tension profile at the lipid protein interface. A recent study indicated the asparagine substitution of the residues near both ends of the transmembrane helices impaired the function of MscS (275). Similarly, it has been shown that introduction of Tyr, Trp, Asn, or Asp residues at the periplasmic end of the transmembrane domains impairs MscL mechanosensitivity (401). Thus MscS shares the same characteristics with MscL in that the interaction with lipids near the polar-apolar boundary is essential to the channel function (36). These findings have general implications for MS channel gating, since they seem to suggest the role of the lipid bilayer in actively modulating the activity of MS ion channels in all types of living cells (184).

4. MscL and MscS homologs

The accessibility of a large number of genome sequences of different evolutionary groups has made possible the analysis of the phylogenetic distribution of MscL and MscS type of channels in these microorganisms. Multiple sequence alignments of homologs of MscL and MscS revealed that they form separate families of prokaryotic MS channels (240, 307). Furthermore, a recent comprehensive analysis of nucleotide composition and codon usage from six phylogenetic groups of prokaryotic MS channel genes indicates that the evolution of the prokaryotic MscL and MscS genes followed separate evolutionary pathways (49). A subfamily group of MscL-type proteins encompasses MS channels of gram-negative and gram-positive bacteria. It also includes MscL-like proteins of a single archaeon, *Methanosarcina acetovorans*, and a fungus, *Neurospora crassa* (163, 181, 307). The archaeal and fungal proteins are the most divergent members of the MscL family, which most closely resemble those of gram-

positive bacteria (307). Compared with the MscL subfamily, the MscS family varies much more in size by including a number of representatives from bacteria, archaea, fission yeast *Schizosaccharomyces pombe*, single-celled alga *Chlamydomonas*, and plant *Arabidopsis thaliana* (266, 307). Although the MscS subfamily is more diverse, it is not ubiquitous. Several organisms with fully sequenced genomes including gram-negative chlamydias, the gram-positive clostridia, mycoplasmas, and ureaplasmas, do not encode recognizable MscS homologs (307). Furthermore, neither of the two subfamilies of MS channels include representatives from animal cells (163, 240, 307).

B. Mechanosensitive Channels of Archaea: MscMJ, MscMJLR, and MscTA

MS channel activities have also been reported in several species of Archaea (Fig. 1*B*) including halophilic *Haloferax volcanii*, thermophilic *Thermoplasma acidophilum*, and methanogenic *Methanococcus jannashii* (162, 240). Like MscL and MscS, archaeal MS channels are gated by tension in the lipid bilayer and are activated by amphipaths. They have large conductance and low selectivity for ions and are weakly voltage dependent. They can also be blocked by submillimolar concentrations of gadolinium, which is a common inhibitor of MS type of ion channels.

MscMJ and MscMJLR are the two types of MS channels found in *M. jannashii* (164, 165). These two channels differ functionally from each other despite sharing 44% sequence identity (240). Although they have similar ion selectivity with preference for cations over anions (P_K/P_{Cl} ~5.0), the conductance of MscMJ of 0.3 nS is much smaller compared with 2.0 nS conductance of MscMJLR (165). Both channels were identified during inspection of the *M. jannashii* genome database using the DNA corresponding to the TM1 helix of MscL as a probe. MscMJ comprises 350 residues, whereas MscMJLR is a slightly bigger protein comprising 361 residues (165). Both channels are members of the MscS subfamily of MS channels, with both proteins exhibiting ~28% sequence identity with overlapping residues of the MscS sequence (163, 165) (Fig. 4).

MscTA is a 15-kDa membrane protein underlying the activity of the MS channel of *Thermoplasma volcanium* (161). It was identified using a functional approach similar to the one used for molecular identification of MscL (366, 367). Like MscL, the channel has a large conductance of 1.5 nS and is nonselective for ions. MscTA seems also structurally related to MscL, since secondary structure analysis revealed two putative α-helical membrane-spanning regions despite that its primary amino acid sequence contains an unusually high proportion of charged residues for a membrane protein.
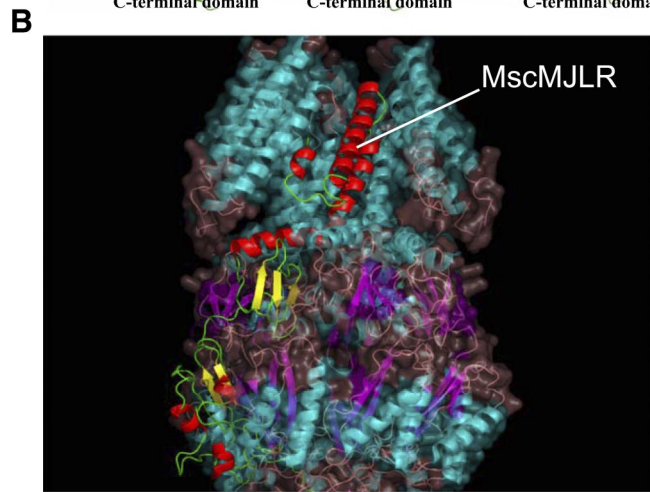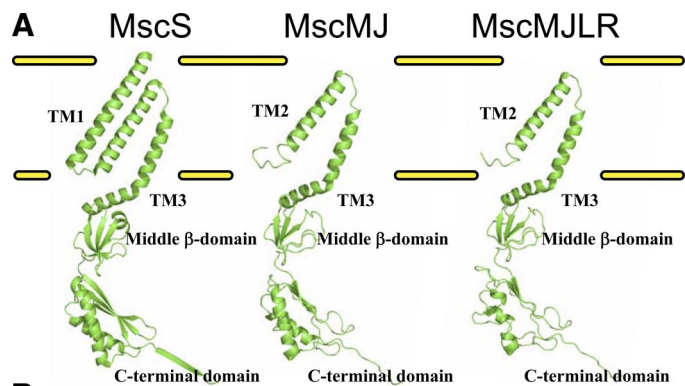

FIG. 4. MscS-like archaeal channels. *A*: MscS monomer (*left*) and structural models of MscMJ (*middle*) and MscMJLR (*right*) monomers based on the MscS crystal structure. Models of the MscMJ and MscMJLR monomers were generated by Swiss-Model (111) and viewed by PyMOL. *B*: MscMJLR monomer superimposed and embedded in the 3-dimensional structure of MscS of *E. coli* viewed by PyMOL. α-Helices of the MscMJLR monomer are shown in red, β-sheets in yellow, whereas loops are depicted in green.

C. Physiological Role of MS Channels in Prokaryotes

Multiple adaptation mechanisms enable bacteria to grow in a wide range of external osmolarities (351, 396). Located in the cytoplasmic membrane (20, 124, 202, 276), MS channels have evolved specifically to serve as emergency valves for fast release of osmolytes in osmotically challenged bacterial cells. The opening of MS channels upon a hyposmotic shock enables rapid loss of cytoplasmic solutes and excess water, which helps to restore a normal cellular turgor and prevent cell lysis. As unambiguously demonstrated for MscL and MscS, these MS channels thus function as "emergency valves" for rapid and nonspecific release of solutes (28, 37, 202). As sensors and regulators of the cellular turgor, they provide a safeguard without which the bacterial cells would lyse. Double knock-out mutants of *E. coli* lacking both MscL and MscS die upon transfer from a medium of high to a medium of

low osmolarity (38, 202). MscM, the third bacterial MS channel whose molecular identity remains unknown to date, is insufficient alone to protect the cells from lysis. Further evidence for the MS channel "safety valve" function has been provided by a study on marine bacterium *Vibrio alginolyticus*, in which introduction of an *mscL* gene was found to alleviate cell lysis by hyposmotic shock (265). Except in the extreme conditions of a hyposmotic shock, knockout bacterial cells lacking MscS, MscL, or both are otherwise fully viable. The multiplicity of MS channels is likely required to provide a safeguard against the deleterious effects during sudden changes in external osmolarity occurring in the living habitats in which prokaryotes exist.

Given that cell turgor is essential for growth and cell wall synthesis, prokaryotic MS channels may also be designed to detect changes in turgor pressure during cell division and cell growth, which are accompanied by an increase in cell volume required for the synthesis and assembly of cell wall components (63). Indeed, it has been demonstrated that the expression of MscS and MscL is stimulated in cells entering into stationary growth phase when they undergo cell wall remodeling and need to relieve the turgor pressure (361). Although the physiological role of MS channels in Archaea has not clearly been established, the archaeal MS channels, however, could be expected to have functions similar to those of their bacterial counterparts.

III. ION-SPECIFIC CHANNELS OF PROKARYOTES

Unlike the study of mechanosensitive channels above, studies of prokaryotic ion-specific channels are not systematic. Historically, they are largely the extensions of crystallographic studies and not originated with microbial-physiological concerns. The recent decade saw the three-dimensional structures at atomic resolutions of prokaryotic K^+ channels, Na^+ channels, glutamate receptors, etc. These structures provided unprecedented insights into the molecular mechanisms of ion channels and revolutionalized the field of ion-channel research. While these high-resolution structures now serve as the foundation of our ion-channel understanding and its biomedical extensions, these channels have not been studied extensively or systematically in the bacteria and archaea themselves. The roles they play in the various prokaryotic species are largely unknown. The narrative below will therefore concentrate on the knowledge gained through these structures. The deepest knowledge came from the studies of K^+ channels. We will therefore begin with a simpler K^+ channel, KcsA, from the gram-positive bacterium *Streptomyces lividans*. We will then build on the KscA core other gating modules to describe Ca^{2+}-, cNMP-,

or voltage-gated K^+ channel. We will then discuss glutamate receptor, a type of ligand-gated K^+ channel in bacteria. This will then be followed with prokaryotic Na^+ channel, akin to K^+ channels, before describing mechanistically different types of channels including NH_4^+ channels and Cl^- "channels." In this narrative, examples from both bacterial and archaeal channels will be used, largely depending on the availability of crystal structures. Animal ion channel pores have associated partners that play auxiliary or regulatory roles. Often, the channel proper is called the α or the pore-forming subunit, and the other are called $\beta1$, $\beta2$, γ, etc. Some homologs of the non-pore-forming subunits are found in microbes, but are not reviewed here because of space consideration.

A. K^+ Channels

K^+ is the major cation in any cytoplasm. Correspondingly, K^+ channel genes are found in nearly all genomes. These include those of bacteria and archaea, except the greatly reduced genomes of parasites and organelles (190, 192). Because of the crystal structures of prokaryotic channels, far more is known about prokaryotic K^+ channels than most eukaryotic channels or other microbial channels, except MscL and MscS (above). This knowledge has tremendous impact on ion-channel biology and is extensively reviewed and discussed in the literature of animal physiology. For current discussions on K^+-channel structures and functions in general, see References 107 and 278. For more on microbial K^+ channels, see Kuo and co-workers (190, 192).

The study of ion channels is deeply rooted in neurophysiology. Excitation of nerves or muscles entails the sequential rise and fall of Na^+ (Ca^{2+}) and K^+ permeability of the membrane. Permeation to a specific ion implies selectivity; rise and fall imply portal control. These functional characteristics have their conceptual structural counterparts: the "filter" and the "gate," formulated long before we have clear structural information. These two key structures became "crystal clear" with the arrival of prokaryotic channels and are described below.

The puzzling feature of the ion filter is its very key properties: permeation and selectivity. A K^+ channel can pass some 10^7 K^+ per second and discriminate against the smaller Na^+ at the same time (P_K: P_{Na} >1,000:1). These properties challenge our common intuition about binding energy and binding specificity. The structure of the bacterial K^+ channel, KcsA, readily explains these properties. The puzzling feature of the gate is how it can be controlled, and, in different channels, apparently controlled by all the known stimuli including ligands, second messengers, voltage, heat, and mechanical force. To more clearly summarize our current knowledge of cation channels, this review will first give a global view of the KcsA

channel and then proceed with the description of its filter, its gate, and its lipid environment.

1. KcsA at a glance

Most cation-specific channels, including K^+-, Na^+-, Ca^{2+}-, and the cation-nonspecific TRP channels, have a similar structural motif. Each channel has four subunits, converging to enclose the ion pathway. The first K^+ channel with high-resolution crystal structure is KcsA of *Streptomyces lividans* (80). The primary structure predicts each subunit of the tetramer to have, at its core, a TM1-P-TM2 arrangement, comprising two transmembrane helices (TM1, TM2), flanking a short "pore helix" and the filter sequence (together referred to as P) (Fig. 5a). Note that the well-known crystal structure of KcsA was that of its core (80) but not the entire KcsA peptide. Even in this simple channel, there is an additional helix upstream of TM1 and one downstream from TM2 (60). The simplest K^+ channels with only TM1-P-TM2 are found in certain viruses. As shown below and in Figure 5, a common motif of K^+ channel subunits is TM1-TM2-TM3-TM4-TM5-P-TM6, where TM5-P-TM6 is structurally and functionally homologous to the TM1-P-TM2 of KcsA. Genes predicting TM1-TM2-TM3-P-TM4 are found in prokaryotes (190). Two pore-domain K^+ channels each with two TM1-P1-TM2-TM3-P2-TM4 subunits are found in animals (292, 293); those with two TM1- TM2-TM3-TM4-TM5-P1-TM6-TM7-P2-TM8 are found in fungi. Genes predicting K^+-channel subunits with 12 TMs and 2Ps are also found in ciliates (see below) (187).

The KcsA tetramer is shaped like an inverted teepee (Fig. 6, *a–c*). The periplasmic side has a diameter of ~40 Å, the cytoplasmic side ~25 Å. The portion embedded in the lipid is ~35 Å long. TM1 transmembrane domains are the outer helices facing the lipids. TM2 domains are the inner helices, the COOH-terminal ends of which form the gate at the cytoplasmic side. Between TM1 and TM2 is the short "pore helix" cradling the ion-selective filter located towards the periplasmic side of the channel. The KsA protein has two belts of aromatic amino acids, positioned to extend into the lipid bilayer near the lipid-water interface (Fig. 6e). The one towards the outside includes a cuff that surrounds the selectivity filter (80).

A) THE K^+ FILTER OF KCSA. To restate, the channel resembles an inverted teepee, with the gate closing towards the cytoplasmic end, and the filter located at the other end. The K^+-filter sequence TXGY(F)GD is the most evolutionarily conserved sequence in the protein and is used as the diagnostic feature for K^+ channels from all sources. In the tetramer, the four successive layers of carbonyl oxygens from the residues in the signature GYG sequence (residue 77–79 of KcsA) face inward, lining the filter (Fig. 6D). In KcsA, these oxygens are held in positions to provide the coordinates for the naked K^+ in transit (80, 414). Five sites of K^+ coordinations can be recognized, site 0 to site 4, counting from the outside. Since this coordination is essentially the same as that by water, these oxygens act as surrogate waters allowing the passage of dehydrated K^+ through the filter to be nearly energetically costless, much like K^+ diffusing through water, exchanging its hydration shell. The spatial geome-
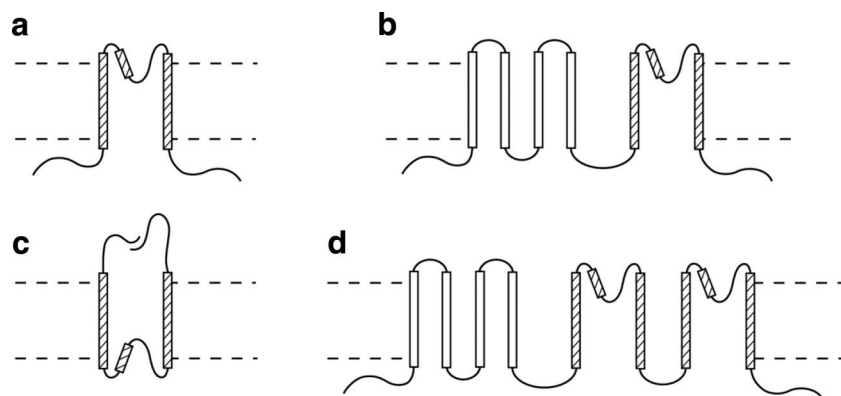

FIG. 5. Topologies of K^+ channel subunits. Each channel is a tetramer in forms of a, b, or c, or a dimer of d. *a*: A simple form of the subunit comprises two α-helices (TM1 and TM2, left and right rods) that traverse the membrane (marked with broken lines, separating the outside above and the cytoplasm below). Between the two are the pore helix (short rod) and the filter sequence (line between the pore helix and TM2). Certain viral K^+ channels, KcsA, Kir, MthK, TvoK, have this topology, though helices preceding TM1 or trailing TM2 exist (not shown) in some of these channels forming structures in the cytoplasm. *b*: A common form of subunit comprising 6 transmembrane helices, in which the last two helices and the pore helix (TM5-P-TM6, right portion) form the permeation and filtration core, similar to the structure in *a*. The preceding four helices (TM1–TM4, left portion) form a separate domain, housing other structures, such as the voltage sensor. This 6-TM motif is found in KvAP, MVP, KvLm, Kch, MloK, and MmaK. The subunit of the bacterial Na^+ channels, NaChBac, also has this structure, although it has a slightly altered filter sequence. *c*: The subunit structure of GluR0, a prokaryotic glutamate receptor. The pore helix and the filter sequence are arranged in the direction opposite that of *a*. The portion outside the membrane forms the glutamate-binding site. *d*: The subunit structure of TOK1, the K^+ channel of budding yeast. Here the first four TM helices are followed by two core structures, each similar to that in *a*.
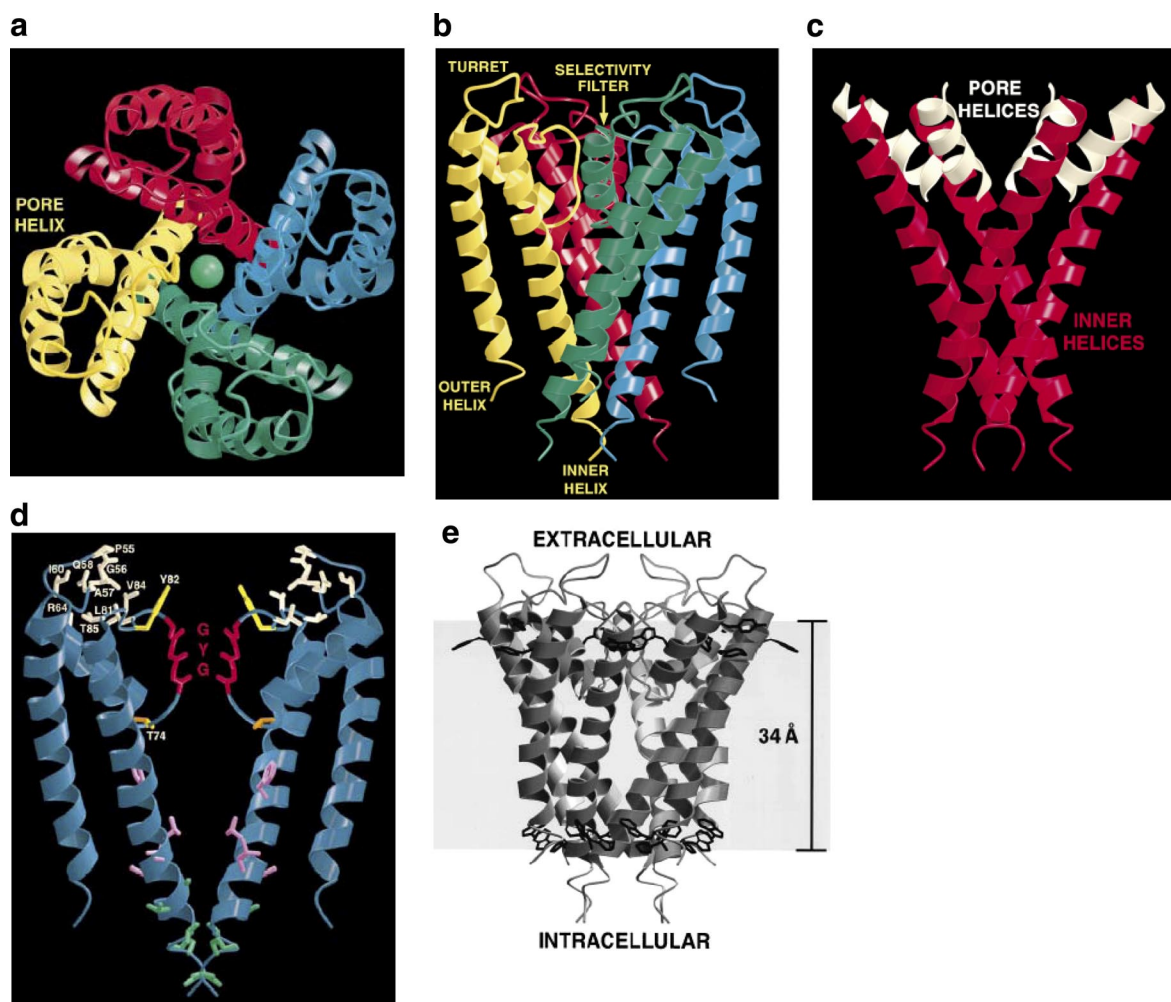
FIG. 6. The crystal structure of KcsA. KcsA is a homotetramer of subunits each with a TM1-P-TM2 core as diagrammed in Fig. 5a. a: Viewed from the outside, with each subunit represented in one color and a K^+ at the center. b: Side view of the membrane-embedded portion of the channel in form of an inverted teepee. Each subunit comprises an outer transmembrane helix (TM1), a short pore helix (P), and an inner transmembrane helix (TM2). Between TM1 and P are residues facing the outside (up), forming a turret. Between P and TM2 is the filter sequence. c: Same view as b, but with the outer TM1 helices removed to show more clearly the inner TM2 helices (red) and pore helices (white). d: The tetramer with the front and back subunit removed to show clearly the turret (white), the filter (GYG, red), and gate region (green). e: Side view of the KcsA tetramer, giving dimension, and showing the two belts of aromatic amino acids facing the membrane (black). [From Doyle et al. (80). Reprinted with permission from AAAS.]

try of these coordinates does not fit other cations such as Na^+ or Ca^{2+}, let alone anions, the passage of which is therefore energetically costly. Thus the crystal structure of this K^+ filter neatly solves the age-old puzzle of how the filter can be specific and efficient at the same time. In the three-dimensional structure, the ion filter is located near the outer surface of the membrane and is held in place by bonds between the amino acid residues in the filter sequence and those in the pore helices, including a network of aromatic-aromatic bonding (80). The conceptual separation of specific permeability to K^+ and Na^+ that form the foundation of membrane excitability and therefore neurophysiology has been formulated for more than half a century. It is ironic that the puzzling basis of ion specificity is finally solved in concrete terms with a channel

from a "lowly" bacterium, and its true function in the life of the bacterium is unknown.

Compared with the gate that makes major movement (below), the filter is often viewed as a fixture. However, the filter is far from static. Its conformations are determined by the number and nature of the occupying ions (77) as well as the bonds between its constituent amino acid residues and those of the surrounding pore helices (56, 278). For example, the activation of KcsA is naturally followed by an inactivation (56), akin to the so-called "C inactivation" of other K^+ channels. (Inactivation means the loss of channel current while the conditions of activation are maintained.) This inactivation occurs when the gate remains open (298) and explains why the observed open probability of KcsA is so low. Apparently, in the

conducting state, the network of hydrogen bonds between the filter sequence and the pore helix has the tendency to drive the filter into a new and nonconductive conformation. Chakrapani et al. (2007) models this network of bonds as a spring, set on the filter to balance the activated and inactivated conformations (42). The network includes bonds between charged residues, explaining why the entry into the inactivated state is voltage dependent (42, 43). A nonconductive conformation of the filter is observed when KscA was crystallized in a low K^+ concentration. This conformation likely corresponds to in vivo state when the bottom gate is closed (below) and the filter is facing a lumen of low $[K^+]$ (414). When there is no K^+ to occupy the filter, it collapses. This property explains C-inactivation, the voltage dependence of KcsA channel (149, 324), and the dependence on K^+ driving force in the case of the yeast TOK1 K^+ channel (219) (below).

Many variants of the filter were found in a survey of 270 K^+-channel sequences (190, 192). Instead of the usual TVGYG found in the KcsA filter, genes predicting channel subunit with TVGDG and TVGDA filter sequence, but otherwise similar to KcsA were found in *Bacillus cereus* and *B. anthracis*, respectively. The former channel protein has been crystallized and its structure solved (347). It shows that K^+ coordination sites 3 and 4 are like those of KcsA, but sites 1 and 2 have become a vestibule where cations cannot bind specifically. Competition experiments of $^{86}Rb^+$ flux showed that K^+ and Na^+ compete, but Li^+ or N-methyol-D-glucamine$^+$ does not. Such channels are now called NaK channels. A molecular dynamics simulation indicates that the lack of selectivity of NaK reflects the differences in hydration of the ions in the filter (278).

B) THE KCSA GATE. Except in the filter, the K^+ in transit is surrounded by shells of polarized water molecules. Correspondingly, except in the filter, the pathway is lined largely with hydrophobic amino acids of four TM2 inner helices, preventing the lingering of the hydrated K^+. The ion pathway of the filter is connected to a gate near the opposite surface facing the cytoplasm. The gate of KcsA is formed by the convergence of the four TM2 helices that are slightly tilted and kinked (80). These helices come into contact at the point near the bundle crossing to occlude the ion pathway in the closed conformation. In KcsA, the contact is at residue 112–119, at the COOH-terminal end of TM2 (31, 80). Near the center of KcsA's TM2 is glycine, which acts as the "gating hinge," allowing the COOH-terminal half to move. The gate likely opens at the hinge and by rotating the TM2 helices counterclockwise away from the central axis. There are concerted movements of the TM1 helices as well (31, 298). As described below, various "gating principles" (physiologically relevant ligands, voltage, stretch force, etc.) are believed to dilate the gate by moving the COOH-terminal ends of the inner helices outward. Note that parts of the NH$_2$- and the COOH-terminal sequence are not represented in the KcsA crystal structure. EPR spectroscopy shows that the NH$_2$-terminal peptide forms a helix lying at the membrane-water interface, and the COOH-terminal peptide forms a helical bundle in the cytoplasm (60). The functions of these helices are unclear.

The movement of the gate and the dynamic filter, which is often referred to as the "second gate," accounts for complex kinetic behavior, even for a relatively simple channel like KcsA (11, 42, 43). In general, a channel rarely visits its open state without a stimulus, which is referred to as the "gating principle" in channel biology. In the case of KcsA, proton opens the channel in the laboratory, although the physiological significance of this pH gating in vivo is unknown. In this case, pH apparently affects both the inner gate as well as the filter (42, 43, 55). Opening and closing of the gate entail a concerted movement of the inner helix (TM2) and the outer helix (TM1) that interact in a hand-and-handle manner (see below).

C) THE LIPIDS AROUND KCSA. Unlike soluble proteins, ion channels reside in the membrane and function to ferry ions across the lipid bilayer, a special environment. There is obviously an intimate relation between channels and their surrounding lipids. The KcsA tetramer is more stable in lipid bilayer compared with detergent micelles. In NMR studies, KcsA dissociating organic solvent has a large effect on the acyl-chain ordering, suggesting that the bilayer stabilizes KcsA by the lateral pressure in the acyl chain region (377, 378).

Two types of protein-lipid interactions can be distinguished: annular or nonannular. Annular interactions occur between the embedded portion of protein surface and the surrounding lipids. Nonannular interactions entail tighter association of the lipid into crevices between transmembrane helices. Such a tightly bound lipid often acts like a subunit or cofactor of the protein. Valiyaveetil et al. (376) showed in a KcsA crystal that there are four lipid molecules, each located between two subunits at the part of the channel that faces the periplasmic side. This is surprising because the KcsA protein examined here has been purified and crystallized in detergent with no added lipids. Note that the conditions required for crystallization are extremely harsh. Cocrystallization indicates specific and strong binding. The head group of the bound lipid was not resolved, but biochemical analyses showed that the lipids are likely phosphatidylglycerol (PG), even though the *E. coli* membrane, in which the KcsA is produced, has more of the neutral (zwitterionic) phosphatidylethanolamine (PE) than the anionic PG. The head group is apparently held in place by nearby arginines and its fatty acid tails wedged into crevices formed by helices from adjacent subunits. Fluorescence quenching experiments largely agree with these findings. They showed that charged interaction is crucial in this nonannular binding

(4). The nonannular binding constant of PG was determined to be ~3 mole fraction^{-1}, corresponding to ~40% occupancy by PG in the *E. coli* membrane (233). The details of arginine-lipid binding are revealed in a molecular dynamics simulation (73). Using ^{86}Rb$^+$-uptake to assess KcsA function in reconstituted lipid vesicles, Valiyaveetil et al. (376) showed that uptake occurs in vesicles containing negatively charged lipids (3PE:1PG) but not in those with only neutral lipids (3PE:1PC). It seems likely that this functional requirement of PG is at least in part to fulfill the binding seen in the crystal structure (376). Mass spectrometry by others showed that KcsA forms noncovalent complexes preferentially with PG, less so with PE but little with PC (71). In a separate assay, Valiyaveetil et al. (376) investigated the requirement for KcsA refolding. KcsA is a very stable tetramer, requiring organic solvents to unfold into monomers. They found that lipids are required to refold the monomers into functional tetramers (376). Here the lipids apparently do not act as cofactors, but provide the bilayer environment. Negatively charged lipids are not required for the refolding.

Unlike KcsA, purification and crystallization of Kv1.2, an animal voltage-gated K$^+$ channel (below), required a mixture of phospholipids and detergents (210). When channels are crystallized in a lipid-detergent mixture, many lipids surrounding the channel can be resolved or partially resolved. A hybrid voltage-gated K$^+$ channel has been shown to be surrounded by 64 lipids, 16 per subunit. These lipids are organized in two layers, reminiscent of the membrane. The outer layer, especially, resembles the outer leaflet of the bilayer. The lipid heads are not at the same level, and the tails wedge between proteins filling up space. It appears that the protein-lipid interaction displaces the lipids from their position in the pure lipid bilayer (212).

The more general interactions between the channel protein and the surrounding annular lipids are more difficult to investigate. Such lipid-protein interactions are less likely to survive the harsh condition of crystallization and cannot be revealed by crystallography, especially not in proteins purified through detergents. In fluorescence quenching experiments, annular binding at the periplasmic side of KcsA was found to be nonspecific with respect to the lipid's head group charge. Binding of anionic lipids are stronger at the cytoplasmic side, however, reflecting the pattern of surface charge distribution of KcsA itself (233). In a molecular dynamics simulation (73), the channel protein reduces the lateral mobility of the lipids that dynamically interact with its surface, reducing their diffusion to half the rate of the bulk lipids in the bilayer. About 30 lipid molecules contact KcsA with their head groups, which include the glycerol and the acyl oxygens. About 40 make contact with their acyl tails. Interactions, defined as protein-lipid interatomic distance being ≤3.5 Å, are concentrated in two broad bands (~10 Å) that level

with the two interfaces of the bilayer. Few contacts are made near the bilayer's center, reflecting the mobility of the acyl tails.

Most membrane proteins of known 3-D structures have aromatic belts at the interface, because aromatic amino acids favor this location (390, 397). Such belts apparently stabilize the protein structure and may play roles in membrane-protein folding (390) and possibly in conformation changes (78). Tryptophan and tyrosine, amphipathic aromatic residues, are found to form bands on membrane proteins at levels corresponding to the interfaces (390, 397). Experiments showed that, when properly placed, they help transmembrane peptides to resist dislocation and are thought to anchor membrane proteins to the bilayer. As summarized above, KcsA has two such belts of aromatic amino acids (Fig. 6E). In simulation, the aromatic rings of KcsA are found to be roughly normal to the bilayer plane, with the polar moieties (the ring nitrogen of Trp and the hydroxyl of Tyr) nearest the membrane interfacial region. So oriented, these aromatics apparently have their polar regions interacting with the lipid head groups and their hydrophobic region with the lipid tails. Basic residues, arginines in the case of KcsA, are also seen to form hydrogen bonds with the lipid phosphates, mostly at the intracellular interface (73).

2. K$^+$ channels with additional modules

A tetrameric assembly of subunits each with an inner transmembrane helix, a short pore helix, filter sequence, and an outer transmembrane helix is apparently the core of all K$^+$ channels. This core motif is found in other cation channels including Na$^+$ channels, Ca^{2+} channels, cyclic nucleotide-gated (CNG) channels, and TRP channels. It is likely an early evolutionary design, onto which later embellishments can be added. Such embellishments include voltage-sensing domain, glutamate-, Ca^{2+}-, or cyclic nucleotide-binding domains, etc. It illustrates that, like other proteins, channels are modular, and the permutation of modules yields the diversity we see in the biological world. The modularity of channel's construction is not only evident by surveying existing channel variations, but has been shown in two experiments.

KcsA with the TM1-P-TM2 structure is activated by a proton. On the other hand, the subunit of the depolarization-activated *Shaker* channel comprises six TM helices with a TM5-P-TM6 core similar to KcsA. Lu et al. (221) conferred voltage sensitivity to KcsA by adding the segment TM1-TM4 of *Shaker* to the TM1-P-TM2 sequence of KcsA. The juncture between the two moieties apparently needs to be precise for the chimera to function in a voltage-dependent manner. The graft needs to include both the TM4-TM5 linker as well as the lower end of TM6 from *Shaker*. As revealed later by the structures of voltage-gated KvAP (148) and Kv1.2 (210, 211), the TM4-TM5

linker acts as the "hand" and the lower end of S6 receptacle acts as the "handle" of the gate. Because the hand-and-handle interaction is stereochemically specific, they need to be homologous. This set of experiments illustrates the modular principle of channel construction and anticipated some of the conclusions derived from crystal structures.

The modularity of K^+ channel construct is also evident in the chimera experiment by Ohndorf and Mackinnon (282). They added cyclic nucleotide-binding domain (CNBD) of *Rhodopseudomonas palustris* to the COOH-terminal ends of KcsA's inner helices and showed that the construct opens upon the addition of cAMP. As described below, CNBD is a module in the cytosol and is attached to the membrane-embedded core at the end of its inner helix directly by peptide linkage. Here the force that opens the gate is presumably directly transmitted through this linkage and not by a hand-and-handle mechanism of the voltage-gated channels.

A) CNMP-GATED K^+ CHANNELS (MLOK, MMAK). Several K^+-channel cores trailed by sequences of CNBD can be found in α-proteobacteria and a cyanobacterium (190, 192). A 6-TM K^+ channel (Fig. 5B) with CNBD from *Mesorhizobium loti*, MloK1, has been expressed, and its $^{86}Rb^+$ flux shown to be activated by cyclic nucleotide (274). The crystal structure of MloK1's CNBD has been solved (53). In this structure, the CNBD domains are in forms of dimers, leading to the proposal that the gate operates possibly as a dimer of dimers. A recent electron microscopy structure of the entire MloK1 protein, however, found that each CNBD in the tetramer to be independent, supporting the mode of gate opening by cyclic nucleotide (cNMP) similar to that in the animal CNG or HNG channels (50). MloK1 continued to be analyzed functionally with $^{86}Rb^+$ flux but not by electrophysiology (273). A cNMP-gated channel, MmaK, from the gram-positive bacterium *Methanobacterium thermoautotrophicum*, has recently been cloned and expressed in *E. coli* (191). Here, the authors generated giant *E. coli* spheroplasts (see sect. IC), excised membrane patches from them, and examined the electric activities of MmaK therein. Both macroscopic and microscopic currents can be observed. Activation by cNMP and inactivation by acidic pH are evident. The growth of *E. coli* expressing *mmaK* is suppressed by the external addition of K^+ but not Na^+. This K^+-specific phenotype should make future genetic dissection of MmaK promising.

B) RCK-OPERATED K^+ CHANNELS (MTHK, KCH, TVOK). In eukaryotes, Ca^{2+} actuates the changes in actin-myosin and dynein-tubulin based motility. This key second messenger also controls secretion, fertilization, and many important animal functions. Like many enzymes, some ion channels are also directly controlled by Ca^{2+}. Ca^{2+} binding inactivates some channels but activates others. Channels that are opened by Ca^{2+} are found in archaea and bacteria, although they seem to require much higher concentrations of Ca^{2+} than the eukaryotic channels do.

MthK, a Ca^{2+}-activated K^+ channel of the archaeon *Methanobacterium thermoautotrophicum*, has been crystallized and its structure in an open conformation solved (147). In its primary structure, each MthK subunit has the TM1-P-TM2 sequence (Fig. 5A) followed by an extension of some 200 amino acid residues. These residues form a module that contains the Rossmann fold, which has a scaffold of α-helices and β-sheets in a dimeric arrangement. This fold has a key sequence, GXGXXG, indicative of NAD binding. Such modules are found in many K^+ transporters or K^+ channels in a variety of prokaryotes and is called the KTN (K^+ transport and NAD-binding) domain (324, 325). A related structure, called the RCK (for regulator of the conductance of K^+) domain, retains the $\alpha\beta$-scaffold and the dimeric arrangement without the GXGXXG. Instead of dinucleotides, RCK of MthK binds divalent cations, such as Ca^{2+} (147, 149). KTN or RCK assembles in pairs, and the ligand (dinucloetides or Ca^{2+}) is coordinated at the dimer interface.

Surprisingly, besides the full-length 200 kDa *mthk* gene product, purified MthK channel protein contains a 26-kDa peptide, indicative of translation from an internal AUG. This smaller peptide corresponds to a free RCK domain. The crystal structures (147, 149) and other studies led to a model in which the channel is a hetero-octamer, with the MthK transmembrane tetramer assembles with eight RCK domains: four covalently linked to the four TM2 helices and four additional ones assembled onto them at the cytoplasmic side. The crystal was formed in the presence of 200 mM Ca^{2+} and eight Ca^{2+} found coordinated in clefts between adjacent RCK domains. MthK reconstituted into lipid bilayers can indeed be activated by Ca^{2+}. It was proposed that the eight RCKs form a preassembled gating ring. Ca^{2+} binding changes the conformation of the "gating ring" generating the outward force to pull apart the converged ends of the four TM2 helices, through a 17-residue linker not resolved in the crystal structure. However, there are reasons to question the need of the free RCK domains in gating from the studies of other RCK-bearing bacterial channels (193, 314). Recently, the MthK activities were examined in patches excised from *mthK*-expressing giant *E. coli* spheroplasts (191). Besides Ca^{2+}, Cd^{2+} also activates this channel. MthK desensitizes in the continued presence of these ligands and inactivates in acidic pH. Unlike the "gating-ring" model, biochemical studies of isolated RCK domains showed that they are dimeric in acid pH, regardless of Ca^{2+}. In basic pH, however, they convert from monomers to multimers upon the addition of Ca^{2+}. These findings led to another model in which multimerization is a part of the gating mechanism (191). The physiological meaning of this activation with millimolar Ca^{2+} is unclear,

since Ca^{2+} as a second messenger operates at micromolar concentrations in eukaryotes, and the signaling roles of Ca^{2+} in prokaryotes, if any, are uncertain.

An RCK-containing K^+ channel from the archaeon *Thermoplasma volcanium*, TvoK, has recently been cloned and reconstituted into planar lipid bilayers for functional analyses (289). The 160-pS K^+ conductance was found to be activated by millimolar Ca^{2+} or Mg^{2+}. The molecular mass and subunit composition of TvoK are consistent with the hetero-octameric structures proposed for MthK.

In 1994, Milkman (247) recognized a gene in *E. coli* that corresponds to a K^+ channel, called Kch, because it predicts six transmembrane helices (Fig. 5*B*) similar to the *Shaker* channel of *Drosophila*. Its TM6 is attached to an RCK domain, which was later isolated and crystallized, solving the first RCK structure (149), though its potential ligand is yet to be identified. The electric activities of Kch have never been reported, despite various attempts. However, genetic experiments indicate the Kch does function in vivo. Kuo et al. (2003) isolated GOF *kch* mutants that failed to grow in millimolar added K^+ but not Na^+ (193). This K^+ susceptibility phenotype vanished when the canonical K^+ filter sequence is further mutated, showing that it is the passage of K^+ that kills cells. All seven GOF mutations selected with this phenotype after a random mutagenesis were found to be in the RCK domain. Removing the internal ATG of the GOF mutants does not change the phenotype, indicating that the corresponding free RCK is not needed for K^+ passage in vivo. External H^+ suppresses the GOF phenotype. This observation supports a model that Kch is not for bulk K^+ uptake, but functions to regulate membrane potential under certain stress (189, 190, 193).

C) VOLTAGE-GATED CHANNELS (KVAP, MVP, KVLM). The intellectual history of ion channel is rooted in the study of the excitable membrane. A big step forward was the separation of the regulated rise and fall of Na^+ and K^+ permeability that underlie the generation of action potential axons in the 1950s. Voltage-clamp experiments show that the specific channels involved are governed by membrane voltage. The material basis of the permeability was not firmly established until the cloning of channel genes. A *Drosophila* K^+-channel mutation, *Shaker*, presents an overexcitation phenotype, leg shaking even under anesthesia. Cloning and heterologously expressing the *Shaker* gene in 1987 set another milestone in channel biology. The *Shaker* product is predicted to comprise six transmembrane helices (Fig. 5*B*). TM5-P-TM6 is now recognized to be similar to the KcsA core structure, described above. The fourth, TM4, bears positively charged residues spaced regularly at every third residue and is now well established to be the voltage sensor (41). These charges following voltage changes move to drive the channel to open or close. The movement of these "gating charges"

has been measured biophysically long before their structural bases are understood. Much of our knowledge on how voltage drives open the gate is derived from the crystal structure of archaeal KvAP and the animal Kv1.2 solved by the MacKinnon laboratory (148).

KvAP is a depolarization-activated K^+ channel of the hyperthermophilic archaeon *Aeropyrum pernix*. Like the *Shaker* channel, each KvAP subunit comprises six transmembrane helices (Fig. 5*B*), with TM4 bearing the gating charges and the canonical K^+-filter sequence. The TM5 and TM6 flank the pore helix and the filter sequence. In the tetramer, they converge to enclose the pore and form the filter, much like the TM1 and TM2 of KcsA (148). This portion is therefore the core, or the permeation domain of the protein. TM1 through TM4 of each subunit forms a separate domain, surrounding this core. In this structure, TM1 and TM2 are near the TM5-P-TM6 core with the TM3 and TM4 at the periphery. There is surprisingly little direct contact between the core and the four peripheral domains, considered the voltage-sensing domains. This modular arrangement has been anticipated by a chimera experiment described above, in which a precise grafting of *Shaker*'s voltage-sensing domain onto the core of KcsA confers voltage sensitivity (221). Purified KvAP has been incorporated into planar lipid bilayers and found to correspond to a K^+-specific unitary conductance of 170 pS. Its macroscopic current is found to be activated by depolarization (327).

The current understanding of voltage sensing, based on the structures of KvAP and Kv1.2, is as follows. The voltage sensor is an electromechanical coupling device, allowing the transmembrane voltage to bias the conformation of the domain. The sensor consists of the voltage paddle and the S1-S2 region with which the paddle interacts. ("S," same as "TM," is used here to make easier the narrative and reference to the original papers) The voltage paddle is a helix-turn-helix structure comprising S3b (the COOH-terminal portion of S3) and S4 helices running antiparallel (3). S4 bears positively charged arginines spaced 3 residues apart, named R0, R1, etc. counting from the NH_2 terminus. Seen in the open state, the paddle is located near the outer surface, with one side facing the lipids, and the other side resting on the outer half of S1 and S2 helices, with R0, R1, and R2 interacting with the phosphoester head groups of lipids, and R3 and R4 with a cluster of glutamates of surrounding helices, including S2 (212). The position of the paddle in the closed state is uncertain, since there is no clear closed state structure as yet. Accessibility and other studies suggest that the paddle translates inward, moving all the gating charges beneath a S2 phenylalanine at the midpoint (212).

In the KvAP structure, the voltage-sensing paddle lies along the membrane plane positioned at the inner lipid-cytoplasm interface. The detergent used apparently distorted the native structure (200). The resolution of Kv1.2,

a *Shaker* homolog from rat brain, amended the KvAP structure (210, 211). Here, the TM1-TM4 module remains outside the core, but with the TM3-TM4 voltage-sensor paddle erected, crossing the bilayer. TM4 is seen as a long helix with its NH_2-terminal side bearing the regularly spaced arginines. At its COOH-terminal end, it connects to a helical S4-S5 linker through a bend. Raising the paddle from the position in the KvAP crystal fits the Kv1.2 structure almost perfectly. Long et al. (212) recently showed in the crystal of an open-state Kv2.1-Kv1.2 chimera, formed in lipids and detergent, that the voltage paddle tilts outward, with one entire face exposed to the lipids. It is postulated that the paddle moves between this outward and an inward position upon voltage changes to drive the conformation (state) changes of the protein. The S4-S5 linker is an amphipathic helix running parallel to the membrane plane on the cytoplasmic side. It crosses over TM6 and makes many amino acid contacts with TM6's cytoplasmic end. In the open state, TM6 bends at a hinge near the region of contact to be nearly parallel with the membrane, forming the "handle" for the S4-S5 linker. The presumed flexible hinge allows the lower end of TM6 to dilate or constrict the pathway. In many voltage-gated K^+-channels, the hinge is a glycine (e.g., KvAP) as in KcsA and KirBac; in others, it is the sequence Pro-X-Pro (X being any residue, e.g., Kv1.2). By analogy, the S4-S5 linker can be viewed as the "hand" and the COOH-terminal end of TM6 the "handle," such that the gating force from the movement of TM4 is transmitted to the TM6 bundle crossing.

Alabi et al. (3) recently showed that voltage paddle is itself a portable domain. When the portion from the junction between S3a and S3b to just past the first four critical Arg residues of S4 from KvAP replaces the comparable portion in Kv2.1, the chimera channel retains voltage sensitivity. Different tarantula toxins attack different voltage-sensitive channels specifically. The chimera shows sensitivity to the toxin that is specific for KvAP. Note that the voltage paddles of KvAP and Kv2.1 are not very similar in sequence. Therefore, this work not only shows that the voltage sensor is modular, but also that the paddle is not packed tightly with other protein domains forming extensive bonds. It appears to be in a relatively unconstrained environment, most likely the lipids. Nature uses this voltage-sensing module in a different context. Besides these K^+ channels, they are found in the voltage-activated proton channel (Hv1) (319, 336) and the voltage-sensitive phosphatase of *Ciona* (Ci-VSP) (258).

A gene homologous to *Shaker* and relatives is found to encode MVP, a hyperpolarization activated 37-pS K^+ channel from the archaeon *Methanococcus jannaschii* (344). *MVP* transgene complements the K^+-uptake defects of both mutant *E. coli* (133) and yeast (344). Although MVP responds to hyper- instead of depolarization, it is modeled to have the same S4 movement, but S4's cou-

pling with the gate is such that the S4 position corresponding to open in *Shaker* is close in MVP.

A survey shows that there is a far greater variation in the S4 gating charges among prokaryotes than in animals. S4's with as little as one and as many as eight charges can be found (192). KvLm, the *Shaker*-type channel from the gram-positive bacterium *Listeria monocytogenes*, with only the three of the positively charged S4 residues has been investigated. Expressed and examined in giant *E. coli* spheroplasts, the open probability of KvLm nonetheless shows a steep dependence on depolarization (335). Further mutational investigation shows that the voltage sensor of KvLm likely has a structure similar to that of animal *Shaker* channels (224).

D) INWARD RECTIFIERS (KIRBAC). Inward rectifiers are K^+ channels that behave like diodes. They open when the membrane is polarized or hyperpolarized, allowing K^+ to enter the cell, but the open channel is blocked by internal Mg^{2+} or polyamines when the polarity is reversed to prevent K^+ exit. Durell and Guy (82) recognized a family of prokaryotic inward-rectifier K^+ channels (KirBacs) by sequence similarity to eukaryotic homologs, including the sequence of the large COOH-terminal region unique to inward rectifiers (82). KirBacs are found in many species of *Burkholderia*, *Magentospirillum magnetotacticum*, *Nostoc punctiforme*, (82) *Synechocystis sp.*, *Ralstonia solanacearum*, *Solibacter usitatus*, *Chromobacterium violaceum* (369), and others. The crystal structure of KirBac1.1, the inward rectifier channel from the bacterium *Burkholderia pseudomallei*, has been solved in a closed state by Kuo et al. (189). Like the full-length KcsA, a "slide helix" at the NH_2 terminus positioned at the level of the lipid-water interface, precedes a TM1-P-TM2 core (Fig. 5*A*). The slide helix apparently interacts with the phospholipid head groups (76). In this crystal structure, the core of KirBac1.1 is similar to that of KcsA, except that the pore helices do not point at the center of the channel, a feature considered a key to the closed channel here. The structure of the filter is largely the same as KcsA. Similar dynamics of the filter are seen in a molecular dynamics (MD) simulation (73). This core is trailed by a large COOH-terminal cytoplasmic domain, which is made of β-sheet structures and contains the putative Mg^{2+}-biding glutamate residues. Although the core is in a fourfold radial symmetry, the cytoplasmic domains are in forms of a dimer of dimers. The channel closes at the end of TM2, forming a hydrophobic seal by the convergence of phenylalanines. The inner helix (TM2) of KirBac1.1 has a hinge glycine like in KcsA. Channel opening is modeled to be a concerted outward movement of the slide helices and the TM1 helices, making room for the TM2 helices to bend at their glycine hinges. This notion is further supported by the electron crystallography of two-dimensional crystals of KirBac3.1 of *M. magnetotacticum* in two conformations at 9-Å resolution (188). In a molecular dynamics

simulation, aromatic residues appear to be more evenly distributed in the closed state but shift toward lipid-water interface, suggesting that aromatics preference to be at the interface is being used in gating or conformational stabilization (78).

Sun et al. (369) tested a large number of KirBacs for their ability to complement the K^+ auxotrophy of a TK strain of *E. coli* lacking the three major K^+ uptake mechanisms (Kdp, Trk, Kup). Some of them complement; some complement less well at a higher temperature; some do not complement. The results show differences among KirBacs in their ability to take up bulk K^+ in this heterologous setting.

A current topic in animal channel physiology is the modulation by phosphatidylinositol 4,5-bisphosphate (PIP_2). Pure KirBac1.1 and KcsA have been reconstituted into liposomes of defined lipid composition and assayed for $^{86}Rb^+$ uptake. KcsA is not affected but Kir. Bac1.1 is inhibited by PIP_2. This result shows that there is a direct interaction between PIP_2 and KirBac, excluding modulation through cytoskeletal or other intermediary elements (91). The physiological significance needs to be addressed, since phosphatidylinositol has limited distribution and is in small amounts among bacteria.

E) GLUTAMATE RECEPTORS (GLUR0). GluR, glutamate receptors, bind glutamate or related neurotransmitters to open a cation conductance in excitatory postsynaptic membranes. Animal GluR are sorted into subfamilies depending on their ligands (NMDA, AMPA, or kainate). Each GluR is a tetramer. The core of each subunit of animal GluR consists of an extracellular region called S1 followed by the first transmembrane TM helix called M1, the pore P (with the filter sequence), the second TM helix M2, the second extracellular region S2, and a third TM helix M3. The external S1 and S2 form the glutamate-binding site. There are additional NH_2- and COOH-terminal domains up- and downstream of this core. A sequence homolog was found in *Synechocystis* PCC6803 that has the S1-M1-P-M2-S2 core, but lacks M3 and the additional NH_2- or COOH-terminal domains. It was named GluR0 (47). S1 is followed by TM1 beginning from the outside instead of the cytoplasmic side, thus placing the TM1-P-TM2 permeation and filtration core in an orientation opposite that of KcsA (Fig. 5C). Key residues for glutamate binding in animal GluRs are conserved in the S1 and S2 region of GluR0, and the corresponding protein overexpressed in *E. coli* has the expected ligand-binding properties. The pore region contains the perfect K^+-selectivity sequence TVGYGD identical to that of KcsA. GluR0 expressed in HEK cells or *Xenopus* oocytes indeed produce K^+-specific rather than cation-nonspecific currents, found to flow through animal ionotropic glutamate-receptor channels (47). The ligand-binding core of GluR0 was crystallized and its structure solved. This core consists of two domains separated by a deep cleft. The larger Domain 1 includes α helices A, B, C, from S1 and J, K, from S2. Domain 2 includes α helices F,C, H of S2. L-Glutamate, the ligand, binds in the cleft between the domains. The symmetry of the ligand-binding core suggests that the tetrameric channel is assembled from two dimers (243). A molecular dynamics simulation of GluR0 shows that concerted K^+-water move along the selectivity filter, as in the simulations of KcsA and the K^+ exit is associated with the opening of the hydrophobic gate formed by the M2 termini (8). GluR0 homologs can be found in other bacteria. Interestingly, those from *Prochloroccus marinus*, *Trichodesmium erythraeum*, and two species of *Synechococcus* have the canonical K^+-filter sequence, and those from *Silicibacter pomeroyi*, *Magnetospirillum magnetotacticum*, and two sequences of *Nostoc punctiforme* have the filter and pore sequences more like those of the cation nonspecific eukaryotic glutamate receptors (182). A preliminary X-ray crystallographic analysis of the one from *Nostoc punctiforme* has been reported (199).

B. Na$^+$ Channels (NaChBac)

The animal depolarization-activated Na^+ or Ca^{2+} channels are similar to K^+ channels in structure. However, each Na^+ or Ca^{2+} channel comprises 24 TM domains that are covalently linked, with each 6-TM repeat being comparable to a *Shaker*-type 6TM K^+-channel subunit. Although high-resolution structures are not yet available, the Na^+/Ca^{2+} channel filter is likely lined with four glutamic or aspartic residues. A 6-TM gene product from *Bacillus halodurans*, an extremophile that lives in high salt and high pH, has been expressed in mammalian cells and found to form a 12-pS channel that is activated by depolarization, followed by in- and deactivation. It is similar to L-type Ca^{2+} channel in being blocked by dihydropyridines, nifedipine, and nimodipine. However, this channel is selective for Na^+, not Ca^{2+}, and is named NaChBac (321). It is speculated that the Ca^{2+} selectivity may require a flexible tertiary structure around the acidic residues provided by the four nonidentical repeats in the animal channels, but are not provided by the NaChBac homotetramer (321). Mutational analyses showed that increasing the number of aspartic substitutions in the filter sequence (LESWAS) increases the Ca^{2+} selectivity. In the series of mutations LESWAD, LEDWAS, LEDWAD, and LDDWAD, the first has the lowest and the last the highest Ca^{2+} selectivity (404). The TM4 of NaChBac subunit bears arginine residues spaced every third residue apart, as in KvAP and Kv1.2 (321). The gating-charge movement of NaChBac has been studied electrically (197) and by real-time fluorescence spectroscopy (32). The acidic residues on TM2 and TM3 of NaChBac that likely neutralize the arginines of TM4 have also been mutated and analyzed (26). NaChBac has homologs in at least 11 other bacteria,

forming a family called Na_vBac. Two members, Na_vPZ from *Paracoccus zeaxanthinifaciens* and Na_vSP from *Silicibacter pomeroyi*, have also been expressed and examined in mammalian cells (169). A role in controlling the Na^+-driven flagellar motility for some Na_vBac channels has been proposed (321). Na_vBac channels appear to be a good source for material for crystallography towards a better understanding of Na^+ and Ca^{2+} filtration.

C. Ammonium Channel (Amt, Mep)

Ammonium channels have no relation to the K^+ or Na^+ channels described above. Transport of nitrogen is important to most organisms, since it is a major element in life and available nitrogen is often limited in the environment. Though toxic to animals, ammonium is used by prokaryotes, fungi, and plants as the preferred nitrogen source. Most cellular organisms have AMT/Rh family proteins to transport ammonium, except some parasites and those that use specialized nitrogen source, such as urea. Ammonium channels are called Amts (ammonium transporters) in the bacteria literature and Meps (methylamine permeases) in the fungal literature. They have some sequence homology to Rh, the Rhesus blood group antigens in human, which may function as CO_2 channels. *E. coli amt* mutants grow poorly in ammonium-limiting conditions. The AmtBs, the Amts of *Aquifex aeolicus* and *E. coli*, have been crystallized. Each was found to be a trimer, and each subunit comprises 11 transmembrane α-helices arranged in a twofold quasi-symmetry. Instead of three subunits enclosing a single pore, in the center of each subunit is a hydrophobic pore lined by two highly conserved histidines, which form hydrogen bonds. It is proposed that a ring of aromatic residues at the periplasmic entrance recruits and deprotonates NH_4^+. NH_3 remains uncharged because of the histidines and is then conducted and reprotonated at the cytoplasmic end (158, 407). There are debates on whether NH_4^+ or NH_3 is actually the substrate and whether Amt acts as a channel (195, 222). The confusion apparently originated from the practice of using the kinetics of substrate label accumulation in live cells to deduce mechanisms. Unlike more reduced systems, such as liposomes, ammonium in vivo is rapidly metabolized and assimilated into glutamine and other metabolites, vastly complicating the understanding of the very first step, i.e., how ammonium is taken up. A mutation of one of the putative recruiting aromatics at the *E. coli*'s AmtB (W148L) was recently found to be a GOF mutation that allows rapid accumulation of substrate consistent with a flux driven by electric gradient (98). These results question the role of the ammonium-recruiting role of the aromatics and erase some of the difference previously thought to exist between the bacterial Amt and the plant Amt. The latter has been investigated electrophysi-

ologically and shown to have classical channel characteristics (223).

D. Cl^- "Channels" (ClC-ec1)

Cl^- channels are entirely different from the cation channels described above. As with the cation channels, Cl^- channels were first studied electrophysiologically in animal cells. These studies showed that the Cl^- channel behaves as "double barreled", i.e., two ~8-pS units that can gate independently and rapidly (ms) as well as together and slowly (s). There is also a strong coupling between Cl^- conduction and gating. First cloned from the fish *Torpedo*, the animal ClC-0 has many homologs including those in bacteria, such as the enteric species of *Escherichia*, *Salmonella*, *Shigella*, *Vibrio*, and *Yersinia* (145). The ones from *Salmonella typhimurium* and *E. coli* (ClC-ec1) have been crystallized and their structures solved at high resolution (83). As predicted from the double-barrel gating, it exists as a homodimer. The two subunits meet at an extensive contact surface, but each has its own pore. Each subunit comprises 18 α-helices (A through R) arranged in two structurally similar halves. Helix A–G and helix H–R have only weak sequence homology, but are packed similarly. The two halves ran antiparallel, creating a pseudo-twofold symmetry, and wrap around a common center forming the Cl^--binding sites. The helices vary in length and are all tilted with respect to the membrane normal. It is so arranged that the NH_2 termini of helix D, F, N, and R, i.e., the positive ends of their helical dipoles, point into the central Cl^--binding site. In the crystals, a Cl^- or Br^- occupies this site coordinated by main-chain nitrogens and side-chain oxygens of nearby helices. This central binding site is connected through tunnels to the wider, water-filled vestibules, exposed to the intra- and extracellular solutions. Several crystal structures taken together show that the permeant anion likely passes through three binding sites, the central one being the one described above. All three sites have been seen occupied in various crystals with different anions (271). In the first set of crystals, just above the pseudo-twofold axis, Glu148 of helix F projects into the pore, blocking the presumed external Cl^--binding site. The crystallized form appears to be that of a "closed" channel. This glutamate residue likely swings out of the way in the open conformation to allow Cl^- passage. Mutation analysis indeed shows that the carboxyl group of this glutamate acts as a pseudosubstrate, occupying the external site to block passage (84).

Accardi et al. (1) succeeded in reconstituting pure ClC-ec1 into planar bilayer and made the surprising discovery that it acts like an exchanger rather than a channel. Only the macroscopic current of ClC-ec1 can be registered, with noise properties consistent only with very small unitary conductance (<0.1 pS). The current has no

voltage or time dependence, prominent in animal ClCs. Its reversal potential deviates significantly from the one expected from the Nernst's equation of Cl^- gradient and from the Goldman-Hodgkin-Katz equation of various Cl^- and H^+ gradients, but is consistent with the expectation of a strictly coupled transport of ~ 2 Cl^- for 1 H^+. Furthermore, either ion can be made to flow against its own electrochemical gradient. How H^+ is transported remains unclear. Glu148 is apparently crucial. E148A mutation causes ClC-er1 to allow Cl^- to flow down gradient and not to show the H^+-dependent transport. The exact mechanisms of ion permeation through ClCs are under investigation. The ClC-ec1 finding echoes a finding in *Paramecium*, where the XntA gene product behaves as channel in electrophysiology but shows an exchanger-like sequence (see sect. IV*A1*). The current understanding challenges the classical distinction made between ion channels and ion exchangers. Current literature now divides the animal ClCs into two classes: those in the plasma membrane (ClC-0, -1, etc.) acting as channels and those in vesicular membranes (ClC-4, -5, etc.), being more homologous to the bacterial ClCs, acting as antiporters. As to the role of bacterial ClCs, evidence supports the view that they are employed in the extreme acid-resistance response. In low-pH medium, the H^+ of the entered HCl is evicted by an amino acid decarboxylase and an electrogenic amino acid antiporter. ClC lets out Cl^- to maintain electroneutrality (145). A 100-pS unitary anion conductance in patches of the surface of giant *E. coli* spheroplast has been reported (178), but its molecular identity is unknown.

Cl^- channels exemplified by ClC are thus structured very differently from the cation channels such as KcsA. Nonetheless, some basic physicochemical principles, however, are conserved. For example, the filter binds the ions through partial charges instead of strong electrostatic forces, making possible specificity but not retarding passage. The dipoles of α-helices are employed to focus the electric field on the binding site (83).

E. Roles of Ion-Specific Channels in Prokaryotic Physiology

The role of Cl^- channel/exchanger in enteric bacteria is described above (145). However, the roles of the cation channels (KcsA, KvAP, MthK, KirBac, NaK, NaChBac, etc.) are unknown. Their roles in the native settings are sometimes difficult to investigate, since some are extermophiles, requiring special laboratory conditions for cultivation. Even more frustrating is the fact that we cannot yet fathom the roles in bacteria commonly studied in microbiology, including *E. coli*, *B. subtilis*, and *S. lividans* (132). In the study of the Kch GOF mutants of *E. coli*, external H^+ suppresses the ability of K^+ to block growth of these mutants. About a 10 times increase in $[H^+]$ suppresses the toxicity caused by a 10 times increase in $[K^+]$ on these mutants. This finding implies that the parameter being regulated has a logarithmic relation to $[K^+]$, probably the equilibrium potential of K^+ (E_K). *E. coli* growth depends on the proton-motive force Δp. Δp comprises membrane potential (V_m) and ΔpH, the pH gradient across the membrane. It is therefore thought likely that the GOF Kch channels open uncontrollably, locking the V_m near the E_K. When external $[K^+]$ is raised, E_K and therefore V_m are small and the total Δp is too small to sustain growth. Increasing external $[H^+]$ raises the ΔpH, compensating the loss of V_m and restoring growth in the GOF mutants. This work shows that Kch is apparently functional in vivo, in the sense that it can pass K^+ along its electrochemical gradient and that the membrane potential apparently controls it. If this model is correct, many prokaryotic K^+ channels, like Kch of *E. coli*, may function like their counterparts in animal cells. While the work of the *E. coli* GOF mutants is informative, it begs the question of the stimuli (stresses?) that normally opens the wild-type Kch channel. Extensive attempts fail to register the electric current through the membrane of giant *E. coli* spheroplasts, including those generated from the GOF mutants. Studies of $kch\Delta$ have failed to discover a clear Kch LOF phenotype in the laboratory (Kuo, Haynes, Saimi, and Kung, unpublished results). On the other hand, the widespread presence of K^+-channel genes in prokaryotic genomes clearly indicate the selective advantages they confer. More creative ways to simulate nature in the laboratory are needed to solve this puzzle.

The *E. coli* GOF mutant studies suggest, though cannot prove, that K^+ channel regulates membrane potential, like they do in animal cells. In plant roots, there is evidence that certain K^+ channels are used to take up bulk K^+. Interestingly, the MthK-like K^+ channel of *Helicobacter pylori*, called HpKchA, apparently serve such a function. *hpkchA*Δ mutant grows poorly at low K^+ concentration, but well when K^+ is supplemented. HpKchA is apparently required to colonize murine stomach (359). However, *H. pylori*, unlike free-living bacteria, are devoid of other K^+ uptake mechanisms. Bulk K^+ uptake is unlikely to play a role for K^+ channels in free-living bacteria, which invariably have several non-channel K^+ uptake mechanisms (193). In *E. coli*, three non-channel K^+ uptakers are well known (Trk, Kdp, Kup), which transport or scavenge K^+ when needed. $kch\Delta$ *E. coli* cells are not K^+ auxotrophic (193), and prior search for K^+ auxotrophs did not identify Kch.

IV. ION CHANNELS OF MICROBIAL EUKARYOTES

Research on ion channels focused largely on channels of vertebrates and larger invertebrates. These studies have greatly contributed to our knowledge of the role that ion channels play in the physiology of muscles and the nervous system. Research on microbial channels, on the other hand, offers a unique opportunity for answering questions on the evolution of ion channels as the microbes display large varieties of channels in their cellular membranes. This is best illustrated by the fact that the structures and biophysical properties of microbial channels exhibit variations not seen in plants and animals. The *Paramecium* genome, for example, reveals a 12-TM subunit of S1 S2 S3 S4 S5 P1 S6 S7 S8 S9 S10 S11 P2 S12 arrangement (190), whereas yeast has an 8-TM, two-pore-domain K^+ channel subunit of an S1 S2 S3 S4 S5 P1 S6 S7 P2 S8 arrangement (157, 413).

Ionic currents have been recorded from a number of microbial cells including *Dictyostelium* (slime mold) (256), *Chlamydomonas* (a green flagellate) (355, 399) *Paramecium* and *Stylonychia* (ciliates) (65, 67, 128, 262, 311), *Neurospora* (bread mold) (203, 323), *Uromyces* (a parasitic bean rust fungus) (412), and single-celled fungi *Schizosaccharomyces pombe* (fission yeast) (410) and *Saccharomyces cerevisiae* (baker's yeast) (114, 115). Although the functions of a number of ion channels in ciliates are well understood and interpreted using concepts developed in animal biology, the roles of most ion channels in eukaryotic microbes still remain to be elucidated. Given that fungi and protozoa are highly diverse and occupy widely different ecological niches, there is a great deal to be learned from studies of ion channels in these microorganisms. The yeast K^+ channel may illustrate the point. It is gated by the total K^+ electrochemical gradient instead of voltage, and this gate has been thoroughly dissected by genetic and biophysical means (218).

The fact that microbes can be genetically modified with relative ease provides significant advantages for functional studies of ion channels. In *S. cerevisiae* as a key experimental model gain-of-activity mutants have been isolated, the expression of which hampers growth (220). However, the loss of ion channel activities, as in the case of the knock-out mutants, does not necessarily always lead to a discernable phenotype in the laboratory. The inability to discern a laboratory phenotype indicates that these channels serve functions in conditions not yet simulated in the laboratory. In other words, the channel functions cannot easily be converted into differences in growth rates or cell survival, which are commonly monitored as laboratory microbiological phenotypes. Although we may expect that the basic physical and chemical principles underlying channel activities should be universal, the biological roles of ion channels in the physiology of microbial cells will likely be much broader than the roles they play in the physiology of muscles and the nervous system.

A. Ciliates *Paramecium* and *Stylonychia*

In ciliates *Paramecium* and *Stylonychia*, ion channels are known to generate receptor potentials and action potentials comparable to those found in cell membranes of neurons or sensory organs in metazoans. The perception and transduction of external stimuli in these microorganisms occur at the unicellular level. Consequently, for studies of membrane excitability ciliates may be perceived as "swimming sensory neurons" (68). Such studies in *Paramecium* and *Stylonychia* have demonstrated a crucial role that ion channels play in modulating the behavior of these ciliates by generating electrical membrane activity for signal integration and by controlling ion fluxes across their cell membranes.

Paramecium was the first microbial cell penetrated with a microelectrode (150). Being some 100–300 μm in length, *Paramecium* can easily be investigated by the classical two-microelectrode intracellular recording. Voltage-clamp experiments revealed that membrane depolarization can trigger a Ca^{2+}-dependent action potential leading to an increase in intracilliary calcium concentration, which causes 5,000–6,000 cilia covering the body of a *Paramecium* cell to beat in a reversed direction ("avoiding reaction") (146) to propel the cell backward (85, 262). Membrane hyperpolarization can trigger other ion currents causing the cell to spurt forward due to a more rapid ciliary beat in a normal direction ("escape response") (262, 264). These experiments helped to dissect the K^+, Ca^{2+}, and Na^+ currents that constitute various action potentials encountered in a *Paramecium* cell. In addition, as a model organism for genetic studies, *Paramecium*, and *P. tetraurelia* in particular, provided means to isolate behavioral mutants, whose avoiding reactions to a range of stimuli were missing or altered, identify the corresponding electrophysiological changes with intracellular microelectrodes (330), and clone the genes of some of the corresponding mutations (331). Since the entire genome of *P. tetraurelia* has recently been sequenced, many genes corresponding to K^+, Ca^{2+}, and Na^+ channels as well as nonspecific cationic or anionic channels could be identified (9).

The freshwater hypotrichous ciliate *Stylonychia* is another ciliate that was extensively examined by the classical two-microelectrode current- and voltage-clamp methods. Because of a variety of outstanding structural and physiological properties characteristic of this unicellular microorganism *Stylonychia* has served as a valuable model system for cellular physiology (227). For example, simultaneous recording of responses of compound cilia

(membranelles and cirri) in *Stylonychia* using membrane voltage-clamp and high-frequency cinematography showed that membranelles beat at high frequency, whereas the frontal and marginal cirri are quiescent at the membrane resting potential. In contrast, membrane hyperpolarizations and depolarizations specifically activate the cirri, but leave the membranellar frequency unchanged (69). These results indicate that the activity of both frontal and marginal cirri is coupled to the membrane potential similar to the ciliary activity in *Paramecium*, whereas membranelles should have a mechanism of motor control independent of the membrane potential. Although unicellular, *Stylonychia* thus exhibits complexity characteristic of metazoan organisms. This may not be that surprising given that from the view of ion channel evolution, most of the various types of ion channels and their gating mechanisms had already been operating by the time the ciliates emerged some 200 million years ago (183, 186).

1. Ca^{2+}-dependent channels

At least six types of K^+ currents could be identified in *Paramecium* using a combination of genetics and electrophysiology (311). The recently completed *Paramecium* genome-sequencing project (75), however, provided surprising evidence for the existence of 298 K^+ genes, a number three times bigger than the number of K^+ channel genes found in human genome (190); this is a humbling and potentially disturbing fact for an anthropocentrically minded reader. Based on their open reading frames (ORF), 239 genes of the *Paramecium* K^+ channels encode channels similar to the animal channels gated by cyclic nucleotides (CNG-type). The remaining 57 genes encode channels similar to animal ion channels such as inward rectifier, depolarization or hyperpolarization-activated K^+ channels, as well as Ca^{2+}-dependent BK or SK type K^+ channels. Combined, *Paramecium* also has some 30 Na^+- and Ca^{2+}-channel genes, which is approximately the number found in the human genome.

Studies of *Paramecium* mutants made it possible to identify a number of Ca^{2+}-dependent currents controlling its motile behavior. "Pantophobiacs," a group of behavioral mutants in *Paramecium*, called so because of their overreaction to a variety of stimuli, helped to show that microinjection of the wild-type cytoplasm was able to restore Ca^{2+}-dependent outward potassium currents lacking in voltage-clamp experiments (329). By fractionating the wild-type cytoplasm, the curing element was later identified as calmodulin, a 17-kDa soluble protein highly conserved in eukaryotes (331). When microinjected to a pantophobiac cell, calmodulin restored the current and cured the misbehavior.

Another group of *Paramecium* mutants called "fast-2" have an opposite phenotype to "panthophobiacs" due to a lack of a Ca^{2+}-dependent Na^+ inward current.

Fast-2 mutants were also identified as having defects in their calmodulin (159). Interestingly, studies of "panthophobiacs" and "fast-2" mutants indicated that Ca^{2+}-dependent K^+ channels are regulated by the C lobe, whereas Ca^{2+}-dependent Na^+ channels interact with the N lobe of the calmodulin molecule. This finding was later confirmed in patch-clamp experiments showing that the *Paramecium* Na^+ channel could be directly activated by the Ca^{2+}-calmodulin complex acting as a detachable subunit (332). Detailed information on regulation of Ca^{2+}-dependent currents in *Paramecium* by calmodulin can be found in a review by Preston et al. (311). In contrast to the multitude of ion channel genes, there is only a single calmodulin gene in the *Paramecium* genome.

Other Ca^{2+}-dependent channels found in a *Paramecium* cell include a Ca^{2+}-dependent Mg^{2+}-specific current and a hyperpolarization-activated Ca^{2+}-dependent K^+ channel. Mg^{2+}-specific current is activated by membrane depolarization as well as by membrane hyperpolarization (310). Divalent ions such as Co^{2+} and Mn^{2+} and, to a lesser extent also Sr^{2+} and Ba^{2+}, can substitute for Mg^{2+} as charge carriers through the Mg^{2+} channels. A physiological role of the Mg^{2+}-specific current consists most likely in maintaining intracellular free Mg^{2+} at low concentrations (0.1–0.7 mM). This current was found to be affected in some of the calmodulin mutants. Single gene mutants of *P. tetraurelia* with a reduced ability to respond behaviorally to Mg^{2+} were isolated and called "eccentrics" (*xntA* and *xntB*). Voltage-clamp experiments show a deficit of the Ca^{2+}-dependent Mg^{2+} current in these mutants (312, 313). Because the macronucleus of *Paramecium* is large, DNA can be directly injected through a micropipette into a mutant macronucleus to effect phenotypic transformation. It is possible to clone certain genes through such complementation by sorting a library of wild-type genomic DNA fragments to be injected. With the use of this method, the XntA gene was cloned and its predicted product found to be unlike any known ion channels but similar to animal Na^+/Ca^{2+} exchanger (126). This is the first example of an exchanger-like entity behaving like an ion channel electrophysiologically. This surprising finding is recently echoed in the study of ClC-ec1, the bacterial chloride "channel" behaving like an exchanger (see sect. III*D*).

A hyperpolarization-activated Ca^{2+}-dependent K^+ channel with a conductance of $\sim$70 pS was recorded from the *Paramecium* plasma membrane blisters using the patch-clamp technique (333) (Fig. 2). This channel is weakly voltage dependent, requiring $\sim$41 mV/*e*-fold change in its activity. A treatment of the channel with trypsin, pronase, or thermolysin from the intracellular side in inside-out excised plasma membrane blister patches removed the Ca^{2+} dependence of the channel activation, which suggested that this K^+ channel has a cytoplasmic inhibitory domain that can be removed by

proteolysis (180). The physiological activation of this channel by Ca^{2+} thus could be due to a temporary removal of this inhibition. Hyperpolarization-activated Ca^{2+}-dependent K^+ currents have also been identified and characterized by two-microelectrode voltage-clamp experiments. Since these currents are thought to regulate the resting membrane potential in *Paramecium* (322), the 70-pS hyperpolarization-activated Ca^{2+}-dependent K^+ channel may correspond to one of these currents.

2. Mechanosensitive channels

When observed under a low power microscope, *Paramecium* cells transiently stop or back up briefly by reversing their ciliary beat direction (ciliary reversal). These avoiding reactions (146) occur spontaneously and can also be induced by a variety of stimuli. Mechanical impact at the anterior end of a *Paramecium* cell elicits a Ca^{2+}-based receptor potential (85). Other divalent cations are also able to carry this membrane-depolarizing current (281), which can, in turn, elicit a Ca^{2+}-based action potential underlying the ciliary reversal. Mechanical impact at the posterior end of the cell elicits a K^+-based hyperpolarization (85), prompting the cell to spurt fast forward due to an increase in frequency of the ciliary beat in normal direction. Since cilia in *Paramecium* can be removed with ethanol, the experiments on deciliated cells that were mechanically stimulated showed that deciliated cells retained the depolarizing and hyperpolarizing mechanoreceptor responses, which indicated that mechanosensitive Ca^{2+} and K^+ channels were localized on the cell soma (228). In addition, ciliated and deciliated cells showed a decrease in depolarizing mechanosensitivity and a subsequent increase in hyperpolarizing mechanosensitivity, when the site of stimulation was shifted from the anterior to the posterior end of the cell. These experiments indicated that the Ca^{2+} and K^+ mechanoreceptor channels were distributed over the somatic cell surface in the manner of overlapping gradients (281). Although both mechanosensitive macroscopic currents in *Paramecium* have been well characterized by the voltage-clamp method, the genes and proteins behind these receptor potentials are yet to be identified.

3. Voltage-dependent Ca^{2+} channels

The composition of ionic currents underlying the Ca^{2+} action potential and its relation to ciliary reversal in *Paramecium* are well understood and have been extensively described over the years (85, 226, 250, 337). A depolarization-activated current is carried by Ca^{2+} through voltage-dependent calcium channels, which inactivate in a Ca^{2+}-dependent manner (39, 280). The channels are located in the ciliary membrane, since deciliation abolishes the depolarization-activated Ca^{2+} current (228). This current is abolished or reduced in "pawn" mutants

that show no backward swimming in response to stimulation (185, 280). Microinjection of cytoplasm from a wild-type cell into the pawn mutants belonging to any of the three complementation groups (pawnA, pawnB, pawnC) restored the ability of the mutants to generate action potentials and hence swam backward (116). In addition, the cytoplasm from a pawn of a different complementation group as the microinjected mutant could also restore the action potential and backward swimming. Consecutive studies demonstrated further that microinjection of the total wild-type genomic DNA into the macronucleus of a *Paramecium* cell could restore the Ca^{2+} current and excitability in clonal descendants of the microinjected pawnA cell. By sorting a library of total DNA, the factor required for restoring the Ca^{2+} current was identified as a 2.3-kb DNA fragment corresponding to a novel protein that may be glycophosphatidylinositol anchored (129). The same method was used to clone the pawnB gene, which corresponds to a peptide with two transmembrane domains but no clear homology to known proteins (127).

Similar to *Paramecium*, mechanical stimulation of the anterior part of *Stylonychia* evokes a depolarizing mechanoreceptor potential, which gives rise to an action potential. The action potential in *Stylonychia* is, however, more complex compared with the *Paramecium* action potential. It has two components, which are represented by a first, large graded peak and a second, small "all-or-none" peak (65). The two components were shown to correspond to two types of Ca^{2+} currents based on their differential sensitivity to Co^{2+} and Cd^{2+} (67). In both types of currents Ca^{2+} can be replaced by Ba^{2+} or Sr^{2+}. These Ca^{2+} currents are separable by their localization in the membrane. The smaller Ca^{2+} current corresponding to the "all-or-none" peak is restricted to the membranelles (row of compound cilia) since in cells that spontaneously released their membranellar band the small current disappeared and the larger current corresponding to the graded peak remained unaltered. It has been suggested that the two voltage-dependent Ca^{2+} currents may be functionally related to different beating behavior of membranelles and other types of the compound cilia in *Stylonychia* (67).

B. Slime Mold (*Dictyostelium*)

1. A model system of chemotaxis without ion channel function

Dictyostelium discoideum cycles between free-living single amoebae and social multicellular organisms for spore formation. After starvation, the amoeba secrete cAMP, and cAMP-chemoreception drives the amoebae to form a multicellular slug (chemotaxis), which, in turn, moves around to find an appropriate site to form fruiting

body to develop spores. This chemotaxis is the central study of *Dictyostelium*, since it shares molecular mechanisms with the chemotaxes of neutrophils, lymphocytes, and even cancer cells (46, 100, 288, 309, 391). Briefly, upon reception of external cAMP by G protein-coupled receptor proteins (cAR1 and cAR3), a series of reactions including $G\alpha2\beta\gamma$ activation, small GTPase (Ras and Rho family members) activation (45), PI3K (class 1 phosphatidylinositol-3 kinases, IP3K1, -2, -3) activation (104, 143, 373), phosphorylation of $PI(3,4)P_2$ into $PI(3,4,5)P_3$, and finally F-actin polymerization resulting in pseudopod development for chemotactic movement. Activation of Rho GTPases or their functional homologs, on the other hand, leads to activation of PTEN (PI 3-phosphatase) at the opposite site of the signal source that causes a reduction of $PI(3,4,5)P_3$ (45). Thus, through changing the local concentrations of $PI(3,4,5)P_3$ at the front and back, the amoebae amplify the external cAMP signal (as little as 2% difference) and convert into internal signal gradient to determine for correct polarity in chemotaxis. Although the main cascade of signal transduction has been so established, the chemotactic orientation of *Dictyostelium* cells is hardly affected after genetic deletions of PI3Ks and reduction in $PI(3,4,5)P_3$ contents (213, 373), implying redundant pathways. Genetic screens have identified a second pathway utilizing PLA_{2A} (Patatin-like phospholipase A_2 homolog; Ref. 48). Arachidonic acid has been implicated in the PLA_{2A} pathway (48). There is yet another pathway for chemosensation in *Dictyostelium* that uses phospholipase C (PLC) (156, 174, 381).

Although chemosensation in *Dictyostelium* is often associated with Ca^{2+} fluxes (196, 225, 268, 338) and PLA_{2A} may be regulated by intracellular Ca^{2+} (381), there is no evidence that Ca^{2+} signals are involved in chemotaxis (374), nor is there evidence that membrane potential plays a role in regulation of chemotaxis (380). This lack of ion channel involvement in chemotaxis is in stark contrast to the axonal growth cone that also senses chemical cues and requires TRP channel function (386, 389). The genome of *D. discoideum* has been completely sequenced (88), and one can identify at least two possible TRP channel genes, a Ca^{2+} channel gene, and several K^+ channel genes. Its membrane potential is largely regulated by an electrogenic proton pump like fungi (379). Curiously, there is no recognizable gene for CNG channels in this organism, which is the champion of cAMP chemotaxis. Nuclear pores in nucleus membranes are obviously critical for all eukaryotic cells. Recent efforts on *Dictyostelium* nuclear pores show new features of the pore complex (15). An amoebapore (protozoan pores that affect humans) is also found in the database (405). As to channel activities, three single-channel activities have been reported from the results of patch clamp in the cell-attached mode; DI (11pS), DII (6pS), HI (3 pS) (256, 257). DI and DII are permeable to K^+, and HI may be permeable to Ca^{2+}. DII is quite low in density.

2. P2X, ATP-activated channel

P2Xs are purinergic receptor channels found and studied extensively in animals. These are channels that open upon the binding of extracellular ATP. The channels are multimers of subunits, each with two transmembrane helices (277). *Dictyostelium* has a gene, which has weak homology to these P2X channels. Fountain et al. (99) expressed this gene (*DsP2X*) in HEK cells, where it apparently forms trimeric ATP-gated channels of ~8 pS conductance with some Ca^{2+} selectivity. Permeability to Na^+ is lower ($P_{Ca}/P_{Na} = 1.5$) and those for larger organic cations still lower. The DdP2Xs have key residues for ATP binding, such as Lys67 (Lys71 in rat P2X) and Lys289 (Lys308 in rat P2X), which have critical functions in ATP sensitivity. Unlike mammalian P2X, DdP2X is not activated by ATP analogs. Cu^{2+} blocks DdP2X channels at micromolar concentrations, but not mammalian P2Xs. This gene product in *Dictyostelium*, unlike the HEK cell expression, is localized to the contractile vacuole, the water pumping organelle. Upon osmotic downshock, the DdP2X knockout *Dictyostelium* suffers swelling. Also, HEK cells expressing DdP2X swell upon inhibition by Cu^{2+}. One possible hypothesis is that distension of the contractile vacuole leads to the entry of ATP from the cell cytoplasm, which activates DdP2X receptors, allowing vacuolar Ca^{2+} to pass back into the cytoplasm and initiate contraction (99). Curiously, *Dictyostelium* contractile vacuole apparently includes a voltage- and K^+-dependent K^+ channel, which may also function in water regulation (398).

C. Yeasts and Other Fungi

Much of the current knowledge on fungal channels came from the study of the budding yeast *Saccharomyces cerevisiae*. We will describe the various ion channels studied therein and then point out their homologs in other fungi.

1. Mechanosensitive channels

Like bacteria, yeast cells have to face rapid and large changes in osmolarity. Given the knowledge on prokaryotic mechanosensitive channels, it is not surprising that yeasts and other fungi also have such channels. Possible fungal homologs of MscL and MscS are listed in section II*A4*.

A) PLASMA MEMBRANE MECHANOSENSITIVE CHANNEL. A patch-clamp survey in 1988 of the yeast plasma membrane revealed an ion-nonspecific stretch-activated channel of 36 pS (115). This conductance has poor selectivity, al-

though preferring cations over anions. The *MID1* product is required for Ca^{2+} influx in yeast (see sect. IIIC3). When expressed in mammalian cells, *MID1* was reported to support a pressure-activated, Gd^{3+}-suppressable 32-pS conductance (153, 154). However, the plasma membranes of *mid1Δ* yeast cells retain the 36-pS stretch-activated channels (187). Despite the availability of the complete *S. cerevisiae* genome sequence, the molecular identity of this channel remains unknown to date. At this writing, each ORF that corresponds to recognizable channel sequence in this genome has been individually deleted. None of the deletions remove this 36-pS conductance from the plasma membrane (Zhou, Saimi, and Kung, unpublished results). It, therefore, is likely that it corresponds to a novel channel structure. The surface of protoplast protuberances of the fission yeast *Schizosaccharomyces pombe* has also been examined with the patch clamp (410). There is a 180-pS conductance that prefers K^+ over Cl^-, but discriminates poorly among cations. The spores of the bean-rust fungus *Uromyces appendiculatus* germinate, and the growing germ tubes are apparently guided by the topography of bean-leaf surface to the stomata, where they differentiate into invading structures. A 600-pS mechanosensitive conductance can be registered from the surface of protoplasts derived from the germlings (412). This conductance is cation specific, nearly impermeable to Cl^-. It passes Ca^{2+} and is blocked by Gd^{3+}. It seems possible that this channel can transduce the membrane stress induced by the leaf topography into a flux of Ca^{2+} that initiates differentiation.

B) TRP CHANNELS (YVC1). First identified from a near-blind *Drosophila* with an abbreviated transient receptor potential, TRP channel is now a large superfamily of channels largely studied in animals. Attention is drawn to them in recent years because they apparently underlie sensation of certain tastes, of hot and cold (and the chemical mimics such as pepper and menthol), and of force (osmotic, impact, tension, vibration, etc.). Each TRP channel is believed to be a tetramer of 6-TM subunits akin to *Shaker* K^+ channel (Fig. 5). The seven subfamilies of animal TRPs, however, are quite diverse, with sequence similarity only at TM5-P-TM6 segment and just beyond it (52). The yeast genome includes a gene containing this sequence, and its product forms a channel in the vacuolar membrane. It is called Yvc1, for yeast vacuolar channel, or TRPY1, for a TRP channel in yeast (286). Yeast cell wall can be removed by enzyme digestion; its plasma membrane can be removed by osmotic manipulation. The exposed vacuole can directly be examined with a patch-clamp pipette. Yvc1 displays an inwardly rectifying conductance of 350 pS, rather large for TRP channels. This conductance was first discovered by reconstituting vacuolar membranes into planar lipid bilayers (388). Like other TRP channels, Yvc1 passes cations but discriminates poorly among them, and its open probability is

regulated by H^+ and Ca^{2+} (21, 286). Using transgenic aequorin as an indicator, Denise and Cyert (72) found that Yvc1 releases Ca^{2+} from the vacuole into the cytoplasm upon osmotic upshock. Correspondingly, Yvc1 was found to respond directly to membrane stretch force under patch clamp (409). Combining forward genetics and patch clamp, Yvc1 is being dissected towards understanding its detailed structure-function relationship and the submolecular bases of regulation by force and by Ca^{2+}. GOF mutations were found to be mostly those on aromatic amino acids. A mutation at the base of TM6 near the presumed gate was found to destabilize both the closed and the open state. Of all the 19 variations at this residue, only the aromatics can apparently anchor the gate properly (408). Another aromatic mutation at the cytoplasmic end of TM5 displays a constitutively open channel kinetics, phenocopying a special allele of the *Drosophila* TRP channel (363). Yvc1 has direct homologs in over 30 species of fungi except *Schizosaccharomyces pombe* and the parasitic *Zygomycetes*. The ones from *Kluyveromyces lactis* and *Candida albicans* have been expressed in the vacuole of *S. cerevisiae* and found to also function as mechanosensitive cation channels (411). Yvc1 (TRPY1) and its direct relative are considered more related to TRPML of animal TRP channels (51). A gene in the fission yeast *S. pombe* is reported to encode a channel more similar to animal TRPP (285), although it appears to have minimal homology.

2. K^+ channels (Tok1)

The activities of a K^+ channel were evident in the first patch-clamp examination of the yeast plasma membrane in 1986 (114). The yeast genome was the first eukaryotic genome to be completely sequenced in 1996. Four groups independently recognized a gene that predicted a K^+ channel (157, 201, 320, 413). The cloned gene can be expressed and examined in yeast itself or in *Xenopus* oocytes. Unlike the 2-TM KcsA or 6-TM *Shaker* motif, the channel subunit predicts a peptide with 8 TM helices and 2 P domains (Fig. 5D) and is named TOK1, for two-pore domain K^+ channel (157). It is K^+-specific, rectifies outwardly, and has a unitary conductance of ~30 pS (413). Although TOK1 may take up K^+ in certain mutant context (94), the complete loss of TOK1 function in *tok1Δ* cells has no easily discernible growth phenotype in the laboratory. GOF mutants, however, can be isolated that stop growth when the mutant channel is expressed. Examined in oocytes, such mutant channels are largely unable to enter a closed state distal to the open state. Many mutations are located at the "post-pore" regions, at the cytoplasmic end of the predicted TM6 and TM8 (220). Both are the inner helices comparable to TM2 of KcsA; the "post-pore" region is now shown to be near the K^+-channel gate in crystal structure (80). The proximal

closed state, also called the R (rectifying) state, whose dwell has a low Q_{10}, depends on the total K^+ electrochemical potential and not just the membrane potential. This R state is apparently the behavior of the K^+ filter (219) (see sect. IIIA1A). Second-site mutations that rescue the GOF mutants (intragenic suppressors) were found to be substantial deletions of the COOH-terminal domain predicted to be in the cytoplasm. Detailed analyses showed that this tail domain is needed to maintain the inner-gate closure, and the inner-gate movement conditions the behavior of the filter (218). This COOH-terminal peptide apparently forms a discrete domain that interacts with the channel proper strongly. Expressed as a separate peptide, it binds the channel rigorously to maintain the open state (216). TOK1 homologs can be found in most known fungal genomes that have been sequenced. Curiously, along with the parasitic *Zygomycetes*, the free-living ascomycete *Schizosaccharomyces pombe*, a fission yeast well studied as a eukaryotic cell model, is without a TOK1 homolog or any K^+ channel (217). A nonselective cation conductance has been observed under patch clamp (375). As with the prokaryotic K^+ channels, the physiological role(s) of TOK1 and its fungal homologs are presently unknown.

3. Ca^{2+} channels (Cch1)

Animal Ca^{2+} channels are large proteins of over 2,000 molecular weight. Besides the flanking cytoplasmic domains, the transmembrane body has four repeats, each has a 6-TM arrangement similar to the one described for K^+ channel above. The yeast genome sequence revealed a Ca^{2+} channel, but unlike its animal counterparts, there has been no report on electric current through this channel in situ or in heterologous cells. No Ca^{2+} currents have yet been reported in the plasma or the vacuolar membranes with patch-clamp electrodes at different voltages or stretch force. The studies on this channel are therefore genetic and not electrophysiological.

Mating pheromones induce a Ca^{2+} influx. Two gene products, Cch1 and Mid1, are needed for this Ca^{2+} influx and for the survival through the mating process (95, 284). Mid1 (for mating-pheromone-induced death) is a 548-residue glycoprotein, which has no homologs in animals (140). Cch1 (for calcium channel) is a homolog of animal voltage-gated Ca^{2+} channel (141). Mid1 and Cch1 are both located in the plasma membrane, where they apparently function together and can be coimmunoprecipitated (209). Evidences suggest that they are parts of a homeostatic mechanism analogous to the capacitative calcium entry of animals (209) and play roles in the response to endoplasmic reticulum stress (34). The *cch1Δ mid1Δ* double mutant is apparently sensitive to cold and to high iron concentration in the medium (296). The osmotic upshock-induced cytoplasmic Ca^{2+} response is reduced in the *cch1Δ mid1Δ* double mutant (241). However, a recent examination of a collection of 4,810 yeast-gene deletants shows that this reduction is due to the depletion of Ca^{2+} in the vacuole and not due to defects in the Ca^{2+}-releasing channel Yvc1 (S.H. Loukin, M.M. Kuo, X.L. Zhou, W.J. Haynes, C. Kung, Y. Saimi, unpublished data). Alkaline shock induces a Ca^{2+} flux as evidenced by Ca^{2+}-aequorin luminescence. This flux is largely missing in *cch1Δ* or *mid1Δ*, suggesting a role of Ca^{2+} channel in defense against alkaline stress (384). Even though Cch1 cannot yet be studied directly with electrodes, insights from the dissection of the yeast Cch1 can be transferred to animal Ca^{2+} channels. For example, LOF phenotypes were found in a *cch1* mutant, mutated at a glycine that is completely conserved. The corresponding mutant in an animal Ca^{2+} channel is then found also to be nonfunctional under voltage clamp (142).

4. NH_4^+ channels (Mep)

Fungal Meps (methylamine permeases) are homologous to Amts (ammonium transporters) in the bacteria (see sect. IIIC). The first NH_4^+ channel was cloned as a transporter that complements the yeast *mep1*-mutant defect of poor growth with ammonium as the sole nitrogen source (232). There are three such transporters in yeast, Mep1, Mep2, and Mep3, of different affinity and capacity, as measured by [^{14}C]methylammonium accumulation into live yeast cells (231). Biochemical studies showed that the NH_2 terminus of Mep2 faces outward and is *N*-glycosylated (230), and its function requires the serine/threonine kinase Npr1 (33). Mep2 apparently also functions as a sensor for rapid activation of the protein kinase A pathway (382). Nitrogen starvation of diploid yeast on a fermentable carbon source triggers pseudohyphal growth, presumably to better explore the environment. Mutant of *mep2*, but not *mep1* or *mep3*, abolishes pseudohyphal growth, leading to the suggestion that Mep2 may be the sensor (215). There appears to be no study on Meps in more reduced system such as oocytes or liposomes, and no discussion on interpreting the substrate-accumulation data with the presumed channel mechanism.

5. Cl^- channels (Gef1)

Mutations of a gene called *GEF1* yield the *petite* phenotype that can be suppressed by added iron. *GEF1* was found to give a product of 779-residue, 13-TM structure, similar to the animal Cl^- channel subunits (110) (see sect. IIID). This channel, also called yClC-1 (138), was first found to be located in the Golgi apparatus (343) or prevacuolar fraction. It was found to be a necessary component in the homeostasis of Cu^{2+} and other cations in vesicular compartments by regulating their pH. *gef1* defects can be complemented with certain animal or plant ClCs, indicating functional similarity (105). Gef1 is apparently proteolytically cleaved in the secretory pathway into

a 30- and a 70-kDa fragment, which function together but not individually (387). Electrophysiologically, a 10-pS anion conductance was observed when microsomal fraction of the wild-type, but not the *gef1* mutant, was reconstituted into planar lipid bilayers (97). There is a recent report showing that GEF1 can be expressed in ooctyes or HEK cells and apparently producing a permanently open channel in the plasma membrane, blockable by known ClC blockers. In that study, electron microscopy showed that Gef1 is located in the plasma membrane as well as internal membranes (214). Gef1 homologs can be found in other yeast species as well as in filamentous fungi. Two are found in the human pathogenic yeast *Cryptococcus neoformans*, one of which is required for virulence (415). Three such homologs, AnCLCA, -B, and -C, are found in the filamentous *Aspergillus nidulans* (279).

D. Algae (*Chlamydomonas*)

Green algae comprise single cells or loose colonies of cells. They are true plants with chloroplasts for photosynthesis. Some of them have flagella or cilia to move about, seeking light (phototaxis) and/or avoiding intense light (photophobic response, also called photoshock response) (130, 349, 392). *Chlamydomonas reinhardii* has been exploited as a model system in the studies of photosynthesis and cell motility for a number of years. Recently, its entire genome has been sequenced (245) along with another nonflagellated yet free-living green alga *Ostreococcus tauri* (74). Sixty-one ion channel genes have been predicted in *Chlamydomonas* (245). However, patch-clamp analyses of channel activities have proven to be difficult because of low resistance seal with patch pipettes.

In *Chlamydomonas*, light is detected with the eye spot, which contains rhodopsins. These rhodopsins consist of protein opsins and photopigment retinals, but unlike mammalian rhodopsins (type 2), they mostly consist of all-*trans* retinals, similar to prokaryotic rhodopsins (type 1). These types of rhodopsins have similar structural designs (7 transmembrane domains) but are dissimilar in terms of amino acid contents. In fact, the opsins of *Chlamydomonas* are numerous and mixed. At least six opsin genes have been identified in the genome. Light sensation by the eye spot in *Chlamydomonas* causes membrane depolarization, which in turn activates the Ca^{2+} channels in flagella (14, 121, 135, 136, 349). Ca^{2+} in flagella is known to regulate the flagella motion. At low Ca^{2+}, the flagella movement is in the form of breast stroke (or ciliary type motion), whereas at higher Ca^{2+}, it becomes undulating (or flagellar type). Because the two flagella have different Ca^{2+} sensitivity (152), the net translational movement of the cell can be rotational when the light stimulation is low, resulting in turning the cell body until it orients towards the light source, thereby shielding the eye spot from further excitation. At a high light intensity, both flagella beat in the flagellar type motion, thus moving the cell away from the light source (349).

1. TRP homologs

The general features of TRP channels are given in section IV*C1*B (318). They are found among mammals, worms, insects, yeasts, ciliates, but, mysteriously, largely absent in plants. One exception is *Chlamydomonas*; there are at least seven homologs of TRP-channel genes in its genome. One of them is a homolog of PKD2 or TRPP2, a gene whose mutant forms cause a polycystin disease in kidney (255). In the kidney, the NH_2 terminus of PKD2 interacts with the COOH terminus of PKD1, a protein with multiple transmembrane domains, to form a functional channel unit, which lets Ca^{2+} into the cell (120). These channels reside in the ciliary membrane and probably are activated by mechanical movement of cilia (120, 267). Interestingly, PKD1's NH_2 terminus may be cleaved at GPS domain (G protein-coupled receptor proteolytic site) (315, 403), which may be important for the function of the PKD2-PKD1 complex in the ciliary membrane. Thus PKD2 is the pore-forming subunit, whereas PKD1 may have multiple functions such as chaperone and G protein activation (70). PKD1 does have modest homology to PDK2. Thus PKD1 alone might also form channels (175).

Cilia or flagella are assembled and maintained by the intraflagellar transport (IFT), motorized with kinesin-2 and dynein 1b or 2 (326). IFT particles comprise ~17 proteins that are conserved among mammals, fish, flies, and worms (10, 204). In *Chlamydomonas*, one of the IFT subunits has been identified as a PKD2 homolog (295). *Chlamydomonas* PKD2, CrPKD2, is a protein of 1,626 amino acids with 6 or even more transmembrane domains. Its NH_2 terminus extracellular domain is ~1,000 amino acids long (137). The whole cell extracts show 210-, 120-, and 90-kDa proteins, recognizable by antibodies against CrPKD2. The latter two are the in vivo proteolytic products of the 210-kDa protein after the long extracellular domain, and only these two proteins are found in the flagellar fraction, while the 210-kDa protein is not detected in flagella. CrPKD2 can be visualized with a GFP tag to be in puncta that move along the flagella (137). This movement is dependent on IFT as such fluorescence movement is not observed in the fla10 mutant under a restrictive condition. RNAi knockdown of CrPKD2 causes reduced mating reactions, suggesting CrPKD2 may be necessary for Ca^{2+} influx after flagellar adhesion in the cascade of mating reaction in *Chlamydomonas* (137). Whether CrPKD2 forms the functional channel by itself or with other subunits such as PKD1 in *Chlamydomonas* has yet to be determined. Also, which product(s) of CrPKD2 (the 210 kDa found in the cell body or 120/90 kDa proteins

found in the flagella) actually function as ion channels has to be determined in the future. Some of the other TRP channels may work together with CrPKD2 in the function of Ca^{2+} signaling during the mating reaction. It would also be interesting to see whether the *Chlamydomonas* CrPKD2 has the purported mechanosensitivity of PKD2.

2. Channel rhodopsins

In the study of phototaxis and photophobic responses of *Chlamydomonas*, at least seven eye pigment proteins have been identified. *Cop1* and *Cop2* (splicing variants) (66, 102) are similar to the invertebrate opsins (type 2), which are seven-transmembrane G protein-coupled receptor proteins. RNAi knockdown of these genes indicates that these are not the primary photosensors for phototaxis (103). *Cop3* and *Cop4* [also called channelrhodopsin (ChR) 1, 2 (260, 261); *CSRA, B* (350); *Acop1, 2* (371)] are similar to prokaryotic (type 1) rhodopsins that are H^+ pumps utilizing light energy. Many of the key residues necessary for prokaryotic rhodopsin's H^+ pump activity are preserved in ChRs (350). There are other opsins (*Cop5–7*) similar to prokaryotic "sensory" rhodopsins (356) in the *Chlamydomonas* genome (155). Bacterial and archaeal rhodopsins are type 1 rhodopsins and can be classified into two categories: transporters which pump H^+ or Cl^- and electrogenic [see Stoeckenius (360) for a historic account] and receptors (*SRI* and *SRII*) which interact with their cognate transducers *HtrI* or *HtrII* to activate the cascade of *Che* gene reactions in phototaxis (356). Such type 1 rhodopsins are also found in eukaryotes (345). The structures of some of these rhodopsins have been solved at atomic resolution.

A surprising finding on ChR1, 2 in *Chlamydomonas* is that these ChRs behave more like ion channels than pumps. ChRs are photosensitive, having their peak absorption at 510 and 470 nm, respectively. Both ChRs are expressed in *Chlamydomonas* and can be expressed in *Xenopus* oocytes as well as mammalian cultured cells and yeast cells (12, 260, 261, 350). Patch-clamp examinations revealed that ChR1 are highly selective for H^+ (260). On the other hand, ChR2 is selective for mostly H^+ but also other cations including Ca^{2+} (261). Unlike prokaryotic pump rhodopsins, both currents passed through both ChRs can reverse directions and are dependent on the electromotive force of H^+ or other cations (259–261), indicating that they behave more like ion channels. However, the estimated conductance appears very small (<300 fS) (155). The response time of ChR2 takes less than 200 μs (261), while that of ChR1 is slow (260, 261). Like Cl^- transporters described in section IIID, these ChRs appear to be another case of conversion of ion channels from pumps/exchangers. Activation of ChRs by light leads to depolarization of the *Chlamydomonas* cell, which in turn activates voltage-dependent channels such

as Ca^{2+} channels in flagella (14, 349). RNAi knockdown experiments suggested that these ChRs may be involved in both phototaxis and photophobic responses (350), but further analysis suggests ChR1 is involved in photophobic response under high light intensity stimulation (108). A homolog of ChRs from the green alga *Volvox carteri* has also been cloned, expressed in oocytes and examined biophysically (92). As these ChRs can be heterologously expressed in other cells, they, particular ChR2, have now been utilized as formidable tools (348, 406) to light-stimulate cells in the studies of neuronal networks (7, 205) and behavioral responses (259). The halorhodopsin of *Natronomonas pharaonis*, a Cl^- light-activated pump, has also been used in these studies.

3. Ca^{2+} channels

Depolarization of the *Chlamydomonas* membrane activates voltage-dependent ion channels. There are about 10 Ca^{2+} channel genes and more than 5 K^+ channel genes identifiable in the *Chlamydomonas* genome. Changes in internal Ca^{2+} concentrations have been demonstrated to alter flagellar beat patterns (339). For phototaxis, which results from high intraflagellar Ca^{2+} concentrations, Ca^{2+} channels are suspected to be involved, because Ca^{2+} channel blocker ω-conotoxin blocks phototaxis (131). Such channel activity can be recorded with a macropipette covering part of *Chlamydomonas* cell, where light-induced eye-spot current and flagella-origin current can be measured (14). Partial amputation of flagella causes loss of the current of flagellar origin, which recovers as flagella regenerate to their original length, indicating such channels are distributed along the length of flagella (14). Ca^{2+} channels may also be involved in other aspects of cell biology in *Chlamydomonas*. Deflagellation of *Chlamydomonas* can be induced by Ca^{2+} influx triggered by cytoplasm acidification or Ca^{2+} release from internal storage (317). Such acid-induced Ca^{2+} influx is not sensitive to common Ca^{2+} channel blockers, Cd^{2+}, SKF-96365, or flufenamic acid (316). Most interestingly, isolated flagella do not accumulate Ca^{2+} upon acid stimulation, whereas the cell bodies do, indicating the entity for Ca^{2+} influx is not in the flagellar membrane (316), which is different from the Ca^{2+} channel distribution (see above). Currently, it is not clear whether that entity is an ion channel or transporter.

4. Mechanosensitive channels

In *Chlamydomonas*, there is no reported behavior that is associated with mechanical stimulation or osmotic stress, though in a related green alga S*permatozopsis*, a touch-induced backward movement has been reported (177). However, there are reports on negative pressure-induced mechanosensitive ion channels in *Chlamydomonas* (399), although low seal resistance of the recording

system makes the channel activities less certain. Given the CrPKD2's presence in the flagella and its possible mechanical activation (see above), mechanically sensitive ion channels may indeed exist in the flagella and/or the cell body of *Chlamydomonas*. Note that there are other TRP channels identified in the genome, which could also play a role in the potential mechanosensitivity.

Another mechanosensitive ion channel is *MSC1* (266) that is a homolog of prokaryotic MscS. (see sect. IIA4). *MSC1* has three putative transmembrane domains, and high homology to bacterial MscS can be found in TM3. When expressed in *E. coli*, it corresponds to a ~400 pS conductance, though its NH$_2$-terminal signal sequence has to be removed prior to expression. *MSC1* is activated by membrane tension but not by membrane potential changes. It requires moderate tension, ~80% of tension that activates *MscL* of *E. coli*. The channel activity diminishes upon hyperpolarization despite continued membrane tension, whereas the activity is maintained upon depolarization. The channel prefers anions over cations ($P_K:P_{Cl}:P_{Br}:P_I$ = 1:7:9:9), whereas *E. coli's MscS* is less selective ($P_{Cl}:P_K$ = 1.5–3.0:1) (238, 354, 364, 368). The most astonishing feature of *MSC1* expressed in *E. coli* is its hysteresis behavior depending on how tension is applied to the membrane. It is not clear why *MSC1* exhibits hysteresis. In *Chlamydomonas*, it is localized in chloroplasts. Its homologs of *Arabidopsis* (MSL2, 3) are also known to be localized in chloroplasts and are necessary for maintenance of chloroplast morphology (125). The immunolocalization signals are also found in cytoplasm of *Chlamydomonas*, which appears to be fortuitous cross-reactions (266). RNAi knockdown of *MSC1* reduces chlorophyll autofluorescence. In *Chlamydomonas*, there are at least two additional homologs, but these have yet to be investigated. Given the mechanosensitive function of the *Arabidopsis' MSL3* in rescuing of the mutant *E. coli* lacking mechanosensitive channels upon osmotic downshock (125), it is likely that these eukaryotic *MscS* homologs also function as mechanosensors in vivo. Since these channel proteins are functionally expressed in *E. coli*, it raises a possibility of purification and reconstitution in artificial lipid membrane for further biophysical studies. It also makes it possible that large quantities of these proteins can be used for crystallization in the future.

V. BACTERIAL TOXINS FORMING ION CHANNELS

Bacterial toxins are widely distributed proteins that usually induce an unrestricted flux of ions and molecules across membranes of mammalian cells (106). They are frequently cytotoxic as they perforate the cell membranes by creating unregulated pores across the membrane of susceptible cells, leading to cell death and lysis. Broadly classified into two groups, they are thought to interact with the membrane either through α-helices or β-sheet structures such as β-barrels. The mechanism of pore formation is much better characterized for those toxins, which interact with membranes of target cells through β-sheet structures.

The most widespread bacterial toxin encountered by the human organism is α-hemolysin secreted by *Staphylococcus aureus* (24). The α-hemolysin toxicity is a result of its capacity to form large pores permeant to ions, ATP, and water, leading to irreversible osmotic swelling and cell lysis. α-Hemolysin assembles as a homoheptamer from a water-soluble monomer to form a membrane-bound β-barrel on the surface of targeted cells. The mechanism of heptamer assembly occurs in a stepwise manner, resulting in a water-filled transmembrane channel having a pore of ~40 Å in diameter (252). The three-dimensional structure of α-hemolysin has been solved by X-ray crystallography to 1.9 Å resolution (352), showing the mushroom-shaped heptamer consisting of a 14-strand antiparallel β-barrel. Ion conductance and anionic selectivity of α-hemolysin is sensitive to pH (176). Furthermore, in the presence of divalent and trivalent cations, the α-hemolysin channel can be inactivated by voltage in a dose-dependent manner (244). In very good agreement with the experiments, molecular dynamics simulation studies of α-hemolysin helped to visualize permeation of ions, small solutes, and water through this channel at atomic scale (372).

RTX toxins (repeats in the structural toxin) present another type of pore-forming bacterial peptides with a molecular mass of 100–200 kDa. They are produced by a broad range of pathogenic gram-negative bacteria and, in particular, species of the family *Pasteurellaceae*. RTX toxins mostly exhibit a cytotoxic as well as a hemolytic activity. They were named after a repeated structure of iterative glycine-rich nonapeptides binding calcium on the COOH-terminal half of the protein. The toxic activities of RTX toxins in host cells usually lead to necrosis and apoptosis. The molecular mechanism of their toxicity is currently under investigation (101).

Among the bacterial toxins, the pore-forming colicins were first to be discovered in the process of searching for ways to kill bacteria (109). Colicins are produced by colicinogenic strains of nonpathogenic *E. coli* and some related species of *Enterobacteriaceae*. Colicins primarily target membranes of susceptible bacterial strains to inhibit their growth and thus present a major weapon in the on-going bacterial warfare. They form voltage-dependent ion channels by interacting simultaneously with several components of the complex membrane of susceptible cells and transforming themselves into α-helical membrane-spanning channel proteins (198). Although most colicins kill susceptible bacteria by forming ion channels in the plasma membrane of target cells, other types of colicins, such as E3, E4, E6, and cloacin DF13 or E2 and

E7-E9, function as specific 16S rRNA endonucleases or nonspecific DNA endonucleases, respectively, while other colicins like colicin M or pesticin I inhibit cell wall synthesis or hydrolyze it (171).

A large family of bacterial toxins is formed by the cholesterol-binding toxins (CBTs). CBTs are also known as thiol-activated toxins and cholesterol-dependent cytolysins (106, 253). Among the best-known CBTs are streptolysin from *Streptococcus pyogenes*, pneumolysin from *Streptococcus pneumoniae*, perfringolysin from *Clostridium perfrigens*, and listeriolysin from *Listeria monocytogenes*. They interact with membrane cholesterol at concentrations between 1 and 100 nM. The presence of cholesterol, which has been identified as a CBT receptor in membranes of target cells, is thus a prerequisite for CBTs to form oligomeric pores that can be made up of up to 50 subunits. CBT oligomers exist in two forms, as arc- or ring-shaped oligomers. CBT oligomerization occurs in a concentration-dependent manner (106), such that smaller arc-shaped oligomers form smaller pores compared with the larger pores of ring-formed oligomers. Given that only 10–100 CBT monomers are required for their cytotoxic action, this suggests that arc-formed pores may be more important for the cytotoxic action of CBTs than the larger ring-formed pores.

An interesting case on its own presents VacA, the pore-forming toxin of the stomach ulcer causing bacterium *Helicobacter pylori*. In contrast to most bacterial toxins, which usually form membrane pores without preference for permeating ions, VacA exhibits electrophysiological properties characteristic of the ClC channels of eukaryotic host cells (64). In addition to sharing similar conductance and ionic selectivity with the ClC channels, VacA also shares an open probability dependent on the molar ratio of permeable ions as well as single-channel events resolvable as two independent, voltage-dependent transitions, which are the very characteristic of the ClC channels. The only feature distinguishing VacA from the ClC channels is the membrane potential at which the two channels close. VacA toxin thus largely mimics the electrophysiological behavior of ClC channels of the host cells, suggesting a novel mechanism of toxin action.

VI. VIRAL ION CHANNELS

Before discovery of the microbial world, the term *virus*, which originates from a Latin word meaning "venom," had been used to describe any disease-causing agent. As cellular parasites, viruses depend entirely on their host cell machinery for propagation. The genome of a virus consists of either DNA or RNA, but never both. The viral genome is surrounded by the capsid, a protein coat, which together with the genome

constitutes the nucleocapsid. The nucleocapsid of complex viruses may be surrounded by an additional protein covering, which in enveloped viruses has also a lipid bilayer covering it that contains membrane glycoproteins functioning as ion channels. The ion channels of enveloped viruses, such as influenza A, influenza B, and influenza C virus as well as the human immunodeficiency virus type 1 (HIV-1) form homo-oligomers of short membrane proteins of ~100 amino acids in length. These channels are called M2 (influenza A), NB (influenza B), CM2 (influenza C), Vpu (HIV-1) (93, 96, 370), and Vpr (HIV-1) (304).

The M2 protein from the influenza A virus is a minimalistic primitive ion channel, which has only one 22-residue-long transmembrane domain. Most likely four of these domains assemble in a tetrameric ion channel selective for protons (305, 306). Protons are conducted through the channel pore in response to applied membrane voltage. Proton selectivity of these channels, which is ensured by the presence of four histidines, one from each of the four helices, is essential to viral function. The channels are blocked by the drug amantadine, the only drug against influenza (251). M2, NB, CM2, and Vpu proteins do not share any sequence homology, although they have in common an amino acid sequence of ~22–26 residues with a high content of hydrophobic residues corresponding to the transmembrane domain. NB, Vpu, and Vpr are selective for cations (93, 304, 370), whereas the ion selectivity of CM2 has still to be determined. The exact role of NB and CM2 in the life cycles of the viruses is not yet identified, although they may also play a role in virus entry into a host cell (96). The ion channel activity of Vpu is thought to be associated with the ability of Vpu to facilitate the budding of new virus particles. Except for a partial high-resolution structure available for Vpu, there is no higher order structure available for any of the viral ion channels (251). Another recently identified viral ion channel is the *Chlorella* virus PBCV-1 Kcv protein. A distinguishing property of the Kcv ion channel is its high selectivity for potassium, which is believed to be critical for virus replication, since blocking the channel by amantadine or barium also inhibits virus plaque formation (308).

VII. APPLICATIONS OF MICROBIAL ION CHANNELS AND TOXINS IN NANOTECHNOLOGY AND MEDICINE

Membrane proteins and peptides that form pores and channels in bilayers of biological membranes comprise a diverse class of molecules. The diversity of regulation and selectivity of these membrane pores together with recent advances in redesigning these pro-

teins by means of molecular biology and chemical technology provide excellent prospects for building custom molecules with wide-ranging biotechnological applications. Studies on microbial ion channels have been primarily driven by curiosity to understand structure and function, physiological role, as well as evolutionary origins of these fascinating molecules. Inevitably, as a byproduct of the basic research on these molecules, practical applications in nanotechnology and medicine have recently begun to emerge. The following examples of practical applications resulting from the research on bacterial mechanosensitive channels and the α-hemolysin toxin may illustrate this.

The MscL channel of *E. coli* was used as a template to construct a light-driven channel-nanovalve (168). For this purpose, light-sensitive synthetic compounds that undergo light-induced charge separation were attached to the channel molecule allowing the MscL nanovalve to be opened by long-wavelength ultraviolet radiation and closed by visible light. MscL was subsequently also converted into a pH-sensitive nanovalve. The opening and closing of this pH-sensitive channel can be fine-tuned by changing the pK_a of the chemical compounds modulating the MscL properties (167). Thus the modified MscL channel can be reversibly opened and closed by light instead of by membrane tension. Such a light-driven nanovalve could, for example, find applications in pharmaceutical industry in liposome-based drug delivery systems.

Recently, it has also been recognized that bacterial MscL and MscS channels have a potential as selective targets for novel types of antibiotics (272). Both channels not only can be opened by amphipaths (235, 237) but also by parabens, the alkyl esters of *p*-hydroxybenzoic acid as well as eriochrome cyanine R, a biological stain commonly used as a spectrophotometric reagent for the detection of aluminium (Nguyen and Martinac, unpublished data). The difference between the action of amphipaths and parabens is that parabens appear to interact directly with the gate of the channels (272) and not indirectly via the lipid bilayer, although a recent study seems to suggest that parabens may also act on the bacterial MS channels through their action on the lipid bilayer (151). One could envisage that the novel antibiotics based on parabens or eriochrome cynanine R as lead compounds, for example, would work as channel openers of MscL and MscS. Opening of the large pores of these MS channels should in turn compromise cellular turgor of bacterial cells leading to inhibition of cell growth and proliferation. Given that, to date, MscL has been identified in over 120 prokaryotic species, including many bacterial pathogens (307), but its homologs have not been found in animal and human cells (117), this channel in particular appears as an excellent target for the novel type of antibacterial agents. An antibiotic targeting MscL could be expected to be broad-spectrum, selective for a range of pathogenic bacteria and most likely having minimal side effects to infected patients.

Recent experimental studies exploring a possibility of using the α-hemolysin protein as a model system to decipher ionic signature patterns in the genetic code of nucleic acids present an example of a practical application of basic research on microbial toxins in nanotechnology (40, 61). This application of α-hemolysin is based on the fact that single-stranded nucleic acid polymers can be transported across an α-hemolysin channel under the action of an applied electric field. Given that the translocation of the nucleic acid polymers causes transient blockades in the ion current through the channel pore and each type of nucleic acid seems to have a characteristic "current signature," the α-hemolysin channel could thus function as a "sequencing nano-device." Recently, the physical and chemical details of the interactions between polymer, channel, and ionic solution that lead to the electric current blockade events have been investigated.

Furthermore, the exchange of cationic α-helical peptides between the bulk aqueous phase and the transmembrane β-barrel of the α-hemolysin protein pore were examined at the single-molecule level (254). This exchange was found to be strongly dependent on voltage and peptide length. At high transmembrane potentials, the alanine-based peptides, which include bulky lysine side chains, were found to bind more strongly to the lumen of the α-hemolysin pore than highly flexible polyethylene glycols, for example. In contrast, the peptides bind weakly to the lumen of the pore and the affinity decreases with the peptide length at zero transmembrane potential. Consequently, these results indicate that α-hemolysin may also serve as a versatile nano-device for examining the interactions between positively charged signal peptides and a pore of membrane-spanning β-sheets. In addition to α-hemolysin, numerous other pore-forming peptides are being developed as antimicrobial agents with potential application as antitumorigenic agents as well as biosensors for a range of different analytes (287).

As shown here, besides gaining further knowledge from microbial channels, some of these channels can be used as tools in further research or even in therapy. As another example, transgenic channelrhodopsin of *Chlamydomonas* has become a tool to depolarize neurons with light (291, 341). This then allows us to investigate the roles of the targeted neurons in the network of behaving animals. Other technological opportunities are currently being explored. Besides the existing channel blockers in cardiological use, blockers and activators of other channels hold great promise in medicine, since all cells in the human body, excitable or not, have ion channels in their plasma membrane as well as organelle membranes. Microbial ion channels, with their fundamental similarity to human channels and

their endless variations reflecting microbial diversity, will continue to figure heavily in biomedical research, development, and practice.

VIII. CONCLUSIONS AND OUTLOOK

A. Possible Physiological Roles of Ion Channels in Microbes

The achievement and intellectual significance of the high-resolution structures of microbial channels are indeed astounding. In contrast, current understanding of the physiological roles of these channels in the microbes themselves lags behind. As stated at the outset of this review, ion-channel studies are rooted in animal physiology, especially neurobiology. The study of *Paramecium* ion channels reinforced the connection between channels and motile behavior, even though a *Paramecium* is but a single cell (see sect. IV*A*). Recent research presents two egregious disconnects between motile behavior and ion channels. First, two major models of microbial motile behaviors are currently understood mechanistically without the involvement of ion channels. *E. coli* chemotaxis is understood as a series of phosphate transfers from the receptor to the effector molecules, without an ionic component (89) (although the flagellar motor is constantly driven by H^+ or Na^+). cAMP taxis of *Dictyostelium* amoebae is said to begin with a G protein-coupled receptor and proceed with a series of phosphorylations, again without an ionic component in signal transduction (see sect. IV*B1*). Second, as evident throughout the entire review above, microbes that are immotile and do not have overt animal-like behavior nonetheless have various types of ion channels found in animals. While we do not yet know the true physiological roles of most of the identified ion channels in microbes, it is clear that they function far beyond regulating motilities.

The role of the mechanosensitive channels in protecting bacteria from hyposmotically induced lysis is now well established (see sect. II). The roles of ion-specific channels in microbes, however, are largely unknown. This is especially frustrating, since they include channels in well-known model microbes, such as Kch of *E. coli* (see sect. III*E*) as well as Yvc1 (see sect. IX*C1B*) and Tok1 (see sect. IV*C2*) of *S. cerevisiae*. Knocking out *kch*, *yvc1*, or *tok1* resulted in no discernable growth phenotype in various cultures or under various stresses. These genes, together with some 30% of the genes in the *E. coli* or yeast genome, are annotated as being "nonessential," meaning that they are not required for growth in the pampered conditions of the laboratory. The near-universal existence of ion-channel genes in the highly streamlined microbial genomes, however, strongly indicates selective advantages they confer. It therefore seems clear that these

channels are employed to handle environmental challenges, which we have yet to simulate in the laboratory. The role of the mechanosensitive channels in hyposmotic stress (see sect. II) and ClC-ec1 in extreme acid-resistance response are cases in point (see sect. III*D*). A major task for microbial physiologists now is to find the environmental stresses, in which various microbial channels are called upon to function. It seems likely that these ion channels are components of novel signal transduction pathways.

As reviewed here, microbes harbor a large variety of ion channels in their cell membranes (further reading on bacterial ion channels can be found in Kubalski and Martinac, Ref. 179). The cytoplasmic membranes of bacteria, archaea, algae, and fungi play an essential role in energy transduction that requires tight regulation of ion channels to allow cellular functions. A leaky membrane would not allow for energy transfer according to the chemiosmotic theory (249), because membrane potential is closely linked to proton and sodium electrochemical gradient, which provide an interconvertible energy source that links the chemical energy of the cell to membrane transport and motility (37). Another component contributing to membrane potential in bacterial cells is the K^+ gradient across the cell membrane, since intracellular K^+ in most microbes ranges between 300 and 700 mM. Compared with animal cells, whose resting membrane potential is mainly determined by the K^+ gradient, membrane potential in bacterial cells, for example, is much more negative ranging between -120 and -200 mV, indicating the importance of the proton pumping and sodium-motive force in determining the resting membrane potential in bacteria. Given that the cytoplasmic pH is relatively constant, varying within a narrow range of pH 6.0 for acidophiles and pH 8.5 for some alkalophiles, the pH gradient in microbes varies significantly with the pH of the environment with the consequence that the membrane potential component of the proton and sodium electrochemical gradient varies with external pH (35, 37).

It is obvious that, with such high values for the membrane potential, strong driving forces exist for ion movements through ion channels in bacterial membranes. Given the very small capacitance of the cytoplasmic membrane of a single bacterial or archaeal cells ($\sim$0.1 pF), only a very small number of ions flowing through an ion channel would suffice to cause a substantial change in the resting membrane potential (35). Consequently, most of the time ion channels must remain tightly closed and open only transiently to ensure undisturbed energy transduction in a bacterial cell. MS channels (238) are an exception to this rule as they have evolved specifically to serve as emergency valves for fast release of osmolytes in osmotically challenged bacterial cells. A specific role for K^+ or any other type of ion channels in most microbes has not yet been established, although K^+ channels may, for

example, serve as efflux systems, when fast potassium efflux or rapid hyperpolarization is required. For such physiological studies, development of methods to monitor the membrane potential in vivo from these microbes seems necessary. Although TPP has been successfully used to monitor slow changes in membrane potential, dye-based fluorescent molecules may be useful for faster reactions. Alternately, GFP conjugated to a voltage sensor may also be used in a less invasive manner.

B. Microbial Channels, A Treasure Trove

Life originated from microbes (Fig. 1). They have dominated this planet in number, in mass, and in variety, and they will continue to dominate in the future. Although we do not have instinctive emotional connections to microbes as we have with dogs, cats, and pandas, their importance cannot be denied. If biology is to be a comprehensive understanding of all life forms, we need to pay more attention to microbes.

The biological world is vast. The six "model organisms" chosen for mechanistic investigations by contemporary biologists (the mouse, the fly, the worm, the cress, budding yeast, and *E. coli*) do not even begin to capture the tremendous variations in life forms and life-styles. Such variations are especially evident among microbes. They have conquered nearly all imaginable niches of the planet, in deserts, in ice, deep underground, fathoms beneath the oceans, as well as in and on other life forms. Some thrive in extreme pH, salinity, temperature, aridity, or redox environments. Some even derive energy from sources not traceable to the sun. There are dazzling varieties even among the more familiar microbes: "the swimming neuron" *Paramecium*, the sociable amoebae *Dictyostelium*, and the plant-animal chimera *Clamydomonas*. From phenomena that capture our visual imagination such as bacterial bioluminescence to those that seem beyond our awareness such as metabolism miles under our feet, the microbial world provides endless fascinating frontier for exploration and investigation. Fascinating puzzles beckon the curious mind. Why should a unicellular *Paramecium* have more ion-channel genes than humans? How come the chemotactic migration of *Dictyostelium* amoeboid chemotaxis does not seem to employ ion channels? What are K^+- or Na^+-specific channels for in bacteria and archaea? Why would *Synechocystis* PCC6803 need a glutamate receptor channel? Answers to these questions on "molecular natural history" will certainly enrich our understanding of our living planet.

Even if our biology is ultimately selfish, aiming only at the betterment of human life, understanding microbes is still of utmost importance. History has shown that we learned about intermediary metabolism from studying yeast, learned about photosynthesis from algae, and about DNA, RNA, and their workings from bacteria and their viruses. As to the ion channels reviewed here, we now learned about mechanosensitivity, voltage sensitivity, and ion filtration from microbial ion channels. These momentous advances in our understanding are no accident. On the one hand, evolution dictates that important molecular mechanisms evolve early and therefore are universal, existing in microbes as well as macrobes. On the other hand, microbes offer laboratory advantages for molecular biology, genetics, and crystallography. We can therefore look forward to solving additional molecular mysteries from the study of microbes and their ion channels. Besides those reviewed here, such channels as the sensory channels (e.g., TRPs) and channels gated by various ligand (e.g., neurotransmitter) may also find their roots in the vast and varied microbial world, making their studies easier and deeper.

Beyond understanding, we can now also look forward to the use of microbial ion channels in biomedical practice. As described in section VII, the days may be near when we can sequence DNA through channels, release drugs through engineered MscL, effectively kill pathogens by targeting their channels, or even regulate the behavior of animals and the mental state of humans by opening engineered channels in their brains with a flash of light!

REFERENCES

1. **Accardi A, Kolmakova-Partensky L, Williams C, Miller C.** Ionic currents mediated by a prokaryotic homologue of CLC Cl$^-$ channels. *J Gen Physiol* 123: 109–119, 2004.
2. **Ajouz B, Berrier C, Besnard M, Martinac B, Ghazi A.** Contributions of the different extramembranous domains of the mechanosensitive ion channel MscL to its response to membrane tension. *J Biol Chem* 275: 1015–1022, 2000.
3. **Alabi AA, Bahamonde MI, Jung HJ, Kim JI, Swartz KJ.** Portability of paddle motif function and pharmacology in voltage sensors. *Nature* 450: 370–375, 2007.
4. **Alvis SJ, Williamson IM, East JM, Lee AG.** Interactions of anionic phospholipids and phosphatidylethanolamine with the potassium channel KcsA. *Biophys J* 85: 3828–3838, 2003.

5. **Anishkin A, Gendel V, Sharifi NA, Chiang CS, Shirinian L, Guy HR, Sukharev S.** On the conformation of the COOH-terminal domain of the large mechanosensitive channel MscL. *J Gen Physiol* 121: 227–244, 2003.

6. **Anishkin A, Sukharev S.** Water dynamics and dewetting transitions in the small mechanosensitive channel MscS. *Biophys J* 86: 2883–2895, 2004.

7. **Arenkiel BR, Peca J, Davison IG, Feliciano C, Deisseroth K, Augustine GJ, Ehlers MD, Feng G.** In vivo light-induced activation of neural circuitry in transgenic mice expressing channelrhodopsin-2. *Neuron* 54: 205–218, 2007.

8. **Arinaminpathy Y, Biggin PC, Shrivastava IH, Sansom MS.** A prokaryotic glutamate receptor: homology modelling and molecular dynamics simulations of GluR0. *FEBS Lett* 553: 321–327, 2003.

9. **Aury JM, Jaillon O, Duret L, Noel B, Jubin C, Porcel BM, Segurens B, Daubin V, Anthouard V, Aiach N, Arnaiz O, Billaut A, Beisson J, Blanc I, Bouhouche K, Camara F, Duharcourt S, Guigo R, Gogendeau D, Katinka M, Keller AM, Kissmehl R, Klotz C, Koll F, Le Mouel A, Lepere G, Malinsky S, Nowacki M, Nowak JK, Plattner H, Poulain J, Ruiz F, Serrano V, Zagulski M, Dessen P, Betermier M, Weissenbach J, Scarpelli C, Schachter V, Sperling L, Meyer E, Cohen J, Wincker P.** Global trends of whole-genome duplications revealed by the ciliate *Paramecium tetraurelia*. *Nature* 444: 171–178, 2006.

10. **Avidor-Reiss T, Maer AM, Koundakjian E, Polyanovsky A, Keil T, Subramaniam S, Zuker CS.** Decoding cilia function: defining specialized genes required for compartmentalized cilia biogenesis. *Cell* 117: 527–539, 2004.

11. **Baker KA, Tzitzilonis C, Kwiatkowski W, Choe S, Riek R.** Conformational dynamics of the KcsA potassium channel governs gating properties. *Nat Struct Mol Biol* 14: 1089–1095, 2007.

12. **Bamann C, Kirsch T, Nagel G, Bamberg E.** Spectral characteristics of the photocycle of channelrhodopsin-2 and its implication for channel function. *J Mol Biol* 375: 686–694, 2008.

13. **Bass RB, Strop P, Barclay M, Rees D.** Crystal structure of *Escherichia coli* MscS, a voltage-modulated and mechanosensitive channel. *Science* 298: 1582–1587, 2002.

14. **Beck C, Uhl R.** On the localization of voltage-sensitive calcium channels in the flagella of *Chlamydomonas reinhardtii*. *J Cell Biol* 125: 1119–1125, 1994.

15. **Beck M, Lucic V, Forster F, Baumeister W, Medalia O.** Snapshots of nuclear pore complexes in action captured by cryo-electron tomography. *Nature* 449: 611–615, 2007.

16. **Beckstein O, Sansom MS.** A hydrophobic gate in an ion channel: the closed state of the nicotinic acetylcholine receptor. *Phys Biol* 3: 147–159, 2006.

17. **Beckstein O, Sansom MS.** The influence of geometry, surface character, and flexibility on the permeation of ions and water through biological pores. *Phys Biol* 1: 42–52, 2004.

18. **Beckstein O, Sansom MS.** Liquid-vapor oscillations of water in hydrophobic nanopores. *Proc Natl Acad Sci USA* 100: 7063–7068, 2003.

19. **Berrier C, Besnard M, Ajouz B, Coulombe A, Ghazi A.** Multiple mechanosensitive ion channels from *Escherichia coli*, activated at different thresholds of applied pressure. *J Membr Biol* 151: 175–187, 1996.

20. **Berrier C, Coulombe A, Houssin C, Ghazi A.** A patch-clamp study of ion channels of inner and outer membranes and of contact zones of *E. coli*, fused into giant liposomes Pressure-activated channels are localized in the inner membrane. *FEBS Lett* 259: 27–32, 1989.

21. **Bertl A, Slayman CL.** Cation-selective channels in the vacuolar membrane of *Saccharomyces*: dependence on calcium, redox state, voltage. *Proc Natl Acad Sci USA* 87: 7824–7828, 1990.

22. **Betanzos M, Chiang CS, Guy HR, Sukharev S.** A large iris-like expansion of a mechanosensitive channel protein induced by membrane tension. *Nat Struct Biol* 9: 704–710, 2002.

23. **Bezanilla F, Perozo E.** Structural biology. Force and voltage sensors in one structure. *Science* 298: 1562–1563, 2002.

24. **Bhakdi S, Tranum-Jensen J.** Alpha-toxin of *Staphylococcus aureus*. *Microbiol Rev* 55: 733–751, 1991.

25. **Bilston LE, Mylvaganam K.** Molecular simulations of the large conductance mechanosensitive (MscL) channel under mechanical loading. *FEBS Lett* 512: 185–190, 2002.

26. **Blanchet J, Pilote S, Chahine M.** Acidic residues on the voltage-sensor domain determine the activation of the NaChBac sodium channel. *Biophys J* 92: 3513–3523, 2007.

27. **Blount PSS, Moe P, Martinac B, Kung C.** Mechanosensitive channels in bacteria. *Methods Enzymol* 294: 458–482, 1999.

28. **Blount P, Sukharev SI, Moe P, Kung C.** Mechanosensitive channels of *E. coli:* a genetic and molecular dissection. *Biol Bull* 192: 126–127, 1997.

29. **Blount P, Sukharev SI, Moe PC, Schroeder MJ, Guy HR, Kung C.** Membrane topology and multimeric structure of a mechanosensitive channel protein of *Escherichia coli*. *EMBO J* 15: 4798–4805, 1996.

30. **Blount P, Sukharev SI, Schroeder MJ, Nagle SK, Kung C.** Single residue substitutions that change the gating properties of a mechanosensitive channel in *Escherichia coli*. *Proc Natl Acad Sci USA* 93: 11652–11657, 1996.

31. **Blunck R, Cordero-Morales JF, Cuello LG, Perozo E, Bezanilla F.** Detection of the opening of the bundle crossing in KcsA with fluorescence lifetime spectroscopy reveals the existence of two gates for ion conduction. *J Gen Physiol* 128: 569–581, 2006.

32. **Blunck R, Starace DM, Correa AM, Bezanilla F.** Detecting rearrangements of shaker and NaChBac in real-time with fluorescence spectroscopy in patch-clamped mammalian cells. *Biophys J* 86: 3966–3980, 2004.

33. **Boeckstaens M, Andre B, Marini AM.** The yeast ammonium transport protein Mep2 and its positive regulator, the Npr1 kinase, play an important role in normal and pseudohyphal growth on various nitrogen media through retrieval of excreted ammonium. *Mol Microbiol* 64: 534–546, 2007.

34. **Bonilla M, Cunningham KW.** Mitogen-activated protein kinase stimulation of Ca^{2+} signaling is required for survival of endoplasmic reticulum stress in yeast. *Mol Biol Cell* 14: 4296–4305, 2003.

35. **Booth IR.** Regulation of cytoplasmic pH in bacteria. *Microbiol Rev* 49: 359–378, 1985.

36. **Booth IR, Edwards MD, Black S, Schumann U, Miller S.** Mechanosensitive channels in bacteria: signs of closure? *Nat Rev Microbiol* 5: 431–440, 2007.

37. **Booth IR, Edwards MD, Murray E, Miller S.** The role of bacterial channels in cell physiology. In: *Bacterial Ion Channels and Their Eukaryotic Homologues*, edited by Kubalski A, Martinac B. Washington, DC: ASM, 2005, p. 291–312.

38. **Booth IR, Louis P.** Managing hypoosmotic stress: aquaporins and mechanosensitive channels in Escherichia coli. *Curr Opin Microbiol* 2: 166–169, 1999.

39. **Brehm P, Eckert R.** Calcium entry leads to inactivation of calcium channel in *Paramecium*. *Science* 202: 1203–1206, 1978.

40. **Butler TZ, Gundlach JH, Troll M.** Ionic current blockades from DNA and RNA molecules in the alpha-hemolysin nanopore. *Biophys J* 93: 3229–3240, 2007.

41. **Catterall WA.** Structure and function of voltage-gated ion channels. *Trends Neurosci* 16: 500–506, 1993.

42. **Chakrapani S, Cordero-Morales JF, Perozo E.** A quantitative description of KcsA gating I: macroscopic currents. *J Gen Physiol* 130: 479–496, 2007.

43. **Chakrapani S, Cordero-Morales JF, Perozo E.** A quantitative description of KcsA gating II: single-channel currents. *J Gen Physiol* 130: 479–496, 2007.

44. **Chang G, Spencer RH, Lee AT, Barclay MT, Rees DC.** Structure of the MscL homolog from *Mycobacterium tuberculosis*: a gated mechanosensitive ion channel. *Science* 282: 2220–2226, 1998.

45. **Charest PG, Firtel RA.** Big roles for small GTPases in the control of directed cell movement. *Biochem J* 401: 377–390, 2007.

46. **Charest PG, Firtel RA.** Feedback signaling controls leading-edge formation during chemotaxis. *Curr Opin Genet Dev* 16: 339–347, 2006.

47. **Chen GQ, Cui C, Mayer ML, Gouaux E.** Functional characterization of a potassium-selective prokaryotic glutamate receptor. *Nature* 402: 817–821, 1999.

48. **Chen L, Iijima M, Tang M, Landree MA, Huang YE, Xiong Y, Iglesias PA, Devreotes PN.** PLA$_2$ and PI3K/PTEN pathways act in parallel to mediate chemotaxis. *Dev Cell* 12: 603–614, 2007.

49. **Chen R, Yan H, Zhao KN, Martinac B, Liu GB.** Comprehensive analysis of prokaryotic mechanosensation genes: their characteristics in codon usage. *DNA Sequence* 18: 269–278, 2007.

50. **Chiu PL, Pagel MD, Evans J, Chou HT, Zeng X, Gipson B, Stahlberg H, Nimigean CM.** The structure of the prokaryotic cyclic nucleotide-modulated potassium channel MloK1 at 16 A resolution. *Structure* 15: 1053–1064, 2007.

51. **Christensen AP, Corey DP.** TRP channels in mechanosensation: direct or indirect activation? *Nat Rev Neurosci* 8: 510–521, 2007.

52. **Clapham DE.** TRP channels as cellular sensors. *Nature* 426: 517–524, 2003.

53. **Clayton GM, Silverman WR, Heginbotham L, Morais-Cabral JH.** Structural basis of ligand activation in a cyclic nucleotide regulated potassium channel. *Cell* 119: 615–627, 2004.

54. **Colombo G, Marrink SJ, Mark AE.** Simulation of MscL gating in a bilayer under stress. *Biophys J* 84: 2331–2337, 2003.

55. **Cordero-Morales JF, Cuello LG, Perozo E.** Voltage-dependent gating at the KcsA selectivity filter. *Nat Struct Mol Biol* 13: 319–322, 2006.

56. **Cordero-Morales JF, Jogini V, Lewis A, Vasquez V, Cortes DM, Roux B, Perozo E.** Molecular driving forces determining potassium channel slow inactivation. *Nat Struct Mol Biol* 14: 1062–1069, 2007.

57. **Corry B.** An energy-efficient gating mechanism in the acetylcholine receptor channel suggested by molecular and Brownian dynamics. *Biophys J* 90: 799–810, 2006.

58. **Corry B, Martinac B.** Computational studies of bacterial mechanosensitive channels. In: *Mechanosensitive Ion Channels*, edited by Kamkin A, Kiseleva I. Heidelberg: Springer-Verlag, 2007, p. 103–116.

59. **Corry B, Rigby P, Liu ZW, Martinac B.** Conformational changes involved in MscL channel gating measured using FRET spectroscopy. *Biophys J* 89: L49–51, 2005.

60. **Cortes DM, Cuello LG, Perozo E.** Molecular architecture of full-length KcsA: role of cytoplasmic domains in ion permeation and activation gating. *J Gen Physiol* 117: 165–180, 2001.

61. **Cozmuta I, O'Keeffe JT, Stolc V.** Hybrid MD-PNP simulations of the alpha-hemolysin open ion currents. *Technical Proceedings of the 2004 NSTI Nanotechnology Conference and Trade Show* 1: 143–146, 2004.

62. **Cruickshank CC, Minchin RF, Le Dain AC, Martinac B.** Estimation of the pore size of the large-conductance mechanosensitive ion channel of *Escherichia coli*. *Biophys J* 73: 1925–1931, 1997.

63. **Csonka LN, Epstein W.** Osmoregulation. In: *Escherichia coli and Salmonella: Cellular and Molecular Biology*, edited by Neidhardt FC, Curtiss R III, Ingraham JL, Lin ECC, Brooks Low K, Magasanik B, Reznikoff WS, Riley M, Schaechter M, Umbarger HE. Washington, DC: ASM, 1996, p. 1210–1225.

64. **Czajkowsky DM, Iwamoto H, Szabo G, Cover TL, Shao Z.** Mimicry of a host anion channel by a *Helicobacter pylori* pore-forming toxin. *Biophys J* 89: 3093–3101, 2005.

65. **De Peyer JE, Machemer H.** Membrane excitability in *Stylonychia*: properties of the two-peak regenerative Ca-response. *J Comp Physiol A Sens Neural Behav Physiol* 121: 15–32, 1977.

66. **Deininger W, Kroger P, Hegemann U, Lottspeich F, Hegemann P.** Chlamyrhodopsin represents a new type of sensory photoreceptor. *EMBO J* 14: 5849–5858, 1995.

67. **Deitmer JW.** Evidence for two voltage-dependent calcium currents in the membrane of the ciliate *Stylonychia*. *J Physiol* 355: 137–159, 1984.

68. **Deitmer JW, Machemer H.** Ion channels and behaviour: ciliates as cellular models. In: *Biological Signal Processing*, edited by Lüttgau HCVCH. Weinheim, 1989, p. 45–63.

69. **Deitmer JW, Machemer H, Martinac B.** Motor control in three types of ciliary organelles in the ciliate *Stylonychia*. *J Comp Physiol A Sens Neural Behav Physiol* 154: 113–120, 1984.

70. **Delmas P, Nauli SM, Li X, Coste B, Osorio N, Crest M, Brown DA, Zhou J.** Gating of the polycystin ion channel signaling complex in neurons and kidney cells. *FASEB J* 18: 740–742, 2004.

71. **Demmers JA, van Dalen A, de Kruijff B, Heck AJ, Killian JA.** Interaction of the K$^+$ channel KcsA with membrane phospholipids as studied by ESI mass spectrometry. *FEBS Lett* 541: 28–32, 2003.

72. **Denis V, Cyert MS.** Internal Ca^{2+} release in yeast is triggered by hypertonic shock and mediated by a TRP channel homologue. *J Cell Biol* 156: 29–34, 2002.

73. **Deol SS, Bond PJ, Domene C, Sansom MS.** Lipid-protein interactions of integral membrane proteins: a comparative simulation study. *Biophys J* 87: 3737–3749, 2004.

74. **Derelle E, Ferraz C, Rombauts S, Rouze P, Worden AZ, Robbens S, Partensky F, Degroeve S, Echeynie S, Cooke R, Saeys Y, Wuyts J, Jabbari K, Bowler C, Panaud O, Piegu B, Ball SG, Ral JP, Bouget FY, Piganeau G, De Baets B, Picard A, Delseny M, Demaille J, Van de Peer Y, Moreau H.** Genome analysis of the smallest free-living eukaryote *Ostreococcus tauri* unveils many unique features. *Proc Natl Acad Sci USA* 103: 11647–11652, 2006.

75. **Dessen P, Zagulski M, Gromadka R, Plattner H, Kissmehl R, Meyer E, Betermier M, Schultz JE, Linder JU, Pearlman RE, Kung C, Forney J, Satir BH, Van Houten JL, Keller AM, Froissard M, Sperling L, Cohen J.** *Paramecium* genome survey: a pilot project. *Trends Genet* 17: 306–308, 2001.

76. **Domene C, Grottesi A, Sansom MS.** Filter flexibility and distortion in a bacterial inward rectifier K$^+$ channel: simulation studies of KirBac1.1. *Biophys J* 87: 256–267, 2004.

77. **Domene C, Sansom MS.** Potassium channel, ions, water: simulation studies based on the high resolution X-ray structure of KcsA. *Biophys J* 85: 2787–2800, 2003.

78. **Domene C, Vemparala S, Klein ML, Venien-Bryan C, Doyle DA.** Role of aromatic localization in the gating process of a potassium channel. *Biophys J* 90: L01–03, 2006.

79. **Doolittle WF.** Phylogenetic classification and the universal tree. *Science* 284: 2124–2129, 1999.

80. **Doyle DA, Morais Cabral J, Pfuetzner RA, Kuo A, Gulbis JM, Cohen SL, Chait BT, MacKinnon R.** The structure of the potassium channel: molecular basis of K$^+$ conduction and selectivity. *Science* 280: 69–77, 1998.

82. **Durell SR, Guy HR.** A family of putative Kir potassium channels in prokaryotes. *BMC Evol Biol* 1: 14, 2001.

83. **Dutzler R, Campbell EB, Cadene M, Chait BT, MacKinnon R.** X-ray structure of a ClC chloride channel at 3.0 A reveals the molecular basis of anion selectivity. *Nature* 415: 287–294, 2002.

84. **Dutzler R, Campbell EB, MacKinnon R.** Gating the selectivity filter in ClC chloride channels. *Science* 300: 108–112, 2003.

85. **Eckert R.** Bioelectric control of ciliary activity. *Science* 176: 473–481, 1972.

86. **Edwards MD, Booth IR, Miller S.** Gating the bacterial mechanosensitive channels: MscS a new paradigm? *Curr Opin Microbiol* 7: 163–167, 2004.

87. **Ehrlich B, Finkelstein A, Forte M, Kung C.** Voltage-dependent calcium channels from *Paramecium* cilia incorporated into planar lipid bilayers. *Science* 225: 427–428, 1984.

88. **Eichinger L, Pachebat JA, Glockner G, Rajandream MA, Sucgang R, Berriman M, Song J, Olsen R, Szafranski K, Xu Q, Tunggal B, Kummerfeld S, Madera M, Konfortov BA, Rivero F, Bankier AT, Lehmann R, Hamlin N, Davies R, Gaudet P, Fey P, Pilcher K, Chen G, Saunders D, Sodergren E, Davis P, Kerhornou A, Nie X, Hall N, Anjard C, Hemphill L, Bason N, Farbrother P, Desany B, Just E, Morio T, Rost R, Churcher C, Cooper J, Haydock S, van Driessche N, Cronin A, Goodhead I, Muzny D, Mourier T, Pain A, Lu M, Harper D, Lindsay R, Hauser H, James K, Quiles M, Madan Babu M, Saito T, Buchrieser C, Wardroper A, Felder M, Thangavelu M, Johnson D, Knights A, Loulseged H, Mungall K, Oliver K, Price C, Quail MA, Urushihara H, Hernandez J, Rabbinowitsch E, Steffen D, Sanders M, Ma J, Kohara Y, Sharp S, Simmonds M, Spiegler S, Tivey A, Sugano S, White B, Walker D, Woodward J, Winckler T, Tanaka Y, Shaulsky G, Schleicher M, Weinstock G, Rosenthal A, Cox EC, Chisholm RL, Gibbs R, Loomis WF, Platzer M, Kay RR, Williams J, Dear PH, Noegel AA, Barrell B, Kuspa A.** The genome of the social amoeba *Dictyostelium discoideum*. *Nature* 435: 43–57, 2005.

89. **Eisenbach M.** A hitchhiker's guide through advances and conceptual changes in chemotaxis. *J Cell Physiol* 213: 574–580, 2007.

90. **Elmore DE, Dougherty DA.** Molecular dynamics simulations of wild-type and mutant forms of the *Mycobacterium tuberculosis* MscL channel. *Biophys J* 81: 1345–1359, 2001.

91. **Enkvetchakul D, Jeliazkova I, Nichols CG.** Direct modulation of Kir channel gating by membrane phosphatidylinositol 4,5-bisphosphate. *J Biol Chem* 280: 35785–35788, 2005.

92. **Ernst OP, Sanchez M, Daldrop P, Tsunoda S.** Phtoactivation of channelrhodopsin. *J Biol Chem.* In press.

93. **Ewart GD, Sutherland T, Gage PW, Cox GB.** The Vpu protein of human immunodeficiency virus type 1 forms cation-selective ion channels. *J Virol* 70: 7108–7115, 1996.

94. **Fairman C, Zhou X, Kung C.** Potassium uptake through the TOK1 K^+ channel in the budding yeast. *J Membr Biol* 168: 149–157, 1999.

95. **Fischer M, Schnell N, Chattaway J, Davies P, Dixon G, Sanders D.** The *Saccharomyces cerevisiae* CCH1 gene is involved in calcium influx and mating. *FEBS Lett* 419: 259–262, 1997.

96. **Fischer WB, Sansom MS.** Viral ion channels: structure and function. *Biochim Biophys Acta* 1561: 27–45, 2002.

97. **Flis K, Bednarczyk P, Hordejuk R, Szewczyk A, Berest V, Dolowy K, Edelman A, Kurlandzka A.** The Gef1 protein of *Saccharomyces cerevisiae* is associated with chloride channel activity. *Biochem Biophys Res Commun* 294: 1144–1150, 2002.

98. **Fong RN, Kim KS, Yoshihara C, Inwood WB, Kustu S.** The W148L substitution in the *Escherichia coli* ammonium channel AmtB increases flux and indicates that the substrate is an ion. *Proc Natl Acad Sci USA* 104: 18706–18711, 2007.

99. **Fountain SJ, Parkinson K, Young MT, Cao L, Thompson CR, North RA.** An intracellular P2X receptor required for osmoregulation in *Dictyostelium discoideum*. *Nature* 448: 200–203, 2007.

100. **Franca-Koh J, Kamimura Y, Devreotes P.** Navigating signaling networks: chemotaxis in *Dictyostelium discoideum*. *Curr Opin Genet Dev* 16: 333–338, 2006.

101. **Frey J, Kuhnert P.** RTX toxins in *Pasteurellaceae*. *Int J Med Microbiol* 292: 149–158, 2002.

102. **Fuhrmann M, Deininger W, Kateriya S, Hegemann P.** Rhodopsin-related protein, cop1, co2 and chop1 in *Chlamydomonas reinhardtii*. *In: Photoreceptors and Light Signaling*, edited by Batschauer A. Cambridge, UK: Royal Society of Chemistry, 2003, p. 124–135.

103. **Fuhrmann M, Stahlberg A, Govorunova E, Rank S, Hegemann P.** The abundant retinal protein of the *Chlamydomonas* eye is not the photoreceptor for phototaxis and photophobic responses. *J Cell Sci* 114: 3857–3863, 2001.

104. **Funamoto S, Meili R, Lee S, Parry L, Firtel RA.** Spatial and temporal regulation of 3-phosphoinositides by PI 3-kinase and PTEN mediates chemotaxis. *Cell* 109: 611–623, 2002.

105. **Gaxiola RA, Yuan DS, Klausner RD, Fink GR.** The yeast CLC chloride channel functions in cation homeostasis. *Proc Natl Acad Sci USA* 95: 4046–4050, 1998.

106. **Gilbert RJ.** Pore-forming toxins. *Cell Mol Life Sci* 59: 832–844, 2002.

107. **Gouaux E, Mackinnon R.** Principles of selective ion transport in channels and pumps. *Science* 310: 1461–1465, 2005.

108. **Govorunova EG, Jung KH, Sineshchekov OA, Spudich JL.** *Chlamydomonas* sensory rhodopsins A and B: cellular content and role in photophobic responses. *Biophys J* 86: 2342–2349, 2004.

109. **Gratia A.** Sur un remarquable example d'antagonisme entre deux souches de colibacille. *Compt Rend Soc Biol* 93: 1040–1042, 1925.

110. **Greene JR, Brown NH, DiDomenico BJ, Kaplan J, Eide DJ.** The GEF1 gene of *Saccharomyces cerevisiae* encodes an integral membrane protein: mutations in which have effects on respiration and iron-limited growth. *Mol Gen Genet* 241: 542–553, 1993.

111. **Guex N, Peitsch MC.** SWISS-MODEL and the Swiss-PdbViewer: an environment for comparative protein modeling. *Electrophoresis* 18: 2714–2723, 1997.

112. **Gullingsrud J, Kosztin D, Schulten K.** Structural determinants of MscL gating studied by molecular dynamics simulations. *Biophys J* 80: 2074–2081, 2001.

113. **Gullingsrud J, Schulten K.** Lipid bilayer pressure profiles and mechanosensitive channel gating. *Biophys J* 86: 3496–3509, 2004.

114. **Gustin MC, Martinac B, Saimi Y, Culbertson MR, Kung C.** Ion channels in yeast. *Science* 233: 1195–1197, 1986.

115. **Gustin MC, Zhou XL, Martinac B, Kung C.** A mechanosensitive ion channel in the yeast plasma membrane. *Science* 242: 762–765, 1988.

116. **Haga N, Forte M, Saimi Y, Kung C.** Microinjection of cytoplasm as a test of complementation in *Paramecium*. *J Cell Biol* 92: 559–564, 1982.

117. **Hamill OP, Martinac B.** Molecular basis of mechanotransduction in living cells. *Physiol Rev* 81: 685–740, 2001.

118. **Hamill OP, Marty A, Neher E, Sakmann B, Sigworth FJ.** Improved patch-clamp techniques for high-resolution current recording from cells and cell-free membrane patches. *Pflügers Arch* 391: 85–100, 1981.

119. **Hamill OP, McBride DW Jr.** Induced membrane hypo/hyper-mechanosensitivity: a limitation of patch-clamp recording. *Annu Rev Physiol* 59: 621–631, 1997.

120. **Hanaoka K, Qian F, Boletta A, Bhunia AK, Piontek K, Tsiokas L, Sukhatme VP, Guggino WB, Germino GG.** Co-assembly of polycystin-1 and -2 produces unique cation-permeable currents. *Nature* 408: 990–994, 2000.

121. **Hartz H, Hegemann P.** Rhodopsin-regulated calcium curents in *Chlamydomonas*. *Nature* 351: 489–491, 1991.

122. **Häse CC, Le Dain AC, Martinac B.** Molecular dissection of the large mechanosensitive ion channel (MscL) of *E. coli:* mutants with altered channel gating and pressure sensitivity. *J Membr Biol* 157: 17–25, 1997.

123. **Häse CC, Le Dain AC, Martinac B.** Purification and functional reconstitution of the recombinant large mechanosensitive ion channel (MscL) of *Escherichia coli. J Biol Chem* 270: 18329–18334, 1995.

124. **Häse CC, Minchin RF, Kloda A, Martinac B.** Cross-linking studies and membrane localization and assembly of radiolabelled large mechanosensitive ion channel (MscL) of *Escherichia coli. Biochem Biophys Res Commun* 232: 777–782, 1997.

125. **Haswell ES, Meyerowitz EM.** MscS-like proteins control plastid size and shape in *Arabidopsis thaliana. Curr Biol* 16: 1–11, 2006.

126. **Haynes WJ, Kung C, Saimi Y, Preston RR.** An exchanger-like protein underlies the large Mg^{2+} current in *Paramecium. Proc Natl Acad Sci USA* 99: 15717–15722, 2002.

127. **Haynes WJ, Ling KY, Preston RR, Saimi Y, Kung C.** The cloning and molecular analysis of pawn-B in *Paramecium tetraurelia. Genetics* 155: 1105–1117, 2000.

128. **Haynes WJ, Ling KY, Saimi Y, Kung C.** PAK paradox: *Paramecium* appears to have more K^+-channel genes than humans. *Eukaryotic Cell* 2: 737–745, 2003.

129. **Haynes WJ, Vaillant B, Preston RR, Saimi Y, Kung C.** The cloning by complementation of the pawn-A gene in *Paramecium. Genetics* 149: 947–957, 1998.

130. **Hegemann P.** Vision in microalgae. *Planta* 203: 265–274, 1997.

131. **Hegemann P, Neumeier K, Hegemann U, Kuehnle E.** The role of calcium in *Chlamydomonas* photomovement responses as analysed by calcium channel inhibitors. *Photochem Photobiol* 52: 575–583, 1990.

132. **Hegermann J, Overbeck J, Schrempf H.** In vivo monitoring of the potassium channel KcsA in *Streptomyces lividans* hyphae using immuno-electron microscopy and energy-filtering transmission electron microscopy. *Microbiology* 152: 2831–2841, 2006.

133. **Hellmer J, Zeilinger C.** MjK1, a K^+ channel from *M. jannaschii*, mediates K^+ uptake and K^+ sensitivity in *E. coli. FEBS Lett* 547: 165–169, 2003.

134. **Hodgkin AL.** The ionic basis of nervous conduction (http://nobelprize.org/medicine/laureates/1963/hodgkin-lecture.html).

135. **Holland EM, Braun FJ, Nonnengasser C, Harz H, Hegemann P.** The nature of rhodopsin-triggered photocurrents in *Chlamydomonas*. I. Kinetics and influence of divalent ions. *Biophys J* 70: 924–931, 1996.

136. **Holland EM, Harz H, Uhl R, Hegemann P.** Control of phobic behavioral responses by rhodopsin-induced photocurrents in *Chlamydomonas. Biophys J* 73: 1395–1401, 1997.

137. **Huang K, Diener DR, Mitchell A, Pazour GJ, Witman GB, Rosenbaum JL.** Function and dynamics of PKD2 in *Chlamydomonas reinhardtii* flagella. *J Cell Biol* 179: 501–514, 2007.

138. **Huang ME, Chuat JC, Galibert F.** A voltage-gated chloride channel in the yeast *Saccharomyces cerevisiae. J Mol Biol* 242: 595–598, 1994.

139. **Huxley AF.** The quantitative analysis of excitation and conduction in nerve (http://nobelprize.org/nobel_prizes/medicine/laureates/1963/huxley-lecture.html).

140. **Iida H, Nakamura H, Ono T, Okumura MS, Anraku Y.** MID1, a novel *Saccharomyces cerevisiae* gene encoding a plasma membrane protein, is required for Ca^{2+} influx and mating. *Mol Cell Biol* 14: 8259–8271, 1994.

141. **Iida K, Tada T, Iida H.** Molecular cloning in yeast by in vivo homologous recombination of the yeast putative alpha1 subunit of the voltage-gated calcium channel. *FEBS Lett* 576: 291–296, 2004.

142. **Iida K, Teng J, Tada T, Saka A, Tamai M, Izumi-Nakaseko H, Adachi-Akahane S, Iida H.** Essential, completely conserved glycine residue in the domain III S2–S3 linker of voltage-gated calcium channel alpha1 subunits in yeast and mammals. *J Biol Chem* 282: 25659–25667, 2007.

143. **Iijima M, Devreotes P.** Tumor suppressor PTEN mediates sensing of chemoattractant gradients. *Cell* 109: 599–610, 2002.

144. **Iscla I, Levin G, Wray R, Blount P.** Disulfide trapping the mechanosensitive channel MscL into a gating-transition state. *Biophys J* 92: 1224–1232, 2007.

145. **Iyer R, Iverson TM, Accardi A, Miller C.** A biological role for prokaryotic ClC chloride channels. *Nature* 419: 715–718, 2002.

146. **Jennings HS.** *Behavior of Lower Organisms.* Bloomington: Indiana Univ. Press, 1906.

147. **Jiang Y, Lee A, Chen J, Cadene M, Chait BT, MacKinnon R.** Crystal structure and mechanism of a calcium-gated potassium channel. *Nature* 417: 515–522, 2002.

148. **Jiang Y, Lee A, Chen J, Ruta V, Cadene M, Chait BT, MacKinnon R.** X-ray structure of a voltage-dependent K^+ channel. *Nature* 423: 33–41, 2003.

149. **Jiang Y, Pico A, Cadene M, Chait BT, MacKinnon R.** Structure of the RCK domain from the *E. coli* K^+ channel and demonstration of its presence in the human BK channel. *Neuron* 29: 593–601, 2001.

150. **Kamada T.** Some observations on potential differences across the ectoplasm membrane of Paramecium. *J Exp Biol* 11: 94–102, 1934.

151. **Kamaraju K, Akitake B, Sukharev S.** Membrane-perturbing capacity of parabens and their effects on a mechanosensitive channel directly correlate with hydrophobicity (Abstract). *Biophys J* A598, 2008.

152. **Kamiya R, Witman GB.** Submicromolar levels of calcium control the balance of beating between the two flagella in demembranated models of *Chlamydomonas. J Cell Biol* 98: 97–107, 1984.

153. **Kanzaki M, Nagasawa M, Kojima I, Sato C, Naruse K, Sokabe M, Iida H.** Molecular identification of a eukaryotic, stretch-activated nonselective cation channel. *Science* 285: 882–886, 1999.

154. **Kanzaki M, Nagasawa M, Kojima I, Sato C, Naruse K, Sokabe M, Iida H.** Report clarification. *Science* 288: 1347, 2000.

155. **Kateriya S, Nagel G, Bamberg E, Hegemann P.** "Vision" in single-celled algae. *News Physiol Sci* 19: 133–137, 2004.

156. **Keizer-Gunnink I, Kortholt A, Van Haastert PJ.** Chemoattractants and chemorepellents act by inducing opposite polarity in phospholipase C and PI3-kinase signaling. *J Cell Biol* 177: 579–585, 2007.

157. **Ketchum KA, Joiner WJ, Sellers AJ, Kaczmarek LK, Goldstein SA.** A new family of outwardly rectifying potassium channel proteins with two pore domains in tandem. *Nature* 376: 690–695, 1995.

158. **Khademi S, O'Connell J 3rd, Remis J, Robles-Colmenares Y, Miercke LJ, Stroud RM.** Mechanism of ammonia transport by Amt/MEP/Rh: structure of AmtB at 1.35 A. *Science* 305: 1587–1594, 2004.

159. **Kink JA, Maley ME, Preston RR, Ling KY, Wallen-Friedman MA, Saimi Y, Kung C.** Mutations in paramecium calmodulin indicate functional differences between the C-terminal and N-terminal lobes in vivo. *Cell* 62: 165–174, 1990.

160. **Kloda A, Ghazi A, Martinac B.** C-terminal charged cluster of MscL, RKKEE, functions as a pH sensor. *Biophys J* 90: 1992–1998, 2006.

161. **Kloda A, Martinac B.** Mechanosensitive channel of *Thermoplasma,* the cell wall-less archaea: cloning and molecular characterization. *Cell Biochem Biophys* 34: 321–347, 2001.

162. **Kloda A, Martinac B.** Mechanosensitive channels in archaea. *Cell Biochem Biophys* 34: 349–381, 2001.

163. **Kloda A, Martinac B.** Mechanosensitive channels of bacteria and archaea share a common ancestral origin. *Eur Biophys J* 31: 14–25, 2002.

164. **Kloda A, Martinac B.** Molecular identification of a mechanosensitive channel in archaea. *Biophys J* 80: 229–240, 2001.

165. **Kloda A, Martinac B.** Structural and functional differences between two homologous mechanosensitive channels of *Methanococcus jannaschii. EMBO J* 20: 1888–1896, 2001.

166. **Kloda A, Petrov E, Meyer GR, Nguyen T, Hurst A, Hool L, Martinac B.** Mechanosensitive channel of large conductance. *Intern J Biochem Cell Biol* 40: 164–169, 2008.

167. **Kocer A, Walko M, Bulten E, Halza E, Feringa BL, Meijberg W.** Rationally designed chemical modulators convert a bacterial channel protein into a pH-sensory valve. *Angew Chem Int Ed Engl* 45: 3126–3130, 2006.

168. **Kocer A, Walko M, Meijberg W, Feringa BL.** A light-actuated nanovalve derived from a channel protein. *Science* 309: 755–758, 2005.

169. **Koishi R, Xu H, Ren D, Navarro B, Spiller BW, Shi Q, Clapham DE.** A superfamily of voltage-gated sodium channels in bacteria. *J Biol Chem* 279: 9532–9538, 2004.

170. **Kong YF, Shen YF, Warth TE, Ma JP.** Conformational pathways in the gating of *Escherichia coli* mechanosensitive channel. *Proc Natl Acad Sci USA* 99: 5999–6004, 2002.

171. **Konisky J.** Colicins and other bacteriocins with established modes of action. *Annu Rev Microbiol* 36: 125–144, 1982.

172. **Koprowski P, Kubalski A.** C termini of the *Escherichia coli* mechanosensitive ion channel (MscS) move apart upon the channel opening. *J Biol Chem* 278: 11237–11245, 2003.

173. **Koprowski P, Kubalski A.** Voltage-independent adaptation of mechanosensitive channels in *Escherichia coli* protoplasts. *J Membr Biol* 164: 253–262, 1998.

174. **Korthol A, King JS, Keizer-Gunnink I, Harwood AJ, Van Haastert PJ.** Phospholipase C regulation of phosphatidylinositol 3,4,5-trisphosphate-mediated chemotaxis. *Mol Biol Cell* 18: 4772–4779, 2007.

175. **Kottgen M.** TRPP2 and autosomal dominant polycystic kidney disease. *Biochim Biophys Acta* 1772: 836–850, 2007.

176. **Krasilnikov OV, Sabirov RZ.** Ion transport through channels formed in lipid bilayers by *Staphylococcus aureus* alpha-toxin. *Gen Physiol Biophys* 8: 213–222, 1989.

177. **Kreimer G, Witman GB.** Novel touch-induced, Ca^{2+}-dependent phobic response in a flagellate green alga. *Cell Motil Cytoskeleton* 29: 97–109, 1994.

178. **Kubalski A.** Generation of giant protoplasts of *Escherichia coli* and an inner-membrane anion selective conductance. *Biochim Biophys Acta* 1238: 177–182, 1995.

179. **Kubalski A, Martinac B.** (Editors). *Bacterial Ion Channels and Their Eukaryotic Homologues.* Washington, DC: ASM, 2005.

180. **Kubalski A, Martinac B, Saimi Y.** Proteolytic activation of a hyperpolarization- and calcium-dependent potassium channel in *Paramecium. J Membr Biol* 112: 91–96, 1989.

181. **Kumánovics A, Levin G, Blount P.** Family ties of gated pores: evolution of the sensor module. *FASEB J* 16: 1623–1629, 2003.

182. **Kuner T, Seeburg PH, Guy HR.** A common architecture for K^+ channels and ionotropic glutamate receptors? *Trends Neurosci* 26: 27–32, 2003.

183. **Kung C.** Ion channels of unicellular microbes. In: *Evolution of the First Nervous System,* edited by Anderson PAV. New York: Plenum, 1989, p. 203–214.

184. **Kung C.** A possible unifying principle for mechanosensation. *Nature* 436: 647–654, 2005.

185. **Kung C, Eckert R.** Genetic modification of electric properties in an excitable membrane (paramecium-calcium conductance-electrophysiology measurements-membrane mutant). *Proc Natl Acad Sci USA* 69: 93–97, 1972.

186. **Kung C, Saimi Y, Martinac B.** Mechanosensitive ion channels in microbes and the early evolutionary origin of solvent sensing. In:

Current Topics in Membranes and Transport, edited by Claudio T. New York: Academic, 1990, p. 9451–9455.

187. **Kung Zhou L, Su ZW, Hynes J, Loukin SH, Saimi Y.** Microbial senses and ion channels. In: *Sensing With Ion Channels*, edited by Martinac B. Berlin: Springer-Verlag, 2007, p. 1–23.

188. **Kuo A, Domene C, Johnson LN, Doyle DA, Venien-Bryan C.** Two different conformational states of the KirBac3.1 potassium channel revealed by electron crystallography. *Structure* 13: 1463–1472, 2005.

189. **Kuo A, Gulbis JM, Antcliff JF, Rahman T, Lowe ED, Zimmer J, Cuthbertson J, Ashcroft FM, Ezaki T, Doyle DA.** Crystal structure of the potassium channel KirBac1.1 in the closed state. *Science* 300: 1922–1926, 2003.

190. **Kuo MMC, Kung C, Saimi Y.** K^+ channels: a survey and a case study of Kch of *Escherichia coli*. In: *Bacterial Ion Channels and Their Eukaryotic Homologs*, edited by Kubalski A, Martinac B. Washington, DC: ASM, 2005, p. 1–20.

191. **Kuo MM, Baker KA, Wong L, Choe S.** Dynamic oligomeric conversions of the cytoplasmic RCK domains mediate MthK potassium channel activity. *Proc Natl Acad Sci USA* 104: 2151–2156, 2007.

192. **Kuo MM, Haynes WJ, Loukin SH, Kung C, Saimi Y.** Prokaryotic K^+ channels: from crystal structures to diversity. *FEMS Microbiol Rev* 29: 961–985, 2005.

193. **Kuo MM, Saimi Y, Kung C.** Gain-of-function mutations indicate that *Escherichia coli* Kch forms a functional K^+ conduit in vivo. *EMBO J* 22: 4049–4058, 2003.

194. **Kuo MM, Saimi Y, Kung C, Choe S.** Patch clamp and phenotypic analyses of a prokaryotic cyclic nucleotide-gated K^+ channel using *Escherichia coli* as a host. *J Biol Chem* 282: 24294–24301, 2007.

195. **Kust US, Inwood W.** Biological gas channels for NH_3 and CO_2: evidence that Rh (Rhesus) proteins are CO_2 channels. *Transfus Clin Biol* 13: 103–110, 2006.

196. **Kuwayama H, van Haastert PJ.** cGMP potentiates receptor-stimulated Ca^{2+} influx in *Dictyostelium discoideum*. *Biochim Biophys Acta* 1402: 102–108, 1998.

197. **Kuzmenkin A, Bezanilla F, Correa AM.** Gating of the bacterial sodium channel, NaChBac: voltage-dependent charge movement and gating currents. *J Gen Physiol* 124: 349–356, 2004.

198. **Lakey JH, Slatin SL.** Pore-forming colicins and their relatives. *Curr Top Microbiol Immunol* 257: 131–161, 2001.

199. **Lee JH, Park SJ, Rho SH, Im YJ, Kim MK, Kang GB, Eom SH.** Crystallization and preliminary X-ray crystallographic analysis of the GluR0 ligand-binding core from *Nostoc punctiforme*. *Acta Crystallogr Sect F Struct Biol Cryst Commun* 61: 1020–1022, 2005.

200. **Lee SY, Lee A, Chen J, MacKinnon R.** Structure of the KvAP voltage-dependent K^+ channel and its dependence on the lipid membrane. *Proc Natl Acad Sci USA* 102: 15441–15446, 2005.

201. **Lesage F, Guillemare E, Fink M, Duprat F, Lazdunski M, Romey G, Barhanin J.** A pH-sensitive yeast outward rectifier K^+ channel with two pore domains and novel gating properties. *J Biol Chem* 271: 4183–4187, 1996.

202. **Levina N, Totemeyer S, Stokes NR, Louis P, Jones MA, Booth IR.** Protection of *Escherichia coli* cells against extreme turgor by activation of MscS and MscL mechanosensitive channels: identification of genes required for MscS activity. *EMBO J* 18: 1730–1737, 1999.

203. **Lew RR.** Ionic currents and ion fluxes in *Neurospora crassa* hyphae. *J Exp Bot* 58: 3475–3481, 2007.

204. **Li JB, Gerdes JM, Haycraft CJ, Fan Y, Teslovich TM, May-Simera H, Li H, Blacque OE, Li L, Leitch CC, Lewis RA, Green JS, Parfrey PS, Leroux MR, Davidson WS, Beales PL, Guay-Woodford LM, Yoder BK, Stormo GD, Katsanis N, Dutcher SK.** Comparative genomics identifies a flagellar and basal body proteome that includes the BBS5 human disease gene. *Cell* 117: 541–552, 2004.

205. **Li X, Gutierrez DV, Hanson MG, Han J, Mark MD, Chiel H, Hegemann P, Landmesser LT, Herlitze S.** Fast noninvasive activation and inhibition of neural and network activity by vertebrate rhodopsin and green algae channelrhodopsin. *Proc Natl Acad Sci USA* 102: 17816–17821, 2005.

206. **Li Y, Berke I, Chen L, Jiang Y.** Gating and inward rectifying properties of the MthK K^+ channel with and without the gating ring. *J Gen Physiol* 129: 109–120, 2007.

207. **Li Y, Moe PC, Chandrasekaran S, Booth IR, Blount P.** Ionic regulation of MscK, a mechanosensitive channel from *Escherichia coli*. *EMBO J* 21: 5323–5330, 2002.

208. **Li Y, Wray R, Blount P.** Intragenic suppression of gain-of-function mutations in the *Escherichia coli* mechanosensitive channel, MscL. *Mol Microbiol* 53: 485–495, 2004.

209. **Locke EG, Bonilla M, Liang L, Takita Y, Cunningham KW.** A homolog of voltage-gated Ca^{2+} channels stimulated by depletion of secretory Ca^{2+} in yeast. *Mol Cell Biol* 20: 6686–6694, 2000.

210. **Long SB, Campbell EB, Mackinnon R.** Crystal structure of a mammalian voltage-dependent Shaker family K^+ channel. *Science* 309: 897–903, 2005.

211. **Long SB, Campbell EB, Mackinnon R.** Voltage sensor of Kv1.2: structural basis of electromechanical coupling. *Science* 309: 903–908, 2005.

212. **Long SB, Tao X, Campbell EB, MacKinnon R.** Atomic structure of a voltage-dependent K^+ channel in a lipid membrane-like environment. *Nature* 450: 376–382, 2007.

213. **Loovers HM, Postma M, Keizer-Gunnink I, Huang YE, Devreotes PN, van Haastert PJ.** Distinct roles of $PI(3,4,5)P_3$ during chemoattractant signaling in *Dictyostelium*: a quantitative in vivo analysis by inhibition of PI3-kinase. *Mol Biol Cell* 17: 1503–1513, 2006.

214. **Lopez-Rodriguez A, Trejo AC, Coyne L, Halliwell RF, Miledi R, Martinez-Torres A.** The product of the gene GEF1 of *Saccharomyces cerevisiae* transports Cl^- across the plasma membrane. *FEMS Yeast Res* 7: 1218–1229, 2007.

215. **Lorenz MC, Heitman J.** The MEP2 ammonium permease regulates pseudohyphal differentiation in *Saccharomyces cerevisiae*. *EMBO J* 17: 1236–1247, 1998.

216. **Loukin S, Lin J, Athar U, Palmer CP, Saimi Y.** The carboxyl tail forms a discrete functional domain that nlocks closure of the yeast K^+ channel. *Proc Natl Acad Sci USA* 99: 1926–1930, 2002.

217. **Loukin SH, Kuo MM, Zhou XL, Haynes WJ, Kung C, Saimi Y.** Microbial K^+ channels. *J Gen Physiol* 125: 521–527, 2005.

218. **Loukin SH, Saimi Y.** Carboxyl tail prevents yeast K^+ channel closure: proposal of an integrated model of TOK1 gating. *Biophys J* 82: 781–792, 2002.

219. **Loukin SH, Saimi Y.** K^+-dependent composite gating of the yeast K^+ channel, Tok1. *Biophys J* 77: 3060–3070, 1999.

220. **Loukin SH, Vaillant B, Zhou XL, Spalding EP, Kung C, Saimi Y.** Random mutagenesis reveals a region important for gating of the yeast K^+ channel Ykc1. *EMBO J* 16: 4817–4825, 1997.

221. **Lu Z, Klem AM, Ramu Y.** Ion conduction pore is conserved among potassium channels. *Nature* 413: 809–813, 2001.

222. **Ludewig U, Neuhauser B, Dynowski M.** Molecular mechanisms of ammonium transport and accumulation in plants. *FEBS Lett* 581: 2301–2308, 2007.

223. **Ludewig U, von Wiren N, Frommer WB.** Uniport of NH_4^+ by the root hair plasma membrane ammonium transporter LeAMT1;1. *J Biol Chem* 277: 13548–13555, 2002.

224. **Lundby A, Santos JS, Zazueta C, Montal M.** Molecular template for a voltage sensor in a novel K^+ channel. II. Conservation of a eukaryotic sensor fold in a prokaryotic K^+ channel. *J Gen Physiol* 128: 293–300, 2006.

225. **Lusche DF, Malchow D.** Developmental control of cAMP-induced Ca^{2+}-influx by cGMP: influx is delayed and reduced in a cGMP-phosphodiesterase D deficient mutant of *Dictyostelium discoideum*. *Cell Calcium* 37: 57–67, 2005.

226. **Machemer H.** Motor control of cilia. In: *Paramecium*, edited by Goertz HD. Heidelberg: Springer-Verlag, 1988, p. 216–235.

227. **Machemer H, Deitmer JW.** From structure to behaviour: *Stylonychia* as a model system for cellular physiology. In: *Progress in Protistology*, edited by Corliss JO, Patterson DJ. Bristol: Biopress, 1987, p. 213–330.

228. **Machemer H, Ogura A.** Ionic conductances of membranes in ciliated and deciliated *Paramecium*. *J Physiol* 296: 49–60, 1979.

229. **Mackinnon R.** The atomic basis of selective ion conduction in potassium channels. Nobel Lecture (http://nobelprize.org/chemistry/laureates/2003/mackinnon-lecture.html).

230. **Marini AM, Andre B.** In vivo *N*-glycosylation of the mep2 high-affinity ammonium transporter of *Saccharomyces cerevisiae* reveals an extracytosolic N-terminus. *Mol Microbiol* 38: 552–564, 2000.

231. **Marini AM, Soussi-Boudekou S, Vissers S, Andre B.** A family of ammonium transporters in *Saccharomyces cerevisiae*. *Mol Cell Biol* 17: 4282–4293, 1997.

232. **Marini AM, Vissers S, Urrestarazu A, Andre B.** Cloning and expression of the MEP1 gene encoding an ammonium transporter in *Saccharomyces cerevisiae*. *EMBO J* 13: 3456–3463, 1994.

233. **Marius P, Alvis SJ, East JM, Lee AG.** The interfacial lipid binding site on the potassium channel KcsA is specific for anionic phospholipids. *Biophys J* 89: 4081–4089, 2005.

234. **Markin VS, Martinac B.** Mechanosensitive ion channels as reporters of bilayer expansion. A theoretical model. *Biophys J* 60: 1120–1127, 1991.

235. **Martinac B.** 3.5 billion years of mechanosensory transduction: structure and function of mechanosensitive channels in prokaryotes. In: *Current Topics in Membranes*, edited by Hamill OP. San Diego, CA: Elsevier, 2007, p. 25–57.

236. **Martinac B.** Mechanosensitive channels in prokaryotes. *Cell Physiol Biochem* 11: 61–76, 2001.

237. **Martinac B, Adler J, Kung C.** Mechanosensitive ion channels of *E. coli* activated by amphipaths. *Nature* 348: 261–263, 1990.

238. **Martinac B, Buechner M, Delcour AH, Adler J, Kung C.** Pressure-sensitive ion channel in *Escherichia coli*. *Proc Natl Acad Sci USA* 84: 2297–2301, 1987.

239. **Martinac B, Delcour AH, Buechner M, Adler J, Kung C.** Mechanosensitive ion channels in bacteria. In: *Comparative Aspects of Mechanoreceptor Systems*, edited by Ito F. Heidelberg: Springer-Verlag, 1992, p. 3–18.

240. **Martinac B, Kloda A.** Evolutionary origins of mechanosensitive ion channels. *Prog Biophys Mol Biol* 82: 11–24, 2003.

241. **Matsumoto TK, Ellsmore AJ, Cessna SG, Low PS, Pardo JM, Bressan RA, Hasegawa PM.** An osmotically induced cytosolic Ca^{2+} transient activates calcineurin signaling to mediate ion homeostasis and salt tolerance of *Saccharomyces cerevisiae*. *J Biol Chem* 277: 33075–33080, 2002.

242. **Maurer JA, Dougherty DA.** Generation and evaluation of a large mutational library from the *Escherichia coli* mechanosensitive channel of large conductance, MscL: implications for channel gating and evolutionary design. *J Biol Chem* 278: 21076–21082, 2003.

243. **Mayer ML, Olson R, Gouaux E.** Mechanisms for ligand binding to GluR0 ion channels: crystal structures of the glutamate and serine complexes and a closed apo state. *J Mol Biol* 311: 815–836, 2001.

244. **Menestrina G.** Ionic channels formed by *Staphylococcus aureus* alpha-toxin: voltage-dependent inhibition by divalent and trivalent cations. *J Membr Biol* 90: 177–190, 1986.

245. **Merchant SS, Prochnik SE, Vallon O, Harris EH, Karpowicz SJ, Witman GB, Terry A, Salamov A, Fritz-Laylin LK, Marechal-Drouard L, Marshall WF, Qu LH, Nelson DR, Sanderfoot AA, Spalding MH, Kapitonov VV, Ren Q, Ferris P, Lindquist E, Shapiro H, Lucas SM, Grimwood J, Schmutz J, Cardol P, Cerutti H, Chanfreau G, Chen CL, Cognat V, Croft MT, Dent R, Dutcher S, Fernandez E, Fukuzawa H, Gonzalez-Ballester D, Gonzalez-Halphen D, Hallmann A, Hanikenne M, Hippler M, Inwood W, Jabbari K, Kalanon M, Kuras R, Lefebvre PA, Lemaire SD, Lobanov AV, Lohr M, Manuell A, Meier I, Mets L, Mittag M, Mittelmeier T, Moroney JV, Moseley J, Napoli C, Nedelcu AM, Niyogi K, Novoselov SV, Paulsen IT, Pazour G, Purton S, Ral JP, Riano-Pachon DM, Riekhof W, Rymarquis L, Schroda M, Stern D, Umen J, Willows R, Wilson N, Zimmer SL, Allmer J, Balk J, Bisova K, Chen CJ, Elias M, Gendler K, Hauser C, Lamb MR, Ledford H, Long JC, Minagawa J, Page MD, Pan J, Pootakham W, Roje S, Rose A, Stahlberg E, Terauchi AM, Yang P, Ball S, Bowler C, Dieckmann CL, Gladyshev VN, Green P, Jorgensen R, Mayfield S, Mueller-Roeber B, Rajamani S, Sayre RT, Brokstein P, Dubchak I, Goodstein D, Hornick L, Huang YW, Jhaveri J, Luo Y, Martinez D, Ngau WC, Otillar B, Poliakov A, Porter A, Szajkowski L, Werner G, Zhou K, Grigoriev IV, Rokhsar DS, Grossman AR.** The *Chlamydomonas* genome reveals the evolution of key animal and plant functions. *Science* 318: 245–250, 2007.

246. **Meyer GR, Gullingsrud J, Schulten K, Martinac B.** Molecular dynamics study of MscL interactions with a curved lipid bilayer. *Biophys J* 91: 1630–1637, 2006.

247. **Milkman R.** An *Escherichia coli* homologue of eukaryotic potassium channel proteins. *Proc Natl Acad Sci USA* 91: 3510–3514, 1994.

248. **Miller S, Bartlett W, Chandrasekaran S, Simpson S, Edwards M, Booth IR.** Domain organization of the MscS mechanosensitive channel of *Escherichia coli*. *EMBO J* 22: 36–46, 2003.

249. **Mitchell P.** Coupling of phosphorylation to electron and hydrogen transfer by a chemi-osmotic type of mechanism. *Nature* 191: 144–148, 1961.

250. **Mogami Y, Pernberg J, Machemer H.** Messenger role of calcium in ciliary electromotor coupling: a reassessment. *Cell Calcium* 11: 665–673, 1990.

251. **Montal M.** Structure-function correlates of Vpu, a membrane protein of HIV-1. *FEBS Lett* 552: 47–53, 2003.

252. **Montoya M, Gouaux E.** Beta-barrel membrane protein folding and structure viewed through the lens of alpha-hemolysin. *Biochim Biophys Acta* 1609: 19–27, 2003.

253. **Morgan PJAPW, Mitchell TJ.** Thiol-activated cytolysins. *Rev Med Microbiol* 7: 221–229, 1996.

254. **Movileanu L, Schmittschmitt JP, Scholtz JM, Bayley H.** Interactions of peptides with a protein pore. *Biophys J* 89: 1030–1045, 2005.

255. **Moyer JH, Lee-Tischler MJ, Kwon HY, Schrick JJ, Avner ED, Sweeney WE, Godfrey VL, Cacheiro NL, Wilkinson JE, Woychik RP.** Candidate gene associated with a mutation causing recessive polycystic kidney disease in mice. *Science* 264: 1329–1333, 1994.

256. **Müller U, Hartung K.** Properties of three different ion channels in the plasma membrane of the slime mold *Dictyostelium discoideum*. *Biochim Biophys Acta* 1026: 204–212, 1990.

257. **Müller U, Malcow D, Hartung K.** Single ion channels in the slime mold *Dictyostelium discoideum*. *Biochim Biophys Acta* 857: 287–290, 1986.

258. **Murata Y, Iwasaki H, Sasaki M, Inaba K, Okamura Y.** Phosphoinositide phosphatase activity coupled to an intrinsic voltage sensor. *Nature* 435: 1239–1243, 2005.

259. **Nagel G, Brauner M, Liewald JF, Adeishvili N, Bamberg E, Gottschalk A.** Light activation of channelrhodopsin-2 in excitable cells of *Caenorhabditis elegans* triggers rapid behavioral responses. *Curr Biol* 15: 2279–2284, 2005.

260. **Nagel G, Ollig D, Fuhrmann M, Kateriya S, Musti AM, Bamberg E, Hegemann P.** Channelrhodopsin-1: a light-gated proton channel in green algae. *Science* 296: 2395–2398, 2002.

261. **Nagel G, Szellas T, Huhn W, Kateriya S, Adeishvili N, Berthold P, Ollig D, Hegemann P, Bamberg E.** Channelrhodopsin-2, a directly light-gated cation-selective membrane channel. *Proc Natl Acad Sci USA* 100: 13940–13945, 2003.

262. **Naitoh Y, Eckert R.** Ionic mechanisms controlling behavioral responses of paramecium to mechanical stimulation. *Science* 164: 963–965, 1969.

263. **Naitoh Y, Eckert R, Friedman K.** A regenerative calcium response in *Paramecium*. *J Exp Biol* 56: 667–681, 1972.

264. **Naitoh Y, Eckert R.** Sensory mechanisms in paramecium. II. Ionic basis of the hyperpolarizing mechanoreceptor potential. *J Exp Biol* 59: 53–65, 1973.

265. **Nakamaru Y, Takahashi Y, Unemoto T, Nakamura T.** Mechanosensitive channel functions to alleviate the cell lysis of marine bacterium, *Vibrio alginolyticus*, by osmotic downshock. *FEBS Lett* 444: 170–172, 1999.

266. **Nakayama Y, Fujiu K, Sokabe M, Yoshimura K.** Molecular and electrophysiological characterization of a mechanosensitive channel expressed in the chloroplasts of *Chlamydomonas*. *Proc Natl Acad Sci USA* 104: 5883–5888, 2007.

267. **Nauli SM, Alenghat FJ, Luo Y, Williams E, Vassilev P, Li X, Elia AE, Lu W, Brown EM, Quinn SJ, Ingber DE, Zhou J.** Polycystins 1 and 2 mediate mechanosensation in the primary cilium of kidney cells. *Nat Genet* 33: 129–137, 2003.

268. **Nebl T, Kotsifas M, Schaap P, Fisher PR.** Multiple signalling pathways connect chemoattractant receptors and calcium channels in *Dictyostelium*. *J Muscle Res Cell Motil* 23: 853–865, 2002.

269. **Neǒas O.** Cell wall synthesis in yeast protoplasts. *Bacteriol Rev* 35: 149–170, 1971.

270. **Nee S.** More than meets the eye. *Nature* 429: 804–805, 2004.

271. **Nguitragool W, Miller C.** Uncoupling of a CLC Cl⁻/H⁺ exchange transporter by polyatomic anions. *J Mol Biol* 362: 682–690, 2006.

272. **Nguyen T, Clare B, Guo W, Martinac B.** The effects of parabens on the mechanosensitive channels of *E. coli*. *Eur Biophys J* 34: 389–395, 2005.

273. **Nimigean CM, Pagel MD.** Ligand binding and activation in a prokaryotic cyclic nucleotide-modulated channel. *J Mol Biol* 371: 1325–1337, 2007.

274. **Nimigean CM, Shane T, Miller C.** A cyclic nucleotide modulated prokaryotic K^+ channel. *J Gen Physiol* 124: 203–210, 2004.

275. **Nomura T, Sokabe M, Yoshimura K.** Lipid-protein interaction of the MscS mechanosensitive channel examined by scanning mutagenesis. *Biophys J* 91: 2874–2881, 2006.

276. **Norman C, Liu ZW, Rigby P, Raso A, Petrov Y, Martinac B.** Visualisation of the mechanosensitive channel of large conductance in bacteria using confocal microscopy. *Eur Biophys J* 34: 396–402, 2005.

277. **North RA.** Molecular physiology of P2X receptors. *Physiol Rev* 82: 1013–1067, 2002.

278. **Noskov SY, Roux B.** Ion selectivity in potassium channels. *Biophys Chem* 124: 279–291, 2006.

279. **Oddon DM, Diatloff E, Roberts SK.** A CLC chloride channel plays an essential role in copper homeostasis in *Aspergillus nidulans* at increased extracellular copper concentrations. *Biochim Biophys Acta* 1768: 2466–2477, 2007.

280. **Oertel D, Schein SJ, Kung C.** Separation of membrane currents using a *Paramecium* mutant. *Nature* 268: 120–124, 1977.

281. **Ogura A, Machemer H.** Distribution of mechanoreceptor channels in the *Paramecium* surface membrane. *J Comp Physiol A Sens Neural Behav Physiol* 135: 233–242, 1980.

282. **Ohndorf UM, MacKinnon R.** Construction of a cyclic nucleotide-gated KcsA K^+ channel. *J Mol Biol* 350: 857–865, 2005.

283. **Ou X, Blount P, Hoffman RJ, Kung C.** One face of a transmembrane helix is crucial in mechanosensitive channel gating. *Proc Natl Acad Sci USA* 95: 11471–11475, 1998.

284. **Paidhungat M, Garrett S.** A homolog of mammalian, voltage-gated calcium channels mediates yeast pheromone-stimulated Ca^{2+} uptake and exacerbates the cdc1(Ts) growth defect. *Mol Cell Biol* 17: 6339–6347, 1997.

285. **Palmer CP, Aydar E, Djamgoz MB.** A microbial TRP-like polycystic-kidney-disease-related ion channel gene. *Biochem J* 387: 211–219, 2005.

286. **Palmer CP, Zhou XL, Lin J, Loukin SH, Kung C, Saimi Y.** A TRP homolog in *Saccharomyces cerevisiae* forms an intracellular Ca^{2+}-permeable channel in the yeast vacuolar membrane. *Proc Natl Acad Sci USA* 98: 7801–7805, 2001.

287. **Panchal RG, Smart ML, Bowser DN, Williams DA, Petrou S.** Pore-forming proteins and their application in biotechnology. *Curr Pharm Biotechnol* 3: 99–115, 2002.

288. **Parent CA.** Making all the right moves: chemotaxis in neutrophils and *Dictyostelium*. *Curr Opin Cell Biol* 16: 4–13, 2004.

289. **Parfenova LV, Abarca-Heidemann K, Crane BM, Rothberg BS.** Molecular architecture and divalent cation activation of TvoK, a prokaryotic potassium channel. *J Biol Chem* 282: 24302–24309, 2007.

290. **Park KH, Berrier C, Martinac B, Ghazi A.** Purification and functional reconstitution of N- and C-halves of the MscL channel. *Biophys J* 86: 2129–2136, 2004.

291. **Parrish AR, Wang W, Wang L.** Manipulating proteins for neuroscience. *Curr Opin Neurobiol* 16: 585–592, 2006.

292. **Patel AJ, Honoré E, Lesage F, Fink M, Romey G, Lazdunski M.** Inhalational anesthetics activate two-pore-domain background K^+ channels. *Nat Neurosci* 2: 422–426, 1999.

293. **Patel AJ, Lazdunski M, Honoré E.** Lipid and mechano-gated 2P domain K^+ channels. *Curr Opin Cell Biol* 13: 422–428, 2001.

294. **Pavlov E, Bladen C, Diao C, French RJ.** Bacterial Na channels: progenitors, progeny, or parallel evolution? In: *Bacterial Ion Channels and Their Eukaryotic Homologs*, edited by Kubalski A, Martinac B. Washington, DC: ASM, 2005, p. 191–207.

295. **Pazour GJ, Dickert BL, Vucica Y, Seeley ES, Rosenbaum JL, Witman GB, Cole DG.** *Chlamydomonas* IFT88 and its mouse homologue, polycystic kidney disease gene tg737, are required for assembly of cilia and flagella. *J Cell Biol* 151: 709–718, 2000.

296. **Peiter E, Fischer M, Sidaway K, Roberts SK, Sanders D.** The *Saccharomyces cerevisiae* Ca^{2+} channel Cch1pMid1p is essential for tolerance to cold stress and iron toxicity. *FEBS Lett* 579: 5697–5703, 2005.

297. **Perozo E.** Gating prokaryotic mechanosensitive channels. *Nat Rev Mol Cell Biol* 7: 109–119, 2006.

298. **Perozo E, Cortes DM, Cuello LG.** Structural rearrangements underlying K^+-channel activation gating. *Science* 285: 73–78, 1999.

299. **Perozo E, Cortes DM, Cuello LG.** Three-dimensional architecture and gating mechanism of a K^+ channel studied by EPR spectroscopy. *Nat Struct Biol* 5: 459–469, 1998.

300. **Perozo E, Cortes DM, Sompornpisut P, Kloda A, Martinac B.** Open channel structure of MscL and the gating mechanism of mechanosensitive channels. *Nature* 418: 942–948, 2002.

301. **Perozo E, Kloda A, Cortes DM, Martinac B.** Physical principles underlying the transduction of bilayer deformation forces during mechanosensitive channel gating. *Nat Struct Biol* 9: 696–703, 2002.

302. **Perozo E, Kloda A, Cortes DM, Martinac B.** Site-directed spin-labeling analysis of reconstituted Mscl in the closed state. *J Gen Physiol* 118: 193–206, 2001.

303. **Perozo E, Rees DC.** Structure and mechanism in prokaryotic mechanosensitive channels. *Curr Opin Struct Biol* 13: 432–442, 2003.

304. **Piller SC, Ewart GD, Premkumar A, Cox GB, Gage PW.** Vpr protein of human immunodeficiency virus type 1 forms cation-selective channels in planar lipid bilayers. *Proc Natl Acad Sci USA* 93: 111–115, 1996.

305. **Pinto LH, Dieckmann GR, Gandhi CS, Papworth CG, Braman J, Shaughnessy MA, Lear JD, Lamb RA, DeGrado WF.** A functionally defined model for the M2 proton channel of influenza A virus suggests a mechanism for its ion selectivity. *Proc Natl Acad Sci USA* 94: 11301–11306, 1997.

306. **Pinto LH, Holsinger LJ, Lamb RA.** Influenza virus M2 protein has ion channel activity. *Cell* 69: 517–528, 1992.

307. **Pivetti CD, Yen MR, Miller S, Busch W, Tseng YH, Booth IR, Saier MH Jr.** Two families of mechanosensitive channel proteins. *Microbiol Mol Biol Rev* 67: 66–85, 2003.

308. **Plugge B, Gazzarrini S, Nelson M, Cerana R, Van Etten JL, Derst C, DiFrancesco D, Moroni A, Thiel G.** A potassium channel protein encoded by chlorella virus PBCV-1. *Science* 287: 1641–1644, 2000.

309. **Postma M, Bosgraaf L, Loovers HM, Van Haastert PJ.** Chemotaxis: signalling modules join hands at front and tail. *EMBO Rep* 5: 35–40, 2004.

310. **Preston RR.** A magnesium current in *Paramecium*. *Science* 250: 285–288, 1990.

311. **Preston RR, Kink JA, Hinrichsen RD, Saimi Y, Kung C.** Calmodulin mutants and Ca^{2+}-dependent channels in *Paramecium*. *Annu Rev Physiol* 53: 309–319, 1991.

312. **Preston RR, Kung C.** Inhibition of Mg^{2+} current by single-gene mutation in *Paramecium*. *J Membr Biol* 139: 203–213, 1994.

313. **Preston RR, Kung C.** Isolation and characterization of paramecium mutants defective in their response to magnesium. *Genetics* 137: 759–769, 1994.

314. **Ptak CP, Cuello LG, Perozo E.** Electrostatic interaction of a K^+ channel RCK domain with charged membrane surfaces. *Biochemistry* 44: 62–71, 2005.

315. **Qian F, Boletta A, Bhunia AK, Xu H, Liu L, Ahrabi AK, Watnick TJ, Zhou F, Germino GG.** Cleavage of polycystin-1 requires the receptor for egg jelly domain and is disrupted by human autosomal-dominant polycystic kidney disease 1-associated mutations. *Proc Natl Acad Sci USA* 99: 16981–16986, 2002.

316. **Quarmby LM.** Ca^{2+} influx activated by low pH in *Chlamydomonas*. *J Gen Physiol* 108: 351–361, 1996.

317. **Quarmby LM, Hartzell HC.** Two distinct, calcium-mediated, signal transduction pathways can trigger deflagellation in *Chlamydomonas reinhardtii*. *J Cell Biol* 124: 807–815, 1994.

318. **Ramsey IS, Delling M, Clapham DE.** An introduction to TRP channels. *Annu Rev Physiol* 68: 619–647, 2006.

319. **Ramsey IS, Moran MM, Chong JA, Clapham DE.** A voltage-gated proton-selective channel lacking the pore domain. *Nature* 440: 1213–1216, 2006.

320. **Reid JD, Lukas W, Shafaatian R, Bertl A, Scheurmann-Kettner C, Guy HR, North RA.** The *S. cerevisiae* outwardly-rectifying potassium channel (DUK1) identifies a new family of channels with duplicated pore domains. *Receptors Channels* 4: 51–62, 1996.

321. **Ren D, Navarro B, Xu H, Yue L, Shi Q, Clapham DE.** A prokaryotic voltage-gated sodium channel. *Science* 294: 2372–2375, 2001.

322. **Richard EA, Saimi Y, Kung C.** A mutation that increases a novel calcium-activated potassium conductance of *Paramecium tetraurelia*. *J Membr Biol* 91: 173–181, 1986.

323. **Roberts SK.** TOK homologue in *Neurospora crassa*: first cloning and functional characterization of an ion channel in a filamentous fungus. *Eukaryotic Cell* 2: 181–190, 2002.

324. **Roosild TP, Le KT, Choe S.** Cytoplasmic gatekeepers of K$^+$-channel flux: a structural perspective. *Trends Biochem Sci* 29: 39–45, 2004.

325. **Roosild TP, Miller S, Booth IR, Choe S.** A mechanism of regulating transmembrane potassium flux through a ligand-mediated conformational switch. *Cell* 109: 781–791, 2002.

326. **Rosenbaum JL, Witman GB.** Intraflagellar transport. *Nat Rev Mol Cell Biol* 3: 813–825, 2002.

327. **Ruta V, Jiang Y, Lee A, Chen J, MacKinnon R.** Functional analysis of an archaebacterial voltage-dependent K$^+$ channel. *Nature* 422: 180–185, 2003.

328. **Ruthe HJ, Adler J.** Fusion of bacterial spheroplasts by electric fields. *Biochim Biophys Acta* 819: 105–113, 1985.

329. **Saimi Y, Hinrichsen RD, Forte M, Kung C.** Mutant analysis shows that the Ca^{2+}-induced K$^+$ current shuts off one type of excitation in *Paramecium*. *Proc Natl Acad Sci USA* 80: 5112–5116, 1983.

330. **Saimi Y, Kung C.** Behavioral genetics of *Paramecium*. *Annu Rev Genet* 21: 47–65, 1987.

331. **Saimi Y, Kung C.** Calmodulin as an ion channel subunit. *Annu Rev Physiol* 64: 289–311, 2002.

332. **Saimi Y, Ling KY.** Calmodulin activation of calcium-dependent sodium channels in excised membrane patches of *Paramecium*. *Science* 249: 1441–1444, 1990.

333. **Saimi Y, Martinac B.** Calcium-dependent potassium channel in *Paramecium* studied under patch clamp. *J Membr Biol* 112: 79–89, 1989.

334. **Saimi Y, Martinac B, Delcour AH, Minorsky PV, Gustin MC, Culbertson MR, Adler J, Kung C.** Patch clamp studies of microbial ion channels. *Methods Enzymol* 207: 681–691, 1992.

335. **Santos JS, Lundby A, Zazueta C, Montal M.** Molecular template for a voltage sensor in a novel K$^+$ channel. I. Identification and functional characterization of KvLm, a voltage-gated K$^+$ channel from *Listeria* monocytogenes. *J Gen Physiol* 128: 283–292, 2006.

336. **Sasaki M, Takagi M, Okamura Y.** A voltage sensor-domain protein is a voltage-gated proton channel. *Science* 312: 589–592, 2006.

337. **Satow Y, Kung C.** Genetic dissection of active electrogenesis in *Paramecium aurelia*. *Nature* 247: 69–71, 1974.

338. **Schaloske R, Schlatterer C, Malchow D.** A Xestospongin C-sensitive Ca^{2+} store is required for cAMP-induced Ca^{2+} influx and cAMP oscillations in *Dictyostelium*. *J Biol Chem* 275: 8404–8408, 2000.

339. **Schmidt JA, Eckert R.** Calcium couples flagellar reversal to photostimulation in *Chlamydomonas reinhardtii*. *Nature* 262: 713–715, 1976.

340. **Schrempf H, Schmidt O, Kummerlen R, Hinnah S, Muller D, Betzler M, Steinkamp T, Wagner R.** A prokaryotic potassium ion channel with two predicted transmembrane segments from *Streptomyces lividans*. *EMBO J* 14: 5170–5178, 1995.

341. **Schroll C, Riemensperger T, Bucher D, Ehmer J, Voller T, Erbguth K, Gerber B, Hendel T, Nagel G, Buchner E, Fiala A.** Light-induced activation of distinct modulatory neurons triggers appetitive or aversive learning in *Drosophila* larvae. *Curr Biol* 16: 1741–1747, 2006.

342. **Schumann U, Edwards MD, Li C, Booth IR.** The conserved carboxy-terminus of the MscS mechanosensitive channel is not essential but increases stability and activity. *FEBS Lett* 572: 233–237, 2004.

343. **Schwappach B, Stobrawa S, Hechenberger M, Steinmeyer K, Jentsch TJ.** Golgi localization and functionally important domains in the NH$_2$ and COOH terminus of the yeast CLC putative chloride channel Gef1p. *J Biol Chem* 273: 15110–15118, 1998.

344. **Sesti F, Rajan S, Gonzalez-Colaso R, Nikolaeva N, Goldstein SA.** Hyperpolarization moves S4 sensors inward to open MVP, a methanococcal voltage-gated potassium channel. *Nat Neurosci* 6: 353–361, 2003.

345. **Sharma AK, Spudich JL, Doolittle WF.** Microbial rhodopsins: functional versatility and genetic mobility. *Trends Microbiol* 14: 463–469, 2006.

346. **Sheetz MP, Singer SJ.** Biological membranes as bilayer couples. A molecular mechanism of drug-erythrocyte interactions. *Proc Natl Acad Sci USA* 71: 4457–4461, 1974.

347. **Shi N, Ye S, Alam A, Chen L, Jiang Y.** Atomic structure of a Na$^+$- and K$^+$-conducting channel. *Nature* 440: 570–574, 2006.

348. **Sigrist SJ.** Neurobiology tools: flashdancing worms. *Curr Biol* 16: R100–102, 2006.

349. **Sineshchekov OA, Govorunova EV.** Rhodopsin-mediated photosensing in green flagellated algae. *Trends Plant Sci* 4: 201, 1999.

350. **Sineshchekov OA, Jung KH, Spudich JL.** Two rhodopsins mediate phototaxis to low- and high-intensity light in *Chlamydomonas reinhardtii*. *Proc Natl Acad Sci USA* 99: 8689–8694, 2002.

351. **Sleator RD, Hill C.** Bacterial osmoadaptation: the role of osmolytes in bacterial stress and virulence. *FEMS Microbiol Rev* 26: 49–71, 2001.

352. **Song L, Hobaugh MR, Shustak C, Cheley S, Bayley H, Gouaux JE.** Structure of staphylococcal alpha-hemolysin, a heptameric transmembrane pore. *Science* 274: 1859–1866, 1996.

353. **Sotomayor M, Schulten K.** Molecular dynamics study of gating in the mechanosensitive channel of small conductance MscS. *Biophys J* 87: 3050–3065, 2004.

354. **Sotomayor M, Vasquez V, Perozo E, Schulten K.** Ion conduction through MscS as determined by electrophysiology and simulation. *Biophys J* 92: 886–902, 2007.

355. **Spalding EP.** Ion channels and the transduction of light signals. *Plant Cell Environ* 23: 665–674, 2000.

356. **Spudich JL.** The multitalented microbial sensory rhodopsins. *Trends Microbiol* 14: 480–487, 2006.

357. **Steinbacher S, Bass R, Strop P, Rees DC.** Mechanosensitive channel of large conductance (MscL) PDB (http://www.rcsb.org/pdb/results/results.do).

358. **Steinbacher S, Bass R, Strop P, Rees DC.** Mechanosensitive channel of small conductance (MscS) PDB (http://www.rcsb.org/pdb/results/results.do).

359. **Stingl K, Brandt S, Uhlemann EM, Schmid R, Altendorf K, Zeilinger C, Ecobichon C, Labigne A, Bakker EP, de Reuse H.** Channel-mediated potassium uptake in *Helicobacter pylori* is essential for gastric colonization. *EMBO J* 26: 232–241, 2007.

360. **Stoeckenius W.** Bacterial rhodopsins: evolution of a mechanistic model for the ion pumps. *Protein Sci* 8: 447–459, 1999.

361. **Stokes NR, Murray HD, Subramaniam C, Gourse RL, Louis P, Bartlett W, Miller S, Booth IR.** A role for mechanosensitive channels in survival of stationary phase: regulation of channel expression by RpoS. *Proc Natl Acad Sci USA* 100: 15959–15964, 2003.

362. **Strop P, Bass R, Rees DC.** Prokaryotic mechanosensitive channels. In: *Advances in Protein Chemistry: Membrane Proteins*, edited by Rees DC. New York: Academic, 2003, p. 177–209.

363. **Su Z, Zhou X, Haynes WJ, Loukin SH, Anishkin A, Saimi Y, Kung C.** Yeast gain-of-function mutations reveal structure-function relationships conserved among different subfamilies of transient receptor potential channels. *Proc Natl Acad Sci USA*. In press.

364. **Sukharev S.** Purification of the small mechanosensitive channel of *Escherichia coli* (MscS): the subunit structure, conduction, gating characteristics in liposomes. *Biophys J* 83: 290–298, 2002.

365. **Sukharev S, Betanzos M, Chiang CS, Guy HR.** The gating mechanism of the large mechanosensitive channel MscL. *Nature* 409: 720–724, 2001.

366. **Sukharev SI, Blount P, Martinac B, Blattner FR, Kung C.** A large-conductance mechanosensitive channel in *E. coli* encoded by mscL alone. *Nature* 368: 265–268, 1994.

367. **Sukharev SI, Blount P, Martinac B, Kung C.** Functional reconstitution as an assay for biochemical isolation of channel proteins: application to the molecular identification of a bacterial mechanosensitive channel. *Methods* 6: 51–59, 1994.

368. **Sukharev SI, Martinac B, Arshavsky VY, Kung C.** Two types of mechanosensitive channels in the *E. coli* cell envelope: solubilization and functional reconstitution. *Biophys J* 65: 177–183, 1993.

369. **Sun S, Gan JH, Paynter JJ, Tucker SJ.** Cloning and functional characterization of a superfamily of microbial inwardly rectifying potassium channels. *Physiol Gen* 26: 1–7, 2006.

370. **Sunstrom NA, Premkumar LS, Premkumar A, Ewart G, Cox GB, Gage PW.** Ion channels formed by NB, an influenza B virus protein. *J Membr Biol* 150: 127–132, 1996.

371. **Suzuki T, Yamasaki K, Fujita S, Oda K, Iseki M, Yoshida K, Watanabe M, Daiyasu H, Toh H, Asamizu E, Tabata S, Miura K, Fukuzawa H, Nakamura S, Takahashi T.** Archaeal-type rhodopsins in *Chlamydomonas*: model structure and intracellular localization. *Biochem Biophys Res Commun* 301: 711–717, 2003.

372. **Tajkhorshid E, Cohen J, Aksimentiev A, Sotomayor M, Schulten K.** Towards understanding of membrane channels. In: *Bacterial Ion Channels and Their Eukaryotic Homologues*, edited by Kubalski A, Martinac B. Washington, DC: ASM, 2005, p. 153–190.

373. **Takeda K, Sasaki AT, Ha H, Seung HA, Firtel RA.** Role of phosphatidylinositol 3-kinases in chemotaxis in *Dictyostelium*. *J Biol Chem* 282: 11874–11884, 2007.

374. **Traynor D, Milne JL, Insall RH, Kay RR.** Ca^{2+} signalling is not required for chemotaxis in *Dictyostelium*. *EMBO J* 19: 4846–4854, 2000.

375. **Vacata V, Hofer M, Larsson HP, Lecar H.** Ionic channels in the plasma membrane of *Schizosaccharomyces pombe*: evidence from patch-clamp measurements. *J Bioenerg Biomembr* 25: 43–53, 1993.

376. **Valiyaveetil FI, Zhou Y, MacKinnon R.** Lipids in the structure, folding, function of the KcsA K^+ channel. *Biochemistry* 41: 10771–10777, 2002.

377. **Van den Brink-van der Laan E, Chupin V, Killian JA, de Kruijff B.** Small alcohols destabilize the KcsA tetramer via their effect on the membrane lateral pressure. *Biochemistry* 43: 5937–5942, 2004.

378. **Van den Brink-van der Laan E, Chupin V, Killian JA, de Kruijff B.** Stability of KcsA tetramer depends on membrane lateral pressure. *Biochemistry* 43: 4240–4250, 2004.

379. **Van Duijn B, Vogelzang SA.** The membrane potential of the cellular slime mold *Dictyostelium discoideum* is mainly generated by an electrogenic proton pump. *Biochim Biophys Acta* 983: 186–192, 1989.

380. **Van Duijn B, Vogelzang SA, Ypey DL, Van der Molen LG, Van Haastert PJ.** Normal chemotaxis in *Dictyostelium discoideum* cells with a depolarized plasma membrane potential. *J Cell Sci* 95: 177–183, 1990.

381. **Van Haastert PJ, Keizer-Gunnink I, Kortholt A.** Essential role of PI3-kinase and phospholipase A_2 in *Dictyostelium discoideum* chemotaxis. *J Cell Biol* 177: 809–816, 2007.

382. **Van Nuland A, Vandormael P, Donaton M, Alenquer M, Lourenco A, Quintino E, Versele M, Thevelein JM.** Ammonium permease-based sensing mechanism for rapid ammonium activation of the protein kinase A pathway in yeast. *Mol Microbiol* 59: 1485–1505, 2006.

383. **Vasquez V, Cortes DM, Furukawa H, Perozo E.** An optimized purification and reconstitution method for the MscS channel: strategies for spectroscopical analysis. *Biochemistry* 46: 6766–6773, 2007.

384. **Viladevall L, Serrano R, Ruiz A, Domenech G, Giraldo J, Barcelo A, Arino J.** Characterization of the calcium-mediated response to alkaline stress in *Saccharomyces cerevisiae*. *J Biol Chem* 279: 43614–43624, 2004.

385. **Volk WA.** *Basic Microbiology*. New York: Harper Collins, 1992.

386. **Von Phillipsborn A, Bastmeyer M.** Mechanisms of gradient detection: a comparison of axon pathfinding with eukaryotic cell migration. *Int Rev Cytol* 263: 1–62, 2007.

387. **Wachter A, Schwappach B.** The yeast CLC chloride channel is proteolytically processed by the furin-like protease Kex2p in the first extracellular loop. *FEBS Lett* 579: 1149–1153, 2005.

388. **Wada Y, Ohsumi Y, Tanifuji M, Kasai M, Anraku Y.** Vacuolar ion channel of the yeast, *Saccharomyces cerevisiae*. *J Biol Chem* 262: 17260–17263, 1987.

389. **Wang GX, Poo MM.** Requirement of TRPC channels in netrin-1-induced chemotropic turning of nerve growth cones. *Nature* 434: 898–904, 2005.

390. **White SH, Wimley WC.** Membrane protein folding and stability: physical principles. *Annu Rev Biophys Biomol Struct* 28: 319–365, 1999.

391. **Williams HP, Harwood AJ.** Cell polarity and *Dictyostelium* development. *Curr Opin Microbiol* 6: 621–627, 2003.

392. **Witman GB.** Chlamydomonas phototaxis. *Trends Cell Biol* 3: 403–408, 1993.

393. **Woese CR.** There must be a prokaryote somewhere: microbiology's search for itself. *Microbiol Rev* 58: 1–9, 1994.

394. **Woese CR, Gupta R.** Are archaebacteria merely derived "prokaryotes"? *Nature* 289: 95–96, 1981.

395. **Wood DC.** Membrane permeabilities determining resting, action and mechanosensitive potentials in Stentor coeruleus. *J Comp Physiol* 146: 537–550, 1982.

396. **Wood JM.** Osmosensing by bacteria: signals and membrane-based sensors. *Microbiol Mol Biol Rev* 63: 230–262, 1999.

397. **Yau WM, Wimley WC, Gawrisch K, White SH.** The preference of tryptophan for membrane interfaces. *Biochemistry* 37: 14713–14718, 1998.

398. **Yoshida K, Ide T, Inouye K, Mizuno K, Taguchi T, Kasai M.** A voltage- and K^+-dependent K^+ channel from a membrane fraction enriched in contractile vacuole of *Dictyostelium discoideum*. *Biochim Biophys Acta* 1325: 178–188, 1997.

399. **Yoshimura K.** Mechanosensitive channels in the cell body of *Chlamydomonas*. *J Membr Biol* 166: 149–155, 1998.

400. **Yoshimura K, Batiza A, Schroeder M, Blount P, Kung C.** Hydrophilicity of a single residue within MscL correlates with increased channel mechanosensitivity. *Biophys J* 77: 1960–1972, 1999.

401. **Yoshimura K, Nomura T, Sokabe M.** Loss-of-function mutations at the rim of the funnel of mechanosensitive channel MscL. *Biophys J* 86: 2113–2120, 2004.

402. **Yoshimura K, Usukura J, Sokabe M.** Gating-associated conformational changes in the mechanosensitive channel MscL. *Proc Natl Acad Sci USA* 105: 4033–4038, 2008.

403. **Yu S, Hackmann K, Gao J, He X, Piontek K, Garcia Gonzalez MA, Menezes LF, Xu H, Germino GG, Zuo J, Qian F.** Essential role of cleavage of polycystin-1 at G protein-coupled receptor proteolytic site for kidney tubular structure. *Proc Natl Acad Sci USA* 104: 18688–18693, 2007.

404. **Yue L, Navarro B, Ren D, Ramos A, Clapham DE.** The cation selectivity filter of the bacterial sodium channel, NaChBac. *J Gen Physiol* 120: 845–853, 2002.

405. **Zhai Y, Saier MH Jr.** The amoebapore superfamily. *Biochim Biophys Acta* 1469: 87–99, 2000.

406. **Zhang F, Aravanis AM, Adamantidis A, de Lecea L, Deisseroth K.** Circuit-breakers: optical technologies for probing neural signals and systems. *Nat Rev Neurosci* 8: 577–581, 2007.

407. **Zheng L, Kostrewa D, Berneche S, Winkler FK, Li XD.** The mechanism of ammonia transport based on the crystal structure of AmtB of *Escherichia coli*. *Proc Natl Acad Sci USA* 101: 17090–17095, 2004.

408. **Zhou X, Su Z, Anishkin A, W, J, Haynes E, M, Friske Loukin SH, Kung C, Saimi Y.** Yeast screen show aromatic residues at the end of the sixth helix anchor TRP-channel gate. *Proc Natl Acad Sci USA* 104: 15555–15559, 2007.

409. **Zhou XL, Batiza AF, Loukin SH, Palmer CP, Kung C, Saimi Y.** The transient receptor potential channel on the yeast vacuole is mechanosensitive. *Proc Natl Acad Sci USA* 100: 7105–7110, 2003.

410. **Zhou XL, Kung C.** A mechanosensitive ion channel in *Schizosaccharomyces pombe*. *EMBO J* 11: 2869–2875, 1992.

411. **Zhou XL, Loukin SH, Coria R, Kung C, Saimi Y.** Heterologously expressed fungal transient receptor potential channels retain mechanosensitivity in vitro and osmotic response in vivo. *Eur Biophys J* 34: 413–422, 2005.

412. **Zhou XL, Stumpf MA, Hoch HC, Kung C.** A mechanosensitive channel in whole cells and in membrane patches of the fungus *Uromyces. Science* 253: 1415–1417, 1991.

413. **Zhou XL, Vaillant B, Loukin SH, Kung C, Saimi Y.** YKC1 encodes the depolarization-activated K$^+$ channel in the plasma membrane of yeast. *FEBS Lett* 373: 170–176, 1995.

414. **Zhou Y, Morais-Cabral JH, Kaufman A, MacKinnon R.** Chemistry of ion coordination and hydration revealed by a K$^+$ channel-Fab complex at 2.0 A resolution. *Nature* 414: 43–48, 2001.

415. **Zhu X, Williamson PR.** A CLC-type chloride channel gene is required for laccase activity and virulence in *Cryptococcus neoformans. Mol Microbiol* 50: 1271–1281, 2003.

416. **Zoratti M, Ghazi A.** Stretch-activated channels in prokaryotes. In: *Alkali Transport Systems in Prokaryotes*, edited by Bakker EP. Boca Raton, FL: CRC, 1993, p. 349–358.